LINEAR THEORY OF RADIATION FROM LARGE SPACE STRUCTURES WITH INDUCED AC CURRENT

by

Jiong Wang

B.S., Mechanics and Thermophysics
Tsinghua University, Beijing, China
(1985)

SUBMITTED TO THE DEPARTMENT OF
AERONAUTICS AND ASTRONAUTICS
IN PARTIAL FULFILLMENT OF THE
REQUIREMENTS OF THE DEGREE OF

MASTER OF SCIENCE
IN AERONAUTICS AND ASTRONAUTICS

at the

MASSACHUSETTS INSTITUTE OF TECHNOLOGY
November 1987

Signature of Author.....
Department of Aeronautics and Astronautics
November 9, 1987

Certified by.....
Professor Daniel E. Hastings
Thesis Supervisor, Department of Aeronautics and Astronautics

Accepted by.....
Professor Harold Y. Wachman
Chairman, Department Graduate Committee

LINEAR THEORY OF RADIATION FROM LARGE SPACE STRUCTURES WITH INDUCED AC CURRENT

by

Jiong Wang

Submitted to the Department of Aeronautics and Astronautics
on November 9, 1987, in partial fulfillment of the requirements of
the Degree of Master of Science in Aeronautics and Astronautics

Abstract

This thesis is concerned with the radiation from large space structures with induced AC current. A general theory of cold plasma wave radiation by a moving conductor with AC current in a multi-ion species plasma is presented. The radiation from space systems is studied both analytically and numerically. In order to simulate a realistic situation, the space structure is modeled as a generalized box object carrying currents which can be driven into the system from any direction and the effects of environmental change is considered as well. The radiation impedance and power radiated associated with non-evanescent waves from space station and tethered systems are obtained numerically. The radiation impedance is studied as a function of structure, environment and AC frequency and the underlying physics is explored. Guidelines for the design of large space structures are suggested.

Thesis Supervisor: Daniel E. Hastings

Title: Charles Stark Draper Assistant Professor
of Aeronautics and Astronautics

ACKNOWLEDGMENTS

I wish to thank my research supervisor, Professor D. E. Hastings, for his direct guidance and invaluable assistance throughout this thesis work. His advice and encouragement are greatly appreciated.

I wish to thank Prof. Stan Olbert and Dr. Alan Barnett at the Center for Space Research at MIT. They have been kindly sharing with me their research results and helping me enhance my understanding of this problem.

Thanks also go to my officemates and fellow students for sharing in the friendly atmosphere and offering their help on the computer facilities whenever I asked.

I would like to express my appreciation to my parents, their care and expectation have always been the main motivation since my childhood. Finally, my appreciation to Meng-Huai, who not only came to spend a boring vacation typing the major part of this thesis, but her love has supported me through the past fourteen months of hard work.

This work was supported by NASA grant NAG3-695.

Contents

List of Figures

Chapter 1
Introduction

The electrodynamical interactions between the spacecraft and plasma environment have been investigated since 1950's, when the first artificial satellites were orbited. In 1965, the radiation problem was brought up by Drell et al[7]. Using a cold plasma model in the MHD limit, they predicted that a large conductor moving in the low earth orbit will radiate Alfven waves. This phenomenon was first observed in the plasma flow perturbations generated by Io in the Jovian magnetosphere[2]. The proposed tethered system and space station have caused a revival of interest in the problem of radiation by large space structures and extensive research have been conducted recently. This is a subject of fundamental importance for the design of future space structures and with many applications in space-physics as well.

The basic physics of this problem is as the following: a conductor moving across an external $\vec{B}$ field will see an induced electrical field $\vec{E'} \sim \vec{V} \times \vec{B}$, which causes a potential difference between two terminators in the $\vec{V} \times \vec{B}$ direction. In a "vacuum" environment, there will be net charge accumulated at the two ends, and the induced $\vec{E'}$ field will be balanced inside the conductor. If the conductor moves in a conducting medium such as a plasma, it has been shown that there will be standing waves – Alfven wings – attached the moving body in response to this perturbation. The excitation and radiation of the Alfven

waves were first described by Drell et al[7]. Therefore, there could exist steady electric current flowing inside the conductor and completing its circuit in the environment through those waves[1,15]. Shown in Fig 1.1 and Fig 1.2 are several conceptual views taken from current literatures illustrating the wave radiation by conductor, and particularly by a shuttle tether system . Those pictures also reflect the present understanding of this problem.

As a result of the wave excitation, energy will be carried away from the conductor which can be estimated by integrating the Poynting vector on a closed surface surrounding the conductor:

$$P_{rad} = \frac{c}{4\pi} \oint (\vec{E} \times \vec{B}) \cdot \vec{n} da$$

The energy radiation is especially important for large space structures. For instance, at the low earth orbit, the magnetic field $B \sim 0.33$ $Gauss$ and the induced $E' \sim 0.2V/m$. So a 10 km tether gives an emf of about 2000 Volt. Thus, if a net current of 10 A was flowing in the tether, the energy dissipation associated with this system could be of the order of 10^4 W [15].

The power radiation problem can be studied in the form of an electric circuit as shown in Fig 1.3. In the circuit, there are 1) The electric load, Φ_{load} and r_{load}. For passive case such as a tether used as a power line, $\Phi_{load} = 0$. For active case such as a tether used for communication, then there will be a Φ_{load} used to overcome the induced field Φ'; 2) The conventional Ohmic resistance $R_{ohm} = \rho L/S$; 3) The contactor impedance existing at the interface between conductor and plasma $Z_{contactor}$; and 4) The resistance associated with the ionosphere, the radiation impedance Z_{rad}. So the power radiation associated with plasma waves

can be writen as

$$P_{rad} = I^2 Z_{rad}$$

where

$$I = \frac{\Phi' - \Phi_{load}}{r_{load} + R_{ohms} + Z_{contactor} + Z_{rad}}$$

The radiation impedance Z_{rad} and the power radiation in the ionosphere P_{rad} are the main subjects we are going to study in this thesis.

There have been several publications studying the radiation from space structures, almost all of them are concentrated on the radiation impedance of a tethered system[3,4,6,8,15]. However, the results and conclusions are not mutually consistent. This is not surprising since the field is in its infancy. Because the theory is still incomplete and because the experimental knowledge is limited , the authors are often studying different limiting cases and using different assumptions. First let us briefly review some of the recent research. Either taking the tether to be infinitely long or only studying the MHD regime, Belcastro et al[4] and Rasmussen et al[15] estimated the impedance of a tether to be low , of the order of a few Ohms. Barnett and Olbert carefully examined the wave radiation in the whole frequency regime and developed a general theory for a finite conductor with DC current in a singly ionized plasma. They pointed out that there are three separated radiation bands and the excitation of the lower hybrid waves, which had been neglected by all the previous work, makes a substantial contribution and so the impedance of a tether was estimated of the order of 10^3 Ohms [3]. Neither of the above cited work took into account the "dumbbell" shape of a real tethered system. Estes pointed out that the geometry of the terminators can results in great difference[8], but his model also turns out to be somewhat unrealistic. Besides the research on systems with DC current, at

present, a radiation theory on space structures with AC current is also being developed by Hastings et al[9]. By and large, the knowledge on the radiation problem is still far from satisfactory in both theory and practical applications. Most of the publications are concentrated only on a certain aspect or a specific case of the radiation problem. All the structure models used so far were unrealistically simple, none of them seems to simulate a real space structure in general. All the analysis so far were made in a single ion species plasma, none of them studied the environment as a multi-ion species plasma. No estimations of the radiation by a space station, a problem which has caused more and more concern recently, have been found in the existing publications. Most seriously , there are no answers to fundamental questions such as what factors affect the radiation power and how they affect it,etc, which are crucial for the design of future space structures.

In the present work we make a systematic study on the radiation from large space structures. We shall present a complete and general theory based on the knowledge obtained so far. The goal is not only to give some results which can be applied directly to several practical space structures, but also to explore the underlying physics so that design guidelines can be established. The theoretical base of this thesis is the work by Barnett and Olbert. Using the same formulation, we extend their theory to a multi-ion species plasma and to structures with induced AC current. To simulate the real shape of a space station or a tethered system, the most general case - a box structure with current flowing through the terminator in every directions - is studied. The non-evanescent wave propagating in the multi-ion plasma is solved. The radiation impedance and power radiated by a space station and tethered systems in single and multi-ion species

plasma are estimated. The factors affecting power radiation are discussed. The organization of this thesis is as follows: in chapter 2, we follow the formulation in [3] and present a general theory on wave and power radiation by a conductor with AC current moving in a magnetized plasma. In chapter 3, the impedance and power radiation of a space station and tethered systems are estimated. The power radiation is studied as a function of environment, structure and AC current frequency and the inner relations are analysed. The design guidelines for large space structures are suggested from the radiation point of view. Chapter 4 contains a summary and conclusion.

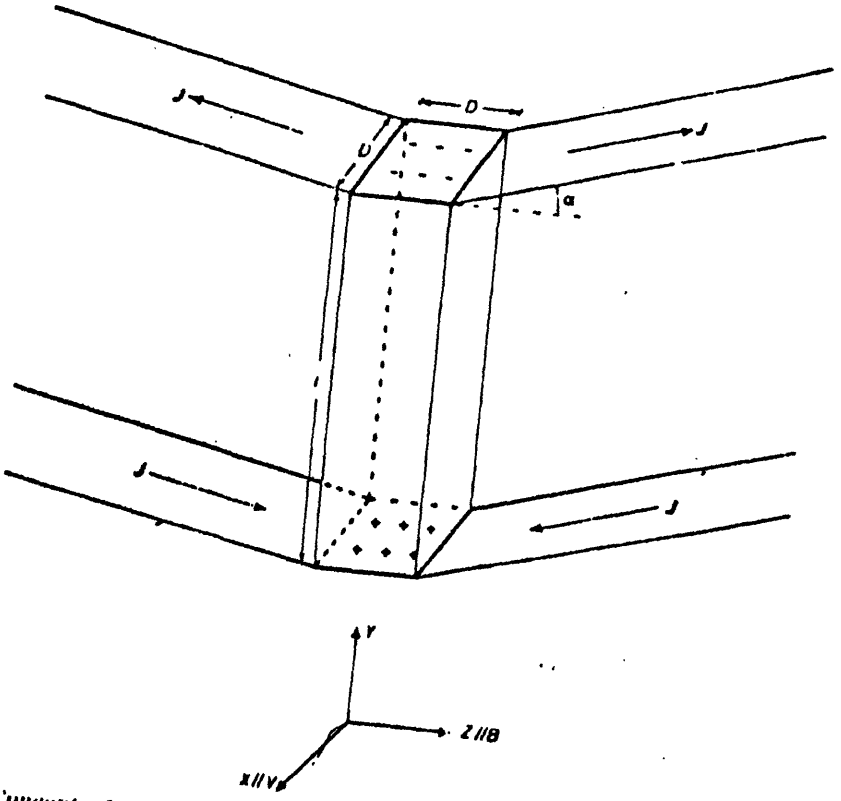

– Concept of Alfvén wings associated with the motion of a conductor through a magnetoplasma.

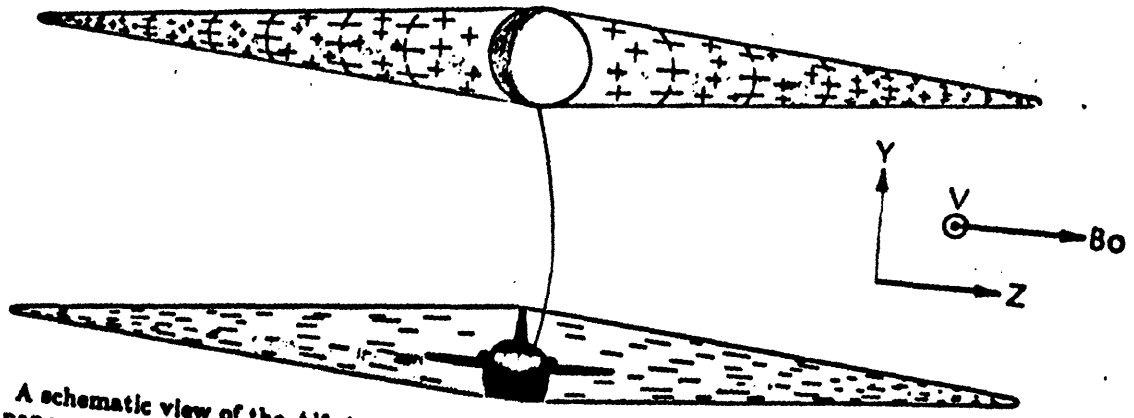

A schematic view of the Alfvén wings. In this figure the tethered system is moving out of the plane of the paper.

Figure 1.1: Illustration of the Alfven wings

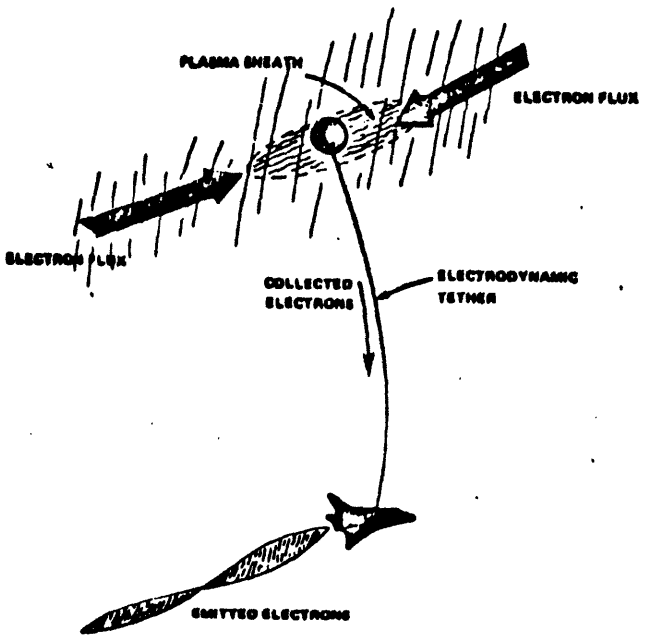

GENERAL CONCEPTUAL VIEW OF THE SHUTTLE ELECTRODYNAMIC TETHER SYSTEM.
A conducting tether 10–20 km long electrically connects a sub-satellite to the Orbiter. Owing to the motion of SETS across geomagnetic field lines, an emf is present which tends to collect electrons at the sub-satellite. Acuve electron emission from the Orbiter completes the circuit.

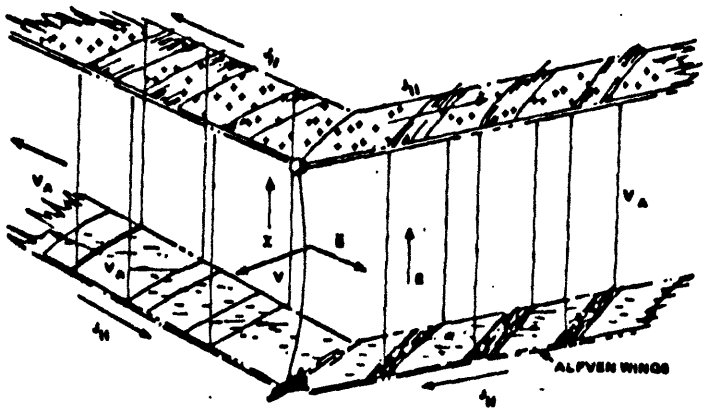

SCHEMATIC VIEW OF THE UPPER AND LOWER CURRENT SHEETS WHICH SPREAD OUTWARD ALONG MAGNETIC FIELD LINES FOLLOWING THE PASSAGE OF SETS.
The periodic darkened regions represent the outward propagation of low frequency Alfvén waves along $\vec{B}$. There is a net positive charge excess on the upper wing and net negative charge density on the lower wing. Currents along $\vec{B}$ are also shown.

Figure 1.2: Conceptual view of the shuttle tether system

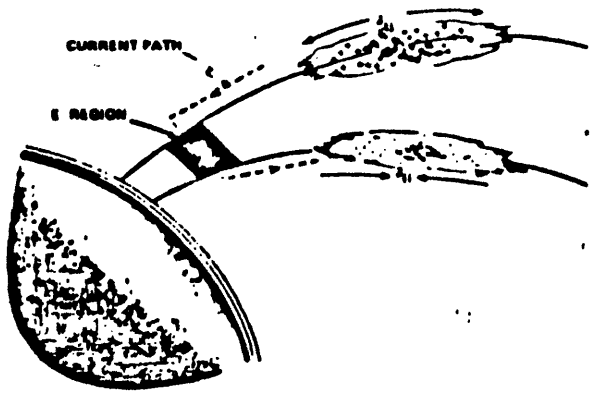

ILLUSTRATING THE REGIONS OF ELECTRICAL CHARGE IMBALANCE CREATED BY THE PASSAGE OF SETS.

These regions spread along the geomagnetic field until they reach the E-region where the transverse electrical resistivity becomes small.

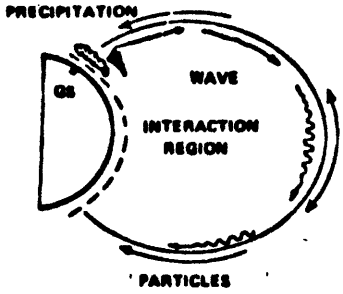

THE PROPAGATION OF VLF AND LOW FREQUENCY WAVES INTO THE MAGNETOSPHERE MAY LEAD TO RESONANT INTERACTIONS WITH GEOMAGNETICALLY TRAPPED ENERGETIC PARTICLES

As a consequence, precipitation of these particles into the atmosphere may occur.

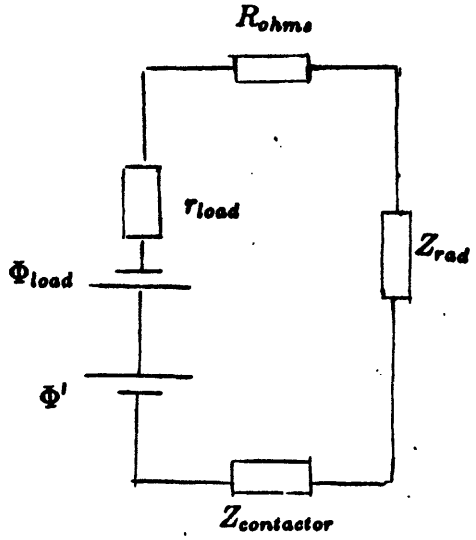

Figure 1.3: Illustration of the circuit composed of the space structure and the environment

Chapter 2

Theory of Plasma Wave Radiation by a Moving Conductor

2.1 Formulation of the Problem

We shall follow the same formulation used in [3][9]. Their formulation was composed of a closed set equations for a "cold" plasma in the linearized approximation and a stationary solution was found in the moving frame.

We start from the Maxwell equations in the rest frame of the ambient plasma.

$$\nabla \cdot \vec{E} = 4\pi\rho_e \tag{2.1}$$

$$\nabla \cdot \vec{B} = 0 \tag{2.2}$$

$$\nabla \times \vec{E} = -\frac{1}{c}\frac{\partial \vec{B}}{\partial t} \tag{2.3}$$

$$\nabla \times \vec{B} = \frac{4\pi}{c}\vec{J} + \frac{1}{c}\frac{\partial \vec{E}}{\partial t} \tag{2.4}$$

The current density $\vec{J}$ is expressed as

$$\vec{J} = \vec{J}_c(x,t)H(x,t) + \vec{J}_p(x,t)[1 - H(x,t)] \tag{2.5}$$

where $\vec{J_c}$ and $\vec{J_p}$ are the current densities in the conductor and in the plasma respectively and $H(x,t)$ is the step function defined as

$$H(x,t) = 1 \quad \textit{for points inside the conductor}$$

$$H(x,t) = 0 \quad \textit{for points outside the conductor}$$

In a frame fixed in the conductor, the current density and the electric field inside the conductor are related by Ohm's law

$$\vec{J'}_c(x') = \sigma \vec{E'}(x') \tag{2.6}$$

The wave equation is obtained from equation(2.3) and (2.4):

$$\nabla \times (\nabla \times \vec{E}) = -\frac{1}{c^2}[\frac{\partial^2 \vec{E}}{\partial t^2} + 4\pi \frac{\partial \vec{J}}{\partial t}] \tag{2.7}$$

In non-relativistic approximation, the field variables can be transfered to a moving frame fixed with the conductor by:

$$\vec{E'} = \vec{E} + \frac{1}{c}\vec{V} \times \vec{B}$$

$$\vec{J'} = \vec{J} - \rho_c \vec{V}$$

$$\rho'_c = \rho_c - \frac{1}{c^2}\vec{V} \cdot \vec{J}$$

$$\vec{B'} = \vec{B}$$

Since the surrounding plasma is a dispersive medium, we go to Fourier space. The four dimensional Fourier transformation is defined as:

$$F(\vec{k}, w) = \frac{1}{(2\pi)^2} \int e^{-i(\vec{k}\cdot\vec{x} - wt)} F(\vec{x}, t) d^3x dt \tag{2.8}$$

$$F(\vec{x},t) = \frac{1}{(2\pi)^2}\int e^{-i(\vec{k}\cdot\vec{x}-wt)}F(\vec{k},w)d^3kdtw \tag{2.9}$$

In Fourier space, wave equation (2.7) is expressed as

$$\vec{k}\times[\vec{k}\times\vec{E}(\vec{k},w)] + \frac{w^2}{c^2}\tilde{K}\vec{E}(\vec{k},w) = -4\pi\frac{iw}{c^2}\vec{J}_s(\vec{k},w) \tag{2.10}$$

where $\tilde{K}$ is the dielectric tensor and $\vec{J}_s(\vec{k},w)$ is the source current term. In ordinary space $\vec{J}_s(\vec{k},w)$ is expressed by:

$$\vec{J}_s(\vec{x},t) = (\vec{J}_c(\vec{x},t) - \vec{J}_p(\vec{x},t))H(\vec{x},t) \tag{2.11}$$

For an alternating current source on a space system moving perpendicular to the magnetic field with velocity $\vec{V}$, $\vec{J}(\vec{x},t)$ can be expressed as:

$$\vec{J}_s(\vec{x},t) = \begin{cases} \vec{J}_s(\vec{x})\cos(w^*t) & \vec{x}\ \textit{inside surface}\ F(\vec{x}_0+\vec{V}t)=0 \\ 0 & \vec{x}\ \textit{elsewhere} \end{cases} \tag{2.12}$$

where at time $t = 0$, the conductor surface is bounded by $F(\vec{x}_0) = 0$. Therefore $\vec{J}_s(\vec{k},w)$ takes the form [9]:

$$\vec{J}_s(\vec{k},w) = \sqrt{2\pi}\vec{j}_s(\vec{k})\frac{1}{2}[\delta(w+w^*-k_1V) + \delta(w-w^*-k_1V)] \tag{2.13}$$

where $\vec{j}_s(\vec{k})$ is the transform of $\vec{J}_s(\vec{x})$. For a known source current and known ambient plasma conditions, the field variables can be solved.

Equation (2.10) can be written as:

$$\tilde{T}\cdot\vec{E}(\vec{k},w) = -4\pi\frac{iw}{c^2}\vec{J}_s(\vec{k},w) \tag{2.14}$$

where $\tilde{T}$ is a tensor:

$$\tilde{T} = -k^2\tilde{I} + kk + \frac{w^2}{c^2}\tilde{K} \tag{2.15}$$

and $\tilde{I}$ is the identity matrix.

Therefore the field variables can be solved formally in Fourier space:

$$\vec{E}(\vec{k},w) = -\frac{4\pi i w}{c^2}\tilde{T}^{-1}\vec{J}_s(\vec{k},w) \tag{2.16}$$

$$\vec{B}(\vec{k},w) = \frac{c}{w}\vec{k}\times\vec{E}(\vec{k},w) \tag{2.17}$$

$$\rho_c(\vec{k},w) = \frac{i}{4\pi}\vec{k}\cdot\vec{E}(\vec{k},w) \tag{2.18}$$

$$\vec{J}_p(\vec{k},w) = -\frac{iw}{4\pi}(\tilde{K}-\tilde{I})\cdot\vec{E}(\vec{k},w) \tag{2.19}$$

These expressions can be transferred back to ordinary space by equation (2.8).

Since

$$\tilde{T}_{ij}^{-1} = C_{ij}^*/D_T \tag{2.20}$$

where D_T is the determinant of $\tilde{T}$ and C_{ij}'s are the cofactors of $\tilde{T}_{ij}$, the electric field in ordinary space is given by

$$E_i(\vec{x},t) = -\frac{i}{\pi c^2}\int \frac{w}{D_T}J_{sj}C_{ji}e^{i(\vec{k}\cdot\vec{x}-wt)}d^3k\,dw \tag{2.21}$$

It was pointed out in [9] that there are two modes or zeros of D_T and D_T can be written as:

$$D_T = p(k_\parallel^2 - \Lambda_1^2)(k_\parallel^2 - \Lambda_2^2) \tag{2.22}$$

where

$$\Lambda_1^2 = s - \frac{1}{2}k_\perp^2(1+\frac{s}{p}) + \frac{1}{2}\sqrt{\triangle} \tag{2.23}$$

$$\Lambda_2^2 = s - \frac{1}{2}k_\perp^2(1+\frac{s}{p}) - \frac{1}{2}\sqrt{\triangle} \tag{2.24}$$

$$\triangle = k_\perp^4(1-\frac{s}{p})^2 + \frac{4d^2}{\beta} \tag{2.25}$$

and

$$s = \frac{w^2}{c^2}S(w)$$

$$p = \frac{w^2}{c^2}P(w)$$

$$d = \frac{w^2}{c^2}D(w)$$

$$\beta = \frac{p}{p-k_\perp^2}$$

In the above expressions $k_\parallel$ is the wave vector component prepaller to $\vec{B}$, $k_\parallel = k_3$ and $k_\perp$ is the wave vector component perpendicular to $\vec{B}$, $k_\perp = \sqrt{k_1^2+k_2^2}$. The functions $S(w), P(w), D(w)$ come from the dielectric tensor of cold plasma [17]. The dielectric tensor can be obtained from the electric-flux-density vector [5]:

$$\vec{D}_e = \epsilon_0\vec{E} + \vec{P}_f =$$

$$\begin{pmatrix} 1+K_T & K_H & 0 \\ -K_H & 1+K_T & 0 \\ 0 & 0 & 1+K_L \end{pmatrix}\begin{pmatrix} E_x \\ E_y \\ E_z \end{pmatrix} = \begin{pmatrix} S & -iD & 0 \\ iD & S & 0 \\ 0 & 0 & P \end{pmatrix}\begin{pmatrix} E_x \\ E_y \\ E_z \end{pmatrix} \tag{2.26}$$

For a cold, multi-ionic plasma, we have[17][5]:

$$S(w) = 1 + \frac{w_{pe}^2}{\Omega_e^2 - w^2} + \sum_{k=1}^{N}\frac{w_{pik}^2}{\Omega_{ik}^2 - w^2} \tag{2.27}$$

$$P(w) = 1 - \frac{w_{pe}^2}{w^2} - \sum_{k=1}^{N} \frac{w_{pik}^2}{w^2} \tag{2.28}$$

$$D(w) = \frac{1}{w}[-\frac{w_{pe}^2 \Omega_e}{\Omega_e^2 - w^2} + \sum_{k=1}^{N} \frac{w_{pik}^2 \Omega_{ik}}{\Omega_{ik}^2 - w^2}] \tag{2.29}$$

where w_{pe} and w_{pik} are electronic angular plasma frequency and angular plasma frequencies for the k'th ion species respectively:

$$w_{pe}^2 = \frac{n_e q_e^2}{\epsilon_0 m_e} \tag{2.30}$$

$$w_{pik}^2 = \frac{n_k q_k^2}{\epsilon_0 m_k} \tag{2.31}$$

and Ω_e and Ω_{ik} are electronic gyrofrequency and ionic gyrofrequencies for the k'th species

$$\Omega_e = \left| \frac{q_e B_0}{m_e} \right| \tag{2.32}$$

$$\Omega_{ik} = \left| \frac{q_{ik} B_0}{m_k} \right| \tag{2.33}$$

The plasma frequency is given by $w_p^2 = w_{pe}^2 + \sum_k w_{pik}^2$.

For a single-ion plasma, $S(w)$,$P(w)$ and $D(w)$ can be simplified to

$$P(w) = 1 - \frac{w_p^2}{w^2} \tag{2.34}$$

$$S(w) = \frac{(w^2 - w_{lh}^2)(w^2 - w_{uh}^2)}{(w^2 - \Omega_i^2)(w^2 - \Omega_e^2)} \tag{2.35}$$

$$D(w) = -\frac{w w_p^2 \Omega_e^2}{(w^2 - \Omega_i^2)(w^2 - \Omega_e^2)} \tag{2.36}$$

where w_{lh} and w_{uh} are the lower and upper hybrid frequencies:

$$w_{lh}^2 \simeq \frac{w_p^2}{w_p^2 + \Omega_e^2} \Omega_i \Omega_e \tag{2.37}$$

$$w_{uh}^2 = \Omega_e^2 + w_p^2 \tag{2.38}$$

Since D_T can be written in the form of Eq(2.22) and the integrand is singular only at the zeros of D_T, one of the integrals in (2.21) can be evaluated by using Cauchy's Theorem. Equation(2.21) is integrated out as [9]:

$$\vec{E} = \vec{E}^{(1)} + \vec{E}^{(2)} \tag{2.39}$$

where

$$E^{(i)} = \int F^i e^{i\Psi^{(i)}} dk_1 dk_2 dw \tag{2.40}$$

$$\Psi^i = \Lambda_i x_\parallel + \vec{k}_\perp \cdot \vec{x}_\perp - wt \tag{2.41}$$

$$F^i = -\frac{\vec{q}_i \cdot \vec{j}_s}{c^2} \vec{q}_i \frac{w}{\beta \Lambda_i k_\perp^2} \alpha_i \tag{2.42}$$

$$\vec{q}_i = \vec{k}_\perp + (1-\beta)\vec{b}\Lambda_i + \delta_i(\vec{b} \times \vec{k}_\perp) \tag{2.43}$$

$$\alpha_i = \frac{-s + k_\perp^2 + \Lambda_i^2}{\Lambda_1^2 - \Lambda_2^2} \tag{2.44}$$

$$\delta_i = \frac{d}{\alpha_i \sqrt{\Delta}} \tag{2.45}$$

and the index i takes values 1 and 2.

For an alternating current source moving perpendicular to $\vec{B}$ field, $E^{(i)}$ is the sum of two terms, one for $w = k_1 V + w^*$ and the other for $w = k_1 V - w^*$. Therefore, the electric field can be written as:

$$\vec{E} = \vec{E}_+^{(1)} + \vec{E}_-^{(1)} + \vec{E}_+^{(2)} + \vec{E}_-^{(2)} \tag{2.46}$$

$$E_\pm^{(i)} = \int dk_1 dk_2 f_\pm^{(i)} exp(i\Psi_\pm^{(i)}) \tag{2.47}$$

where

$$\Psi_\pm^{(i)} = k_1(x_1 - Vt) + k_2 x_2 + k_3 x_3 \pm w^* t \tag{2.48}$$

$$k_1 = \frac{w \pm w^*}{V} \tag{2.49}$$

and

$$f_{\pm}^{(i)} = -\sqrt{\frac{\pi}{2}} \frac{w_{\pm}\alpha_i(\vec{q}_i \cdot \vec{j}_s)\vec{q}_i}{c^2\beta\Lambda_i k_{\perp}^2} \tag{2.50}$$

being evaluated at $w_{\pm} = k_1 V \pm w^*$.

Therefore eq(2.16)through eq(2.19) and eq(2.46) through eq(2.50) provide a formal solution of the field variables to the radiation problem. So the power radiated can be found by integrating the Poynting vector over an arbitary closed surface surrounding the conductor:

$$P_{rad} = \int \vec{S} \cdot \vec{n} dA \tag{2.51}$$

where

$$\vec{S}(\vec{x}, t) = \frac{c}{4\pi} \vec{E}(\vec{x}, t) \times \vec{B}(\vec{x}, t) \tag{2.52}$$

2.2 Radiation by Non-evanescent Waves

The field variables have been solved formally in the above section, but a self-consistant solution of $\vec{E}, \vec{B}$ and $\vec{J}_s$ is almost impossible to obtain because of the extremely complicated nature of these equations. In this section we are going to study only the far field of a known source current, while the determination of the source current pattern will be left to the next section and the near field won't be considered in this thesis.

2.2.1 Non-evanescent Waves

The electromagnetic waves are of the form $E(\vec{x},t) = E_0 e^{i(\vec{k}\cdot\vec{x}-wt)}$ and $B(\vec{x},t) = B_0 e^{i(\vec{k}\cdot\vec{x}-wt)}$, where $\vec{k} = (k_1, k_2, k_3)$ is the wave vector. Since we are only interested in the behaviour of the field far from the structure, the solutions for non-evanescent waves are those whose wave number $\vec{k}$ are always real. The plasma is a dispersive environment, so clearly we can obtain waves only at those frequencies for which the wave numbers are real. The relation between the wave vector $\vec{k}$ and the angular frequency w is restricted by the dispersion relation

$$D_T = 0 \tag{2.53}$$

As discussed in the above section, D_T can be written as:

$$D_T = \frac{w^2}{c^2} P(k_3^2 - \Lambda_1^2)(k_3^2 - \Lambda_2^2)$$

In the realistic situations of interest to us, we have

$$w_p^2 >> \Omega_e^2$$

$$V^2 << c_A << c^2$$

where V is the speed of conductor , c the speed of light and c_A is the Alfven speed:

$$c_A = \frac{B_0}{4\pi[\rho + (B_0^2/4\pi c^2)]^{1/2}}$$

Then Λ_1 and Λ_2 can be simplified to [3]

$$\Lambda_1^2 \simeq -\frac{S(w)}{P(w)}(k_\perp^2 - \frac{w^2}{c^2}P(w)) \tag{2.54}$$

$$\Lambda_2^2 \simeq -(k_\perp^2 - \frac{w^2}{c^2}S(w)) \tag{2.55}$$

The function $S(w)$ and $P(w)$ are defined in Eq(2.27) and Eq(2.28). Examing their behaviours, we can find:

1) in DC current case($w^* = 0$; $w = \vec{k} \cdot \vec{V}$), the frequency ranges for k_1, k_2, k_3 all real are given by solving:

$$S(w) > 0 \quad if \;\; w < w_p$$

$$S(w) < 0 \quad if \;\; w > w_p$$

and also let:

$$k_3 = \Lambda_1$$

Therefore, the non-evanescent waves can only have frequencies in the following seperated bands:

$$\begin{cases} band\ 1 & 0 < w < \Omega_{i1} \\ band\ 2 & w_{lh_1} < w < \Omega_{i2} \\ band\ 3 & w_{lh_2} < w < \Omega_{i2} \\ \cdots & \cdots \\ band\ N+1 & w_{lh_N} < w < \Omega_e \\ band\ N+2 & w_{pe} < w < w_{uh} \end{cases} \tag{2.56}$$

Where w_{lh_i}'s are the i'th roots of the equation:

$$S(w) = 1 + \frac{w_{pe}^2}{\Omega_e^2 - w^2} + \sum_{k=1}^{N} \frac{w_{pik}^2}{\Omega_{ik}^2 - w^2} = 0 \tag{2.57}$$

For a single ion plasma, the results reduce to that in [3]

$$0 < w < \Omega_i, w_{lh} < w < \Omega_e, w_p < w < w_{uh} \tag{2.58}$$

If we take into account the warm plasma effects, the $N+2$'th band $w_p < w < w_{uh}$ can not exist. So from now on we shall only consider radiation frequencies below Ω_e.

2) For AC current case, similarly we can find the same continuous bands described in Eq(2.56). But since

$$w = \pm w^* + \vec{k}_1 \cdot \vec{V} \tag{2.59}$$

where w^* is the angular frequency of AC current, there will be new narrow bands centered at w^* in addition to the continuous bands. A detailed analysis on radiation bands in a single ion plasma has been presented in [9]. Based on their analysis, it can be concluded that: the i=1 mode excites the above discussed continuous bands. In addition, if w^* is located inside the "continuous band" frequency regions expressed by eq(2.56) , then there will be line emissions of the $i = 2$ mode at $w = w^*$. If w^* is in the regions

$$\Omega_{ik} < w^* < w_{lh_k}, \quad k = 1, 2, \cdots, N$$

there will be line emissions by the $i = 1$ mode at $w = w^*$.

Sometimes we also need to know the phase velocity and group velocity. The phase velocity U_{ph} can be obtained from the dispersion relation.

Starting from the wave equation:

$$\vec{k} \times (\vec{k} \times \vec{E}) + \frac{w^2}{c^2} \tilde{K} \cdot \vec{E} = A_{ij} E_j$$

$$= \begin{bmatrix} S - n^2\cos^2\theta_p & -iD & n^2\cos\theta_p\sin\theta_p \\ iD & S^2 - n^2 & 0 \\ n^2\cos\theta_p\sin\theta_p & 0 & P - n^2\sin^2\theta_p \end{bmatrix} \begin{bmatrix} E_x \\ E_y \\ E_z \end{bmatrix} = 0 \qquad (2.60)$$

where θ_p is the angle between the $\vec{B}$ field and the wave vector $\vec{k}$.

So for a given wave frequency w and a propagation direction θ_p the refraction index n is determined by solving $Det(A_{ij}) = 0$, which leads to:

$$An^4 - Bn^2 + C = 0 \qquad (2.61)$$

where

$$A = P - (P - S)\sin^2\theta_p$$

$$B = -2PS + [S(P - S) - (iD)^2]\sin^2\theta_p$$

$$C = P(S^2 + (iD)^2)$$

and S, P and D are defined by eq(2.27),eq(2.28) and eq(2.29).

From eq(2.61), the refraction index is obtained:

$$n_\pm^2 = \frac{B \pm \sqrt{B^2 - 4AC}}{2A} \qquad (2.62)$$

and by definition, the phase velocity is given by

$$U_{ph} = \frac{w}{k} = \frac{c}{n} \qquad (2.63)$$

Equation (2.63) shows that: for a given w and a given θ_p, there are two wave modes propagating in a magnetoplasma. They have different refraction index n, so they propagate at different phase velocity:

$$U_{ph+} = \frac{c}{n_+} \ and \ U_{ph} = \frac{c}{n_-}$$

The energy radiated are carried by wave packages and the wave packages propagate in the speed and direction of the group velocity.

The group velocity is given by[5]

$$\vec{U}_g = (\frac{\partial w}{\partial k_x}, \frac{\partial w}{\partial k_y}, \frac{\partial w}{\partial k_z}) = \frac{\partial w}{\partial k_\perp}\hat{k}_\perp + \frac{\partial w}{\partial k_\parallel}\hat{k}_\parallel \tag{2.64}$$

Therefore

$$U_g = \sqrt{(\frac{\partial w}{\partial k_\perp})^2 + (\frac{\partial w}{\partial k_\parallel})^2} \tag{2.65}$$

and the direction is given by

$$\tan\theta_g = \tan\theta_p \frac{n^2[(S+P) - (P-S)\sin^2\theta] - PS - [S^2 + (iD)^2]}{n^2[2S - (P-S)\sin^2\theta] - 2SP} \tag{2.66}$$

For the wave radiated by a moving source, the constraint $w \pm w^* = \vec{k} \cdot \vec{V}$ implys that

$$U_p = V\cos\theta \tag{2.67}$$

where $\vec{V}$ is the velocity of the conductor and θ is the angle between $\vec{V}$ and $\vec{k}$. Hence, for waves with any w in the non-evanescent frequency bands and at any propagation direction, though there are two modes can be excited, only the mode with $U_p < V$ actually propagates to infinity. The waves with $U_p > V$ damp down quickly. Thus we can identify which mode carries the energy to infinity by comparing U_{p+}, U_{p-} with V.

In summary, the non-evanescent waves excited by a moving conductor are those with real wave vector (k_1, k_2, k_3). This condition can be satisfied only at several seperated frequency bands. At each w and θ, there are 2 wave modes

propagate with phase velocity U_{p+} and U_{p-}. The energy is carried to infinity by the mode with $U_p < V$.

2.2.2 Power Radiation

The power radiated is given by the Poynting's Theorem

$$P_{rad} = \int \vec{S} \cdot \vec{n} dA = \frac{c}{4\pi} \int (\vec{E} \times \vec{B}) \cdot \vec{n} dA$$

The integral surface is chosen to be a rectangular prism surrounding the conductor with surfaces $x_3 = \pm z_0, x_1 = \pm x_0, x_2 = \pm y_0$. For calculating the power radiated to infinity, we let x_0 and y_0 go to infinity, hence only the sufaces defined at $x_3 = \pm z_0$ contribute to the integral. Therefore

$$P_{rad} \simeq \frac{c}{4\pi} \int (\vec{E} \times \vec{B}) dA \mid_{x_3 = \pm z_0} = \frac{c}{2\pi} \int (E_1 B_2 - E_2 B_1) dx_1 dx_2 \mid_{x_3 = z_0} \qquad (2.68)$$

$\vec{E}(\vec{x}, t)$ and $\vec{B}(\vec{x}, t)$ have been solved in section 2.1. Using the obtained results, we get

$$P_{rad} = \frac{c}{2\pi} \int dx_1 dx_2 \left(\int \vec{E}(\vec{k}, w) e^{i(\vec{k} \cdot \vec{x} - wt)} d^3 k dw \right) \times \left(\int \frac{c}{w} \vec{k}' \times \vec{E}(\vec{k}', w') e^{i(\vec{k}' \cdot \vec{x} - w't)} d^3 k' dw' \right) \qquad (2.69)$$

After some algebra [9], the power radiated to infinity can be expressed as

$$P_{rad} = P_+^{(1)} + P_+^{(2)} + P_-^{(1)} + P_-^{(2)} \qquad (2.70)$$

where

$$P_{\pm}^{(i)} = \frac{\pi^2}{c^2}\int\int_{bands} \frac{w(\beta+\delta_i^2)\alpha_i^2\left|q_i\cdot j_i\right|^2}{k_\perp^2\Lambda_i\beta^2}dk_1dk_2 \tag{2.71}$$

and the integration is performed on the previously discussed non-evascant wave frequency bands(Eq(2.56)). Since the radiated power associated with the line emission is expected to be small [9], from now on we shall only concentrate on the continuous bands, which are excited by the $i = 1$ mode. Thus the total power radiated is approximately

$$P_{rad} \simeq P_+^{(1)} + P_-^{(1)} \tag{2.72}$$

$$= \frac{\pi^2}{c^2}\int\int_{bands}[\frac{w(\beta+\delta_1^2)\alpha_1^2\left|q_1\cdot\vec{j}_s\right|^2}{k_\perp^2\Lambda_1\beta^2}|_{k_1=\frac{w-w^*}{V}} + \frac{w(\beta+\delta_1^2)\alpha_1^2\left|q_1\cdot\vec{j}_s\right|^2}{k_\perp^2\Lambda_1\beta^2}|_{k_1=\frac{w+w^*}{V}}]dk_1dk_2 \tag{2.73}$$

Under the conditions

$$w_p^2 >> \Omega_e^2$$

and

$$V^2 << C_A << C^2$$

we have

$$\Lambda_1^2 \simeq -\frac{S}{P}(k_\perp^2 - \frac{w^2P}{c^2})$$

Also since $d \simeq 0$, we have

$$\alpha_1 = \frac{-S+k_\perp^2+\Lambda_1^2}{\Lambda_1^2-\Lambda_2^2} = \frac{-S+k_\perp^2-\frac{S}{P}(k_\perp^2-\frac{w^2P}{c^2})}{\sqrt{\triangle}}$$

$$\simeq \frac{-S+k_\perp^2-\frac{S}{P}(k_\perp^2-\frac{w^2P}{c^2})}{k_\perp^2(1-\frac{S}{P})} = 1 \tag{2.74}$$

and

$$\delta_1^2 = (\frac{d}{\alpha_1\sqrt{\triangle}})^2 \simeq 0 \tag{2.75}$$

Therefore

$$P_{\pm}^{(1)} \simeq \frac{(\pi)^2}{c^2}\int\int \frac{w\beta\left|\vec{q_1}\cdot\vec{j_s}\right|^2}{k_\perp^2\Lambda_1\beta^2}\mid_{k_1=\frac{w\pm w^*}{V}} dk_1dk_2$$

$$= \frac{\pi^2}{c^2}\int\int \frac{\left|\vec{q_1}\cdot\vec{j_s}\right|^2 w}{k_\perp^2\sqrt{-\frac{S}{P}(k_\perp^2-\frac{w^2P}{c^2})\beta}}\mid_{k_1=\frac{w\pm w^*}{V}} dk_1dk_2$$

$$= \int\int \left|\vec{q_1}\cdot\vec{j_s}\right|^2[\frac{\pi^2}{c}\frac{1}{k_\perp^2\sqrt{\beta S}}]\mid_{k_1=\frac{w\pm w^*}{V}} dk_1dk_2 \qquad (2.76)$$

Since we are considering the radiation by large structures in LEO and only the frequencies below Ω_e need to be considered in this limit , we have:

$$\left|\vec{q_1}\cdot\vec{j_s}\right| = \left|\vec{j_s}\cdot\vec{k}-\beta(\vec{j_s}\cdot\vec{b})\vec{b}+i\delta_1 j_s\cdot(\vec{b}\times\vec{k})\right|$$

$$\simeq \left|\vec{j_s}\cdot\vec{k}\right| \qquad (2.77)$$

where

$$j_s(x) = (j_c(x)-j_p(x))H(x)$$

Hence the total power radiated can be simplified to:

$$P_{red} \simeq \int\int \left|\vec{j_s}\cdot\vec{k}\right|^2[\frac{\pi^2}{c}\frac{1}{k_\perp^2\sqrt{\beta s}}]\mid_{k_1=\frac{w-w^*}{V}} + \left|\vec{j_s}\cdot\vec{k}\right|^2[\frac{\pi^2}{c}\frac{1}{k_\perp^2\sqrt{\beta s}}]\mid_{k_1=\frac{w+w^*}{V}} dk_1dk_2 \qquad (2.78)$$

Further assume that $j_p(x)$ is negligible compared to $j_c(x)$

$$j_s(x) \simeq j_c(x)H(x) \qquad (2.79)$$

and since by definition :

$$i\vec{j_s}(\vec{k})\cdot\vec{k} = (\frac{1}{2\pi})^{3/2}\int d^3x(\bigtriangledown\cdot\vec{j_s}(x))e^{-i\vec{k}\cdot\vec{x}}$$

$$= (\frac{1}{2\pi})^{3/2}\int d^3x[H\bigtriangledown\cdot\vec{j_c}+\vec{j_c}\cdot\bigtriangledown H]e^{-i\vec{k}\cdot\vec{x}} \qquad (2.80)$$

Since $\nabla \cdot \vec{j_c} = 0$ inside the conductor, we have:

$$\begin{aligned}\vec{j_s} \cdot \vec{k} &= \frac{1}{i}(\frac{1}{2\pi})^{3/2} \int (\vec{j_c} \cdot \nabla H) e^{-i\vec{k}\cdot\vec{x}} d^3x \\ &= \frac{1}{i}(\frac{1}{2\pi})^{3/2} \int j_{cn} \delta(\vec{x} - \vec{x}_s) e^{-i\vec{k}\cdot\vec{x}} d^3x \qquad (2.81) \\ &= \frac{1}{i}(\frac{1}{2\pi})^{3/2} \oint j_{cn} e^{-i\vec{k}\cdot\vec{x}} ds \qquad (2.82)\end{aligned}$$

where $\vec{x}_s$ is the boundary position—surface of conductor and j_{cn} is the normal componant of the current at boundary.

Therefore the total power radiated can be finally expressed as

$$P_{rad} = P^+ + P^- \qquad (2.83)$$

$$P^{\pm} = \int_{bands} dk_1 dk_2 Q[(\frac{1}{2\pi})^{3/2} \oint j_{cn} e^{-i\vec{k}\cdot\vec{x}} ds]^2 \mid_{k_1 = \frac{w \pm w^*}{V}} \qquad (2.84)$$

$$Q = \frac{\pi^2}{c} \frac{1}{k_\perp^2 \sqrt{\beta S(w)}} \qquad (2.85)$$

The integration in Equation (2.84) is performed on the bands expressed in equation (2.56).

Equation (2.84) can also be written in the form of [13]

$$P^{\pm} = \frac{1}{2\pi}^{3/2} \int \int J'_{cn}(\vec{x}_s) J_{cn}(\vec{x'}_s) w(\vec{x}_s - \vec{x'}_s) dA dA' \qquad (2.86)$$

where

$$w(\vec{\xi}) = \frac{1}{2\pi}^{3/2} \int d^3k e^{i\vec{\xi}\cdot\vec{k}} Q$$

and $\vec{x}_s$ are the boundary points where current flows in and $\vec{x'}_s$ are the boundary points where current flows out.

Equation (2.83) and equation (2.86) indicate that the details of the current flow pattern inside the conductor make no difference on the power radiation. The power radiated depends only on the current flow pattern at boundary and is affected by the coupled effects of the way current flows in and out.

To understand the physics inside, we can roughly explain this in the following way: the field variables $\vec{E}$ and $\vec{B}$ in plasma is the solutions of a set of inhomegenous differential-integral equations. Since the surrounding plasma is still approximately quasi-neutral, for w not too high, the inhomogeneity mainly comes from the boundary condition,i.e., the source current at conductor surface. By analogy to the Green's function theory, the solution of a general inhomogeneous equation

$$LU(x) - \lambda U(x) = f(x)$$

where L is a general operator, is

$$U = \int G(\vec{x}, \vec{x'}) f(\vec{x'}) d^3x' \tag{2.87}$$

where $G(\vec{x}, \vec{x'})$ is the Greens function and is the solution of

$$LG(\vec{x}, \vec{x'}) - \lambda G(\vec{x}, \vec{x'}) = \delta(\vec{x} - \vec{x'})$$

In general , $\vec{E}$ and $\vec{B}$ have similar functional forms as equation (2.87).

Since

$$P_{rad} = \frac{c}{4\pi} \int \vec{E} \times \vec{B} dS$$

P_{rad} also contains the functional form of (2.87) as indicated in (2.86), where $w(\vec{x}_{s1} - \vec{x}_{s2})$ serves as the "Greens function" and $J_{cn}(x_s), J'_{cn}(x_s)$ are the inhomogeneous term. This is the reason why P_{rad} depends on the current flow

pattern at the surface and is affected by the coupled eflect of the way current flows in and out the system. It should be noted that in Eq(2.84), though it seems only the conducting surface(where $j_{cn} \neq 0$) contributes to the integral, the insulated surface(where $j_{cn} = 0$) is of the same importance to the power radiated because it has the same functions of being the boundary condition.

Chapter 3
Radiation from Large Space Structures

3.1 Mathematical Model and Numerical Estimation

In chapter 2, we have presented the basic theory of wave and power radiation by a moving conductor in a magnetized plasma environment. In this chapter we shall apply those basic theories to study the wave and power radiation from large space structures .

3.1.1 Space Structure Model and Power Radiation Formula

The general power radiation by a conductor of arbitary geometry is determinted by:

$$P_{rad} = P^+ + P^- \tag{3.1}$$

$$P^{\pm} = \int_{bands} dk_1 dk_2 Q(\tfrac{1}{2\pi})^{3/2} \left|\vec{j}\cdot\vec{k}\right|^2 |_{k_1} = \tfrac{w \pm w^*}{V} \tag{3.2}$$

$$Q = \frac{\pi^2}{c}\frac{1}{k_\perp^2\sqrt{\beta S(w)}} \tag{3.3}$$

To simulate large space structures such as the proposed space station and shuttle-tether system, we establish a generalized box structure model: a straight oblong main body with two box like terminators . (see Fig 3.1) A typical space station with solar arrays can be simulated by taking $L_{22} \sim 100m$, $L_{21} \sim 80m$, $d_{12} \sim 20m$ and $d_{11} \sim d_{31} \sim 5m$. A typical shuttle-tether: a 10 km tether with space shuttle at one end and a satellite at the other can be simulated by taking $L_{21} = 10\ km$, $d_{11} \sim d_{31} \sim 1mm$, and $d_{12} \sim d_{32} \sim 10m$.

We shall consider the structure always moving perpendicular to the magnetic field. The reference frame fixed with the space structure is taken to be $\vec{x}_3$ in $\vec{B}$ direction, $\vec{x}_1$ in the structure velocity $\vec{V}$ direction and the $\vec{x}_2$ along $\vec{V} \times \vec{B}$ direction. The coordinate axes are placed in accord with the symmetry axes of the box structure.

Since the induced field is $\vec{E}' \sim \vec{V} \times \vec{B}$ and the structure is also oriented along the $\vec{V} \times \vec{B}$direction, the macroscopic motion of electrons inside the conductor is in the $\vec{x}_2$ direction. We take the side surfaces of the middle box to be insulated, thus electric current flows in and out the system only through the conducting surfaces of the two terminators (surface 1,2,3,4, as marked in Fig 3.1). Further the normal boundary current component J_n at each surface are assumed to be uniform. Of course for a real box structure, the boundary current pattern may not be like this way, especially at those edges. Since the box structure is an abstracted object and our purpose is to simulate the effect of different boundary current components, the above established model is considered very satisfactory.

Having established the space structure geometry, the boundary current pat-

tern and the reference frame, now we are able to derive the power radiation formula for our box structure.

1) The simplest case: an oblong body with current I_t (current density $J_t = I_t/A_t$)flowing in and out only in the $\vec{x}_2$ direction at the two end surfaces (A_t, A_t'), we have

$$|\vec{j_s} \cdot \vec{k}| = \frac{2J_t}{(2\pi)^{3/2}} \frac{\sin(k_1 d_{11}/2)}{k_1/2} \frac{\sin(k_3 d_{31}/2)}{k_3/2} sin(k_2 L_{22}/2)$$
$$= \frac{I_t}{A_t} \frac{2}{(2\pi)^{3/2}} [(d_{11} d_{31} \frac{\sin(k_1 d_{11}/2)}{k_1 d_{11}/2} \frac{\sin(k_3 d_{31}/2)}{k_3 d_{31}/2} \sin(k_2 L_{22}/2)] \quad (3.4)$$

So the power radiated is

$$P_r = P_r^+ + P_r^- = J_t^2 S_t = I_t^2 Z_t \quad (3.5)$$

Where the radiation impedance is

$$Z_t = Z_t^+ + Z_t^-$$

$$Z_t^{\pm} = Z_0 \frac{c}{c_A} \frac{1}{(d_{11} d_{31})^2} \int_{band} \frac{2}{(2\pi)^{3/2}} (d_{11} d_{31} \frac{\sin(k_1 d_{11}/2)}{k_1 d_{11}/2})^2 \frac{1}{\sqrt{S(w)}} \frac{L_{22} dw}{V} [f_4(0) - f_4(1)] \quad (3.6)$$

and $Z_t^{\pm}$ are evaluated at $k_1 = \frac{w \pm w^*}{V}$. This formula can be applied to calculate the power radiation from a tether or a space station without solar array.

2) For the box structure, generally current can flow in and out through every surface of the two terminators (see Fig 3.1): I_2 through surface A_2, A_2', I_1 through A_1, A_1', I_3 through A_3, A_3' and I_4 through A_4, A_4'.

So the total current flowing through the system is:

$$I_{tot} = I_2 + I_4 + 2I_1 + 2I_3$$

and the conducting area is:

$$A_a = A'_a = A_2 + A_4 + 2A_1 + 2A_3$$

where

$$A_t = d_{11}d_{31}, \quad A_2 = d_{12}d_{32}, \quad A_4 = A_2 - A_t$$

$$A_3 = d_{12}(L_{22} - L_{21})/2, \quad A_1 = d_{32}(L_{22} - L_{21})/2$$

The current densities at each surface are given by

$$J_1 = I_1/A_1, \;\; J_2 = I_2/A_2, \;\; J_3 = I_3/A_3, \;\; J_4 = I_4/A_4.$$

After some algebra(see Appendix), we have

$$\begin{aligned}
|\vec{j_s} \cdot \vec{k}| = \tfrac{2}{(2\pi)^{3/2}} \{ \tfrac{I_2}{A_2} [(d_{12}d_{32} \tfrac{\sin(k_1 d_{12}/2)}{k_1 d_{12}/2} \tfrac{\sin(k_3 d_{32}/2)}{k_3 d_{32}/2} \\
\sin(k_2 L_{22}/2)] + \tfrac{I_4}{A_4} [(d_{12}d_{32}) \tfrac{\sin(k_1 d_{12}/2)}{k_1 d_{12}/2} \tfrac{\sin(k_3 d_{32}/2)}{k_3 d_{32}/2} \\
-(d_{11}d_{31}) \tfrac{\sin(k_1 d_{11}/2)}{k_1 d_{11}/2} \tfrac{\sin(k_3 d_{31}/2)}{k_3 d_{31}/2}] \sin(k_2 L_{21}/2)] \\
+ \tfrac{I_1}{A_1} [2d_{32} \tfrac{(L_{22}-L_{21})}{2}] [\tfrac{\sin(k_2(L_{22}-L_{21})/4)}{k_2(L_{22}-L_{21})/4} \\
\cos(k_1 d_{12}/2) \tfrac{\sin(k_3 d_{32}/2)}{k_3 d_{32}/2} \sin k_2(L_{22} + L_{21})/4 \\
+ \tfrac{I_3}{A_3} [2d_{12} \tfrac{(L_{22}-L_{21})}{2}] [\tfrac{\sin(k_2(L_{22}-L_{21})/4)}{k_2(L_{22}-L_{21})/4} \\
\cos(k_3 d_{32}/2) \tfrac{\sin(k_1 d_{12}/2)}{k_1 d_{12}/2} \sin k_2(L_{22} + L_{21})/4 \}
\end{aligned} \tag{3.7}$$

If we further assume that the boundary current densities at each direction are the same,

$$J_1 = J_2 = J_3 = J_4 = J_a$$

then

$$|\vec{j_s} \cdot \vec{k}| = \tfrac{2}{(2\pi)^{3/2}} J_a \{ [(d_{12}d_{32} \tfrac{\sin(k_1 d_{12}/2)}{k_1 d_{12}/2} \tfrac{\sin(k_3 d_{32}/2)}{k_3 d_{32}/2} \sin(k_2 L_{22}/2)]$$

$$+[(d_{12}d_{32})\frac{\sin(k_1d_{12}/2)}{k_1d_{12}/2}\frac{\sin(k_3d_{32}/2)}{k_3d_{32}/2}-(d_{11}d_{31})\frac{\sin(k_1d_{11}/2)}{k_1d_{11}/2}\frac{\sin(k_3d_{31}/2)}{k_3d_{31}/2}]\sin(k_2L_{21}/2)]$$

$$+[2d_{32}\frac{(L_{22}-L_{21})}{2}][\frac{\sin k_2(L_{22}-L_{21})/4}{k_2(L_{22}-L_{21})/4}$$

$$\cos(k_1d_{12}/2)\frac{\sin(k_3d_{32}/2)}{k_3d_{32}/2}\sin k_2(L_{22}+L_{21})/4]$$

$$+[2d_{12}\frac{(L_{22}-L_{21})}{2}][\frac{\sin k_2(L_{22}-L_{21})/4}{k_2(L_{22}-L_{21})/4}$$

$$\cos(k_3d_{32}/2)\frac{\sin(k_1d_{12}/2)}{k_1d_{12}/2}\sin k_2(L_{22}+L_{21})/4\} \tag{3.8}$$

So the power radiation formula becomes:

$$P_r = P_r^+ + P_r^- = J_a^2 S_a = I_a^2 Z_a \tag{3.9}$$

and the impedance is:

$$Z_a = Z_a^+ + Z_a^-$$

$$Z_a^{\pm} = Z_0\frac{c}{c_A}\int(\frac{2}{(2\pi)^{3/2}}\frac{1}{\sqrt{S(w)}}\frac{L_{22}dw}{V}$$

$$[d_{12}d_{32}\frac{\sin(k_1d_{12}/2)}{k_1d_{12}/2}]^2[f_2(0)-f_2(1)]$$

$$+[d_{12}d_{32}\frac{\sin(k_1d_{12}/2)}{k_1d_{12}/2}]^2[f_2(0)-f_2(L_{21}/L_{22})]$$

$$+[2d_{32}\frac{(L_{22}-L_{21})}{2}\cos(k_1d_{12}/2)]^2[f_1(0)-f_1(\frac{1+L_{21}/L_{22}}{2})]$$

$$+[2d_{12}\frac{(L_{22}-L_{21})}{2}\frac{\sin(k_1d_{12}/2)}{k_1d_{12}/2}]^2[f_3(0)-f_3(\frac{1+L_{21}/L_{22}}{2})]$$

$$+2[(d_{12}d_{32}\frac{\sin(k_1d_{12}/2)}{k_1d_{12}/2}]^2[f_2(\frac{1-L_{21}/L_{22}}{2})-f_2(\frac{1+L_{21}/L_{22}}{2})]$$

$$+2[d_{12}d_{32}\frac{\sin(k_1d_{12}/2)}{k_1d_{12}/2}][2d_{32}\frac{(L_{22}-L_{21})}{2}\cos(k_1d_{12}/2)]^2$$

$$[f_{21}(\frac{1-L_{21}/L_{22}}{4})-f_{21}(\frac{3+L_{21}/L_{22}}{4})]$$

$$+2[d_{12}d_{32}\frac{\sin(k_1d_{12}/2)}{k_1d_{12}/2}][2d_{12}\frac{(L_{22}-L_{21})}{2}\frac{\sin(k_1d_{12}/2)}{k_1d_{12}/2}]$$

$$[f_{23}(\frac{1-L_{21}/L_{22}}{4})-f_{23}(\frac{3+L_{21}/L_{22}}{4})]$$

$$+2[d_{12}d_{32}\frac{\sin(k_1d_{12}/2)}{k_1d_{12}/2}][2d_{32}\frac{(L_{22}-L_{21})}{2}\cos(k_1d_{12}/2)]$$

$$[f_{21}(\frac{1-L_{21}/L_{22}}{4})-f_{21}(\frac{1+3L_{21}/L_{22}}{4})]$$

$$+2[d_{12}d_{32}\frac{\sin(k_1d_{12}/2)}{k_1d_{12}/2}][2d_{12}\frac{(L_{22}-L_{21})}{2}\frac{\sin(k_1d_{12}/2)}{k_1d_{12}/2}]$$

$$
\begin{aligned}
&[f_{23}(\tfrac{1-L_{21}/L_{22}}{4}) - f_{23}(\tfrac{1+3L_{21}/L_{22}}{4})] \\
&+2[2d_{32}\tfrac{(L_{22}-L_{21})}{2}\cos(k_1 d_{12}/2)][2d_{12}\tfrac{(L_{22}-L_{21})}{2}\tfrac{\sin(k_1 d_{12}/2)}{k_1 d_{12}/2}] \\
&[f_{13}(0) - f_{13}(\tfrac{1+L_{21}/L_{22}}{2})] \\
&+[d_{11}d_{31}\tfrac{\sin(k_1 d_{11}/2)}{k_1 d_{11}/2}]^2[f_4(0) - f_4(L_{21}/L_{22})] \\
&-2[d_{11}d_{31}\tfrac{\sin(k_1 d_{11}/2)}{k_1 d_{11}/2}][d_{12}d_{32}\tfrac{\sin(k_1 d_{12}/2)}{k_1 d_{12}/2}] \\
&[f_{42}(\tfrac{1-L_{21}/L_{22}}{2}) - f_{42}(\tfrac{1+L_{21}/L_{22}}{2})] \\
&-2[d_{11}d_{31}\tfrac{\sin(k_1 d_{11}/2)}{k_1 d_{11}/2}][d_{12}d_{32}\tfrac{\sin(k_1 d_{12}/2)}{k_1 d_{12}/2}] \\
&[f_{42}(0) - f_{42}(L_{21}/L_{22})] \\
&-2[d_{11}d_{31}\tfrac{\sin(k_1 d_{11}/2)}{k_1 d_{11}/2}][2d_{32}\tfrac{(L_{22}-L_{21})}{2}\cos(k_1 d_{12}/2)] \\
&[f_{41}(\tfrac{1-L_{21}/L_{22}}{4}) - f_{41}(\tfrac{1+3L_{21}/L_{22}}{4})] \\
&-2[d_{11}d_{31}\tfrac{\sin(k_1 d_{11}/2)}{k_1 d_{11}/2}][2d_{12}\tfrac{(L_{22}-L_{21})}{2}\tfrac{\sin(k_1 d_{12}/2)}{k_1 d_{12}/2}] \\
&[f_{43}(\tfrac{1-L_{21}/L_{22}}{4}) - f_{43}(\tfrac{1+3L_{21}/L_{22}}{4})] \qquad (3.10)
\end{aligned}
$$

This formula can be applied to calculate the power radiation by a tethered system or a space station with current flowing in and out the system through the conducting end connectors or solar arrays.

In the above expressions, the functions f_1,f_2,etc, are Fourier cosine transformations and they are given by:

$$f_1(x) = \int_0^\infty d\bar{k}_2 \cos(\bar{k}_2 x)\left\{\frac{\sin(k_3 d_{32}/2)}{k_3 d_{32}/2}\frac{\sin(\frac{k_2(L_{22}-L_{21})}{4})}{\frac{k_2(L_{22}-L_{21})}{4}}Q\right\}$$

$$f_2(x) = \int_0^\infty d\bar{k}_2 \cos(\bar{k}_2 x)\left\{[\frac{\sin(k_3 d_{32}/2)}{k_3 d_{32}/2}]^2 Q\right\}$$

$$f_3(x) = \int_0^\infty d\bar{k}_2 \cos(\bar{k}_2 x) \left\{ \cos(k_3 d_{32}/2) \frac{\sin(\frac{k_2(L_{22}-L_{21})}{4})}{\frac{k_2(L_{22}-L_{21})}{4}} Q \right\}$$

$$f_4(x) = \int_0^\infty d\bar{k}_2 \cos(\bar{k}_2 x) \left\{ [\frac{\sin(k_3 d_{31}/2)}{k_3 d_{31}/2}]^2 Q \right\}$$

$$f_{21}(x) = \int_0^\infty d\bar{k}_2 \cos(\bar{k}_2 x) \left\{ [\frac{\sin(k_3 d_{32}/2)}{k_3 d_{32}/2}]^2 \frac{\sin(\frac{k_2(L_{22}-L_{21})}{4})}{\frac{k_2(L_{22}-L_{21})}{4}} Q \right\}$$

$$f_{23}(x) = \int_0^\infty d\bar{k}_2 \cos(\bar{k}_2 x) \left\{ \frac{\sin(k_3 d_{32}/2)}{k_3 d_{32}/2} \cos(k_3 d_{32}/2) \frac{\sin(\frac{k_2(L_{22}-L_{21})}{4})}{\frac{k_2(L_{22}-L_{21})}{4}} Q \right\}$$

$$f_{13}(x) = \int_0^\infty d\bar{k}_2 \cos(\bar{k}_2 x) \left\{ \frac{\sin(k_3 d_{32}/2)}{k_3 d_{32}/2} [\frac{\sin(\frac{k_2(L_{22}-L_{21})}{4})}{\frac{k_2(L_{22}-L_{21})}{4}}]^2 \cos(k_3 d_{32}/2) Q \right\}$$

$$f_{41}(x) = \int_0^\infty d\bar{k}_2 \cos(\bar{k}_2 x) \left\{ \frac{\sin(k_3 d_{32}/2)}{k_3 d_{32}/2} \frac{\sin(\frac{k_2(L_{22}-L_{21})}{4})}{\frac{k_2(L_{22}-L_{21})}{4}} \frac{\sin(k_3 d_{31}/2)}{k_3 d_{31}/2} Q \right\}$$

$$f_{42}(x) = \int_0^\infty d\bar{k}_2 \cos(\bar{k}_2 x) \left\{ \frac{\sin(k_3 d_{32}/2)}{k_3 d_{32}/2} \frac{\sin(k_3 d_{31}/2)}{k_3 d_{31}/2} Q \right\}$$

$$f_{43}(x) = \int_0^\infty d\bar{k}_2 \cos(\bar{k}_2 x) \left\{ \frac{\sin(\frac{k_2(L_{22}-L_{21})}{4})}{\frac{k_2(L_{22}-L_{21})}{4}} \frac{\sin(k_3 d_{31}/2)}{k_3 d_{31}/2} \cos(k_3 d_{32}/2) Q \right\}$$

where $\bar{k}_2 = k_2 L_{22}$.

3) We can also insulate part of the terminators to force the current flow through certain surfaces. Listed in the following are several interesting cases which we shall discuss later.

3.a)For a box structure with current I_2 flowing in and out surfaces A_2 and A_2' (other surfaces are insulated):

$$|\vec{j_s} \cdot \vec{k}| = \frac{I_2}{A_2} \frac{2}{(2\pi)^{3/2}} [d_{12} d_{32} \frac{\sin(k_1 d_{12}/2)}{k_1 d_{12}/2} \frac{\sin(k_3 d_{32}/2)}{k_3 d_{32}/2} \sin(k_2 L_{22}/2)] \qquad (3.11)$$

So the power radiated:

$$P_r = J_2^2 S_2 = I_2^2 Z_2.$$

the radiation impedance:

$$Z_2 = Z_2^+ + Z_2^-$$

$$Z_2^{\pm} = Z_0 \frac{c}{c_A} \frac{1}{(d_{12}d_{32})^2} \int \frac{2}{(2\pi)^{3/2}} (d_{12}d_{32} \frac{\sin(k_1 d_{12}/2)}{k_1 d_{12}/2})^2 \frac{1}{\sqrt{S(w)}} \frac{L_{22}dw}{V} [f_2(0) - f_2(1)] \tag{3.12}$$

3.b) For a box structure with current I_4 flowing in and out only through surfaces A_4 and A_4':

$$\begin{aligned} |\vec{j_s} \cdot \vec{k}| &= \frac{2J_4}{(2\pi)^{3/2}} [\frac{\sin(k_1 d_{12}/2)}{k_1/2} \frac{\sin(k_3 d_{32}/2)}{k_3/2} \\ &\quad - \frac{\sin(k_1 d_{11}/2)}{k_1/2} \frac{\sin(k_3 d_{31}/2)}{k_3/2}] \sin(k_2 L_{21}/2)] \\ &= \frac{2}{(2\pi)^{3/2}} \frac{I_4}{A_4} [(d_{12}d_{32}) \frac{\sin(k_1 d_{12}/2)}{k_1 d_{12}/2} \frac{\sin(k_3 d_{32}/2)}{k_3 d_{32}/2} \\ &\quad -(d_{11}d_{31}) \frac{\sin(k_1 d_{11}/2)}{k_1 d_{11}/2} \frac{\sin(k_3 d_{31}/2)}{k_3 d_{31}/2}] \sin(k_2 L_{21}/2)] \end{aligned} \tag{3.13}$$

The power radiation:

$$P_r = J_4^2 S_4 = I_4^2 Z_4.$$

the radiation impedance:

$$Z_4 = Z_4^+ + Z_4^-$$

$$\begin{aligned} Z_4^{\pm} &= Z_0 \tfrac{c}{c_A} \tfrac{1}{A_4} \int (\tfrac{2}{(2\pi)^{3/2}} \tfrac{1}{\sqrt{S(w)}} \tfrac{L_{22}dw}{V} \\ &\{(d_{12}d_{32} \tfrac{\sin(k_1 d_{12}/2)}{k_1 d_{12}/2})^2 [f_2(0) - f_2(L_{21}/L_{22})] + (d_{11}d_{31} \tfrac{\sin(k_1 d_{11}/2)}{k_1 d_{11}/2})^2 [f_4(0) - f_4(L_{21}/L_{22})] \\ &\quad -2(d_{12}d_{32} \tfrac{\sin(k_1 d_{12}/2)}{k_1 d_{12}/2})(d_{11}d_{31} \tfrac{\sin(k_1 d_{11}/2)}{k_1 d_{11}/2}) [f_{42}(0) - f_{42}(L_{21}/L_{22})]\} \end{aligned} \tag{3.14}$$

3.c) For a box structure with current I_1 flowing in and out only through surfaces A_1 and A_1' in the $\vec{x}_1$ direction:

$$|\vec{j_s} \cdot \vec{k}| = \frac{2J_1}{(2\pi)^{3/2}} \cos(k_1 d_{12}/2) \frac{\sin(k_3 d_{32}/2)}{k_3/2}$$

$$\frac{2\sin(k_2(L_{22}-L_{21})/4)}{k_2/2}\sin(k_2(L_{22}+L_{21})/4)$$

$$= \frac{I_1}{A_1}\frac{2}{(2\pi)^{3/2}}[2d_{32}\frac{(L_{22}-L_{21})}{2}][\frac{\sin(k_2(L_{22}-L_{21})/4)}{k_2(L_{22}-L_{21})/4}]$$

$$\cos(k_1 d_{12}/2)\frac{\sin(k_3 d_{32}/2)}{k_3 d_{32}/2}\sin(k_2(L_{22}+L_{21})/4) \tag{3.15}$$

the power radiation:

$$P_r = J_1^2 S_1 = I_1^2 Z_1.$$

the radiation impedance:

$$Z_1 = Z_1^+ + Z_1^-$$

$$Z_1^{\pm} = Z_0\frac{c}{c_A}\int \frac{2}{(2\pi)^{3/2}}\frac{1}{\sqrt{S(w)}}\frac{L_{22}dw}{V}$$

$$(\frac{1}{2d_{32}(L_{22}-L_{21})/2}\cos(k_1 d_{12}/2))^2[f_1(0) - f_1(\frac{1+L_{21}/L_{22}}{2})] \tag{3.16}$$

3.d) For a box structure with current I_3 flowing in and out only through surfaces A_3 and A_3' in the $\vec{x}_3$ direction:

$$|\vec{j_s}\cdot\vec{k}| = \frac{2J_3}{(2\pi)^{3/2}}\cos(k_3 d_{32}/2)\frac{\sin(k_1 d_{12}/2)}{k_1/2}$$

$$\frac{2\sin(k_2(L_{22}-L_{21})/4)}{k_2/2}\sin(k_2(L_{22}+L_{21})/4)$$

$$= \frac{I_3}{A_3}\frac{2}{(2\pi)^{3/2}}[2d_{12}\frac{(L_{22}-L_{21})}{2}][\frac{\sin k_2(L_{22}-L_{21})/4}{k_2(L_{22}-L_{21})/4}]$$

$$\cos(k_3 d_{32}/2)\frac{\sin(k_1 d_{12}/2)}{k_1 d_{12}/2}\sin(k_2(L_{22}+L_{21})/4) \tag{3.17}$$

So the power radiation is:

$$P_r = J_3^2 S_3 = I_3^2 Z_3.$$

and the radiation impedance:

$$Z_3 = Z_3^+ + Z_3^-$$

$$Z_3^{\pm} = Z_0 \frac{c}{c_A} \int \frac{2}{(2\pi)^{3/2}} \frac{1}{\sqrt{S(w)}} \frac{L_{22} dw}{V}$$
$$(\frac{1}{2d_{12}(L_{22}-L_{21})/2} \frac{\sin(k_1 d_{12}/2)}{k_1 d_{12}/2})^2 [f_3(0) - f_3(\frac{1+L_{21}/L_{22}}{2})] \quad (3.18)$$

To determine the value of the power radiated, we need to know the value of the total current I. The power can be radiated actively or passively so the current is determined by the practical purpose of the space structure.

1) Active state , such as a tethered system used for communication. The current is driven into the system actively by an external source. Then in equation

$$P_r = I^2 Z_r \quad (3.19)$$

$$I = \frac{\Phi - \Phi'}{Z_r + R} \quad (3.20)$$

I is detremined by the practical purpose and is a given parameter in equation (3.19). We desire the P_r as large as possible in order to achieve a higher signal radiation. In this case, a larger Z_r corresponds to a large P_r.

2)Passive state, such as the space station case. The current I is driven into the system by the induced field $\vec{E}' \sim \vec{V} \times \vec{B}$. Therefore

$$P_r = (\frac{\Phi'}{Z_r + R})^2 Z_r \quad (3.21)$$

and

$$I = \frac{\Phi'}{Z_r + R} \quad (3.22)$$

where $\Phi' \sim VBL$ and R is the sum of contactor impedance and Ohmic resistence. In this case, the power radiated is the energy loss so we want P_r as small as possible.

It is easy to see from equation (3.21) that

$$\frac{dP_r}{dz} = \Phi^2 \frac{(R - Z_r)}{(Z_r + R)^3}$$

$$\frac{d^2P_r}{dz^2} = -\frac{\Phi^2}{(Z_r + R)^3}[1 + \frac{3(Z_r - R)}{Z_r + R}]$$

so the power loss is maximum when $Z_r \sim R$. ($\frac{dP_r}{dz} \mid_{Z_r=R} = 0$, $\frac{d^2P_r}{dz^2} \mid_{Z_r=R} < 0$). Therefore if we want a smaller power loss, the value of impedance Z_r is desired to be far away from R.

A comment should be addressed here. Either using I as a given parameter for active case or determining I from eq(3.22) for passive case when we calculate the power radiation, we actually already assume that I satisfies the continuity requirement at the conductor surface

$$I = \int_{boundary} J_n dS \tag{3.23}$$

However, since the continuity is limited by the "collecting ability" of the interface, there may be a limit on the maximum current density $(J_n)_{max}$ that can be collected by the conductor. Thus, if we made a potential difference so large that it could drive a total current $I > \int (J_n)_{max} dS$, then the total current is determined only by

$$I = I_{max} = \int J_{max} ds$$

and there will be net charge accumulated at the two ends. This is a more complicated case and more knowledge of the contactor physics is required to solve this problem. In this thesis, we shall assume that equation(3.23) is always satisfied.

3.1.2 Numerical Estimation

The wave radiation and power radiation are determined numerically. First we have to determine the frequencies of the non-evanescant waves. As discussed in chapter 2, the frequencies can only exist in a few separated bands for continuous radiation. The radiation bands are determined from the regions

$$S(w) > 0 \qquad when \;\; w < w_p \tag{3.24}$$

$$S(w) < 0 \qquad when \;\; w > w_p \tag{3.25}$$

For a single ion species plasma, the radiation band can be determined as $0 - \Omega_i$, $w_{lh} - \Omega_e$ and $w_p - w_{uh}$ where Ω_i,Ω_e,w_{lh}, w_p and w_{uh} are ion and electron cyclotron frequencies, the lower hybrid frequency, the electron plasma frequency and the upper hybrid frequency. Taking into account the warm plasma effect, the third band can not exist. So we only consider $w < w_p$ frequencies. For a multi-ion species plasma, the $S(w) > 0$ range can be determined by solving the equation

$$S(w) = 1 - \frac{w_{pe}^2}{\Omega_e^2 - w^2} + \sum_{k=1}^{N} \frac{w_{pik}^2}{\Omega_{ik}^2 - w^2} = 0 \tag{3.26}$$

numerically and there are $N + 1$ radiation bands given by $0 - \Omega_{i1}$,$w_{lh1} - \Omega_{i2}$, $w_{lh2} - \Omega_{i3}$,...$w_{lhn} - \Omega_e$ (see Eq(2.56)).

We can estimate the power radiated by intergrating over those frequency bands. The integral is performed numerically. A gaussian 64 point integration are used for w frequency intergal and the Fourier cosine integrals on k_2 integration are performed by a special quadrature package designed for highly oscillatory integrands. Warm plasma effects (absorbtion of radiation) are simulated by cutting off the k_2 integration at $(k_\perp \rho_e)^2 > 1$. This crude model gives

an indication of the effect of a warm plasma but it's results should be interpreted with care. Numerical calculations are performed for different geometry structures and different environments. The computer code is listed in the Appendices.

3.2 Radiation from Space Station and Tethered System

3.2.1 Radiation in Single Ion Plasma

The plasma environment at low earth orbit is mainly composed of the O^+ ion species. Here we are going to study the radiation in the O^+ plasma with typical LEO parameters: magnetic field $B = 0.33$ Gauss; the electron and ion number density $n_e = n_i = 2 \times 10^5 cm^{-3}$; electron temperature $T_e = 0.1eV$. The space structure is taken to be moving in a velocity $V_c = 7.3\ km/sec$. In such an environment, the wave radiation bands are found to be:

$$Band\ \ I \qquad 0 < w < \Omega_i = 1.977 \times 10^2\ \ (Hz)$$

$$Band\ \ II \qquad w_{lh} = 3.302 \times 10^4 < w < \Omega_e = 5.508 \times 10^2\ \ (Hz)$$

Now we calculate the radiation impedance of a space station and tethered systems as a function of AC frequency $Z_r(w^*)$.

First we examine the radiation from a space station. A practical space station with solar array can be simulated by our box structure with dimensions:

$$L_{21} = 80m, \quad L_{22} = 100m$$

$$d_{11} = d_{31} = 5m, \quad d_{12} = 20m, \quad d_{32} = 0.5m$$

and the current is assumed to flow through solar array and end surfaces of the main body, i . e ., surfaces $A_1 - A_1'$, $A_2 - A_2'$,$A_3 - A_3'$ and $A_4 - A_4'$ and the normal current densities at each surface are uniform and are assumed the same.

For comparison, the impedance of a space station without flat solar arrays is also calculated. The dimensions are

$$L_{21} = L_{22} = 100m$$

$$d_{11} = d_{31} = d_{12} = d_{32} = 5m$$

and current flows in and out the system only through surface $A_2 - A_2'$.

Shown in Fig 3.2 are the impedances associated with band I and band II (Z_I, Z_{II} *vs.* w^*). The impedances at some typical AC frequencies are shown in table 3.2.1.

$w^*(Hz)$	station with solar array		station without solar array	
	Band I	Band II	Band I	Band II
1	5.52×10^{-2}	3.07×10^{-2}	9.23×10^{-2}	2. 32
5	5.48×10^{-2}	3.07×10^{-2}	9.18×10^{-2}	2. 32
100	1.12×10^{-2}	2.52×10^{-2}	4.69×10^{-2}	2.38
400	2.12×10^{-4}	3.29×10^{-2}	2.78×10^{-2}	2. 96
10^3	2.14×10^{-5}	2.73×10^{-2}	4.49×10^{-3}	2.33
10^4	1.28×10^{-7}	2.17	6.60×10^{-6}	2.12×10^2
2×10^4	4.46×10^{-8}	6.49×10^{-2}	3.53×10^{-6}	1.12×10
10^5	0	3.55×10^{-2}	0	2.26×10^{-1}

Table 3.2.1: Impedances of Space Station (unit: Ohms)

We see that the impedances of both structures from band I decay quickly when $w^* > 10^2 Hz$ while the impedances in band II jump to a peak value around $w^* \sim 10^4 Hz$. The impedances in band II are cut off for $w^* \to \infty$ because of the cutoff indicating warm plasma effects. The total impedances $Z = Z_I + Z_{II}$ *vs.* w^* are shown in Fig 3.17.

Second we examine the proposed shuttle tethered system—a 10 km tether with space shuttle and subsatellite attached at the two ends. The dimensions are

$$L_{21} = 10km, \quad L_{22} = 10.004km$$

$$d_{11} = d_{31} = 1cm, \quad d_{12} = 40m, \quad d_{32} = 20m$$

and the current is assumed to flow through every surfaces of the shuttle and statellite and the normal current densities at each surfaces are uniform and the same. For comparision, we also examine the impedance of a long tether

($L_{22} = 10.04\ km,\ \ d_{11} = d_{31} = 1\ cm$) with current only flowing through the two end surfaces.

The impedances associated with band I and band II are shown in Fig 3.3 and some of the typical values are listed in table 3.2.2.

$w^*(Hz)$	tether system		tether	
	Band I	Band II	Band I	Band II
1	2.30×10^{-1}	1.73×10^{-1}	2.72×10^{-1}	3.06×10^{3}
5	2.47×10^{-1}	1.73×10^{-1}	2.88×10^{-1}	3.06×10^{3}
100	2.72×10^{-3}	2.61×10^{-1}	4.79×10^{-2}	3.07×10^{3}
400	1.37×10^{-4}	2.00×10^{-1}	3.62×10^{-2}	3.07×10^{3}
10^3	1.25×10^{-5}	2.68×10^{-1}	3.00×10^{-2}	3.07×10^{3}
10^4	2.69×10^{-6}	1.02	0	3.43×10^{3}
2×10^4	2.31×10^{-7}	2.27×10^{-1}	0	3.39×10^{3}
10^5	0	2.00×10^{-2}	0	3.32×10^{3}

Table 3.2.2 Impedance of Tether and 10 km Tether Shuttle System (unit: Ohms)

We see that: for band I, as w^* increases, $Z_I^{tether\ system}$ decreases to zero gradually while Z_I^{tether} only decreases to 0.03 ohms when it is cut off at $w^* > 10^3 Hz$. As for band II, the tether has a very high impedance coming from this band which is a very weak dependence on w^* while the tether system gets its maximum value at $w^* \sim 10^4$ Hz. The total impedances $Z = Z_I + Z_{II}$ *vs.* w^* are shown in Fig 3.20.

The third space structure being examined is a 1 Km tether with two cubic terminators:

$$L_{21} = 1km, \quad L_{22} = 1.002km$$

$$d_{11} = d_{31} = 1cm, \quad d_{12} = 1m, \quad d_{32} = 1m$$

and the boundary current condition is the same as above. The impedances associated with band I and band II are shown in Fig 3.4. Some of the values are listed in Table 3.2.3. The behaviour of $Z_r(w^*)$ for this structure is similar to that for the tether shuttle system, except that the impedances from band I are not cut off until $w \sim 10^4$ Hz. The total impedances $Z = Z_I + Z_{II}$ *vs.* w^* are shown in Fig 3.14.

$w^*(Hz)$	tether system		tether	
	Band I	Band II	Band I	Band II
1	1.63×10^{-1}	2.38×10	1.82×10^{-1}	3.06×10^3
5	1.61×10^{-1}	2.83×10	1.80×10^{-1}	3.06×10^3
100	2.84×10^{-2}	2.83×10	4.79×10^{-2}	3.07×10^3
400	1.65×10^{-2}	2.84×10	3.61×10^{-2}	3.07×10^3
10^3	1.00×10^{-2}	2.92×10	3.00×10	3.07×10^3
10^4	1.63×10^{-4}	2.41×10^2	1.50×10^{-2}	3.43×10^3
2×10^4	4.25×10^{-5}	1.18×10^2	9.68×10^{-3}	3.39×10^3
10^5	0	2.71×10	0	3.32×10^3

Table 3.2.3 Impedance for 1km Tether System (unit: Ohms)

The above computation results show that there is great difference between the impedances of the space station with and without solar arrays or a tether with and without end connectors. This fact will be discussed in the next section.

Having obtained the radiation impedance, we are able to calculate the power radiation from equation (3.19) or (3.21). For space station , the current is driven into the system by the induced field and the power is radiated passively. The current flow can be determined from equation (3.21) . For our dimension, the induced potential is $\Phi' = vBL \simeq 24\ Volt$ and the sum of Ohmic resistence and contactor impedance is assumed to be $R \simeq 500 Ohms$. Shown in Fig 3.5 are the power radiated as function of w^*.

For a tether system, the power can be radiated passively or actively depending on practical purpose. In active case, since the value of current is a fixed given parameter in equation (3.19), the value of total impedance represents the power radiated out. For example, if there is a current of 10 A driven into our 10 Km tether shuttle system, the power radiated will be $P_r \simeq 4$ W for low w^* and $P_r|_{max} \simeq 10$W at $w^* \sim 10^4$ Hz. The power radiated passively from a 10 Km tether shuttle system and a 1km tether system are shown in Fig 3.6 and Fig 3.7. For tether shuttle system, the induced potential drop is $\Phi = vBL_{22} \simeq 2410$ V and the sum of Ohmic resistence and contact impedance is taken to be 100 ohms. For 1km tether system, the induced potential drop is $\Phi = vBL_{22} \simeq 240$ volt and R is taken to be $R = 50$ ohms.

In table 3.2.4 the power radiated from the above systems are compared at some typical w^*. We get less power radiated when the value of impedance Z_r is far from R. It should always be remembered that the power radiated also depends on the values of induced potential, Ohmic resistence and contactor impedance etc, therefore the power radiated calculated here are valid only for our assumed values of R.

$w^*(Hz)$	space station		10km tether shuttle system		1km tether system	
	without solar array	with solar array	tether	with connector	tether	with connector
1	5.50×10^{-3}	1.98×10^{-4}	1.77×10^{3}	2.32×10^{2}	1.82×10	2.66×10^{2}
5	5.50×10^{-3}	1.99×10^{-4}	1.77×10^{3}	2.42×10^{2}	1.82×10	2.66×10^{2}
100	5.53×10^{-3}	8.41×10^{-5}	1.77×10^{3}	1.53×10^{2}	1.82×10	2.66×10^{2}
400	6.82×10^{-3}	7.64×10^{-5}	1.177×10^{3}	1.16×10^{2}	1.82×10	2.66×10^{2}
10^3	5.34×10^{-3}	6.31×10^{-5}	1.77×10^{3}	1.55×10^{2}	1.81×10	2.68×10^{2}
10^4	2.41×10^{-1}	4.96×10^{-3}	1.60×10^{3}	5.80×10^{2}	1.63×10	1.64×10^{2}
2×10^4	2.47×10^{-2}	1.49×10^{-4}	1.62×10^{3}	1.31×10^{2}	1.65×10	2.41×10^{2}
10^5	5.21×10^{-4}	8.18×10^{-5}	1.65×10^{3}	1.16×10	1.68×10	2.62×10^{2}

Table 3.2.4: Power Loss from Space Station and Tether System (unit: Watt)

3.2.2 Radiation in Multi-ion plasma

Although in the LEO environment the dominant ion species is O^+ and the number densities of other ion species are very small, there are reasons for us to consider the environment as a multi-ion species plasma. The first reason is, as long as there is a second ion species appearing, no matter how small the number density might be, a new radiation frequency band will be opened and the entire radation behaviour is changed. The second is, the surrounding environment can be changed significantly due to the contamination from the space structure. The space shuttle is observed to have a cloud of water plasma around it[10]. So the regions inside our integral surface could be filled mainly by water ion H_2O^+ plasma. Thus, it is very important to take into account the effect from multi-ion species. In this thesis, we only consider a two-ion species plasma.

To simulate the practical situation that the structure is surrounded by a

water plasma cloud, we consider a plasma composed of water ion and oxygen ion. The densities are taken to be

$$\frac{n_{H_2O+}}{n_e} = 0.9, \quad \frac{n_{O+}}{n_e} = 0.1$$

and

$$n_e = 2 \times 10^5 (cm^{-3})$$

In stead of two bands, there are three radiation bands because of the appearance of the second ion species. The radiation frequency bands for this environment are

$$band\ I \qquad 0 < w < \Omega_{iH_2O+}$$

$$band\ II \qquad w_{lh1} < w < \Omega_{iO+}$$

$$band\ III \qquad w_{lh2} < w < \Omega_e$$

where $\Omega_{iH_2O+} = 1.757 \times 10^2\ Hz$,$w_{lh1} = 1.954 \times 10^2\ Hz$, $w_{lh2} = 3.132 \times 10^4\ Hz$. Ω_{iO+} and Ω_e are the same as before.

Again we calculate the radiation impedance for the space station and the 10 km shuttle tether system discussed in the last section. The radiation impedances associated with each band are shown in Fig 3.8 and Fig 3.9. In Table 3.2.5 and Table 3.2.6 are the impedances at several typical w^*. The total impedance can be found in Fig 3.32 through Fig 3.35.

$w^*(Hz)$	station with solar array			station without solar array		
	band I	band II	band III	band I	band II	band III
1	4.85×10^{-2}	3.36×19^{-4}	3.67×10^{-2}	8.01×10^{-2}	6.80×10^{-4}	4.46
5	4.80×10^{-2}	3.39×10^{-4}	3.67×10^{-2}	7.96×10^{-2}	6.80×10^{-4}	4.46
100	9.47×10^{-3}	1.23×10^{-4}	3.48×10^{-2}	3.97×10^{-2}	4.76×10^{-4}	4.33
400	1.80×10^{-4}	2.16×10^{-6}	2.95×10^{-2}	2.36×10^{-2}	2.76×10^{-4}	2.81
10^3	1.81×10^{-5}	2.22×10^{-7}	2.54×10^{-2}	3.81×10^{-3}	4.46×10^{-5}	1.95
10^4	1.09×10^{-7}	1.29×10^{-9}	7.66×10^{-1}	5.60×10^{-6}	6.37×10^{-8}	9.95×10
2×10^4	3.77×10^{-8}	4.46×10^{-10}	4.49×10^{-2}	3.00×10^{-6}	3.25×10^{-8}	2.07
10^5	0	0	1.47×10^{-2}	0	0	1.51×10^{-1}

Table 3.2.5: Impedance of Space Station in 90 $\%H_2O^+$ - 10% O^+ Plasma (unit:Ohms)

$w^*(Hz)$	10km tether shuttle system			tether		
	band I	band II	band III	band I	band II	band III
1	2.22×10^{-1}	2.79×10^{-4}	2.69×10^{-1}	2.57×10^{-1}	7.16×10^{-4}	3.09×10^3
5	2.17×10^{-1}	2.88×10^{-4}	2.68×10^{-1}	2.52×10^{-1}	7.24×10^{-4}	3.09×10^3
100	2.24×10^{-3}	3.97×10^{-5}	1.85×10^{-1}	4.05×10^{-2}	4.95×10^{-4}	3.09×10^3
400	1.18×10^{-4}	1.16×10^{-6}	2.44×10^{-1}	3.06×10^{-2}	3.67×10^{-4}	3.09×10^3
10^3	1.02×10^{-5}	1.91×10^{-7}	1.90×10^{-1}	2.54×10^{-2}	3.05×10^{-4}	3.09×10^3
10^4	2.31×10^{-6}	2.17×10^{-8}	5.85×10^{-1}	0	1.52×10^{-4}	3.41×10^3
2×10^4	1.85×10^{-7}	4.17×10^{-9}	6.41×10^{-1}	0	1.04×10^{-4}	3.39×10^3
10^5	0	0	1.95×10^{-3}	0	0	3.34×10^3

Table 3.2.6: Impedances of 10 km Tether Shuttle System in 90 $\%H_2O^+$ - 10% O^+ Plasma (unit: Ohms)

These results show that the behaviour of impedances in band I and band III are almost the same as that in O^+ plasma and the impedance associated with band II is always very small. This is not to be surprised. On examining the function $S(w)$, we see that the effect of multi-ion plasma comes from the mass of the ions. Since the mass of H_2O^+ ($m_{H_2O^+} = 18$ amu) is almost the same as the mass of O^+ ($m_{O^+} = 16$amu), the environment of 90 % H_2O^+ 10% O^+ is

almost the same as 100% O^+ plasma for the radiation problem.

For the purpose of exploring the effect of multi-ion species now we chose two ion species with very different ion mass: H^+ and O^+. The environment is taken to be

$$\frac{n_{O+}}{n_e} = 0.5, \quad \frac{n_{H+}}{n_e} = 0.5$$

and other parameters are the same as before. In this environment, the radiation bands are found to be

$$band\ I \qquad 0 < w < \Omega_{iO+}$$

$$band\ II \qquad w_{lh1} < w < \Omega_{iH+}$$

$$band\ III \qquad w_{lh2} < w < \Omega_e$$

where $\Omega_{iH+} = 3.163 \times 10^3\ Hz$,$w_{lh1} = 7.9047 \times 10^2\ Hz$, $w_{lh2} = 9.638 \times 10^4\ Hz$. The impedance of a space station and tethered system are shown in Fig 3.10 and Fig 3.11 and some of the values are shown in Table 3.2.7 and Table 3.2.8. The total impedances can be found in Fig 3.31 through Fig 3.35.

The results show that multi-ion plasma environment such as $H^+ - O^+$ plasma may result in significant difference on radiation impedance. This will be studied in next section.

$w^*(Hz)$	station with solar array			station without solar array		
	band I	band II	band III	band I	band II	band III
1	7.63×10^{-2}	2.09×10^{-1}	9.70×10^{-3}	1.28×10^{-1}	2.80	5.15×10^{-1}
5	7.56×10^{-2}	2.10×10^{-1}	9.70×10^{-3}	1.27×10^{-1}	2.80	5.15×10^{-1}
100	1.55×10^{-2}	4.84×10^{-1}	1.12×10^{-2}	6.50×10^{-2}	2.99	5.05×10^{-1}
400	2.94×10^{4}	4.95×10^{-1}	9.28×10^{-3}	3.86×10^{-2}	2.50	3.81×10^{-1}
10^3	2.98×10^{-5}	4.43×10^{-3}	1.04×10^{-2}	6.24×10^{-3}	5.16×10^{-1}	3.08×10^{-1}
10^4	1.78×10^{-7}	1.03×10^{-5}	2.12×10^{-2}	9.22×10^{-6}	8.76×10^{-4}	1.29
2×10^4	6.19×10^{-8}	4.13×10^{-6}	4.21	4.96×10^{-6}	2.20×10^{-4}	3.00×10^{2}
10^5	0	0	8.82×10	0	0	1.06×10^{3}

Table 3.2.7: Impedance of Space Station in 50 $\%H^+$ - 50% O^+ Plasma (unit:Ohms)

$w^*(Hz)$	10km tether shuttle system			tether		
	band I	band II	band III	band I	band II	band III
1	3.17×10^{-1}	1.74×10^{-2}	8.26×10^{-2}	3.74×10^{-1}	3.24	2.36×10^{3}
5	3.39×10^{-1}	1.77×10^{-2}	8.24×10^{-2}	3.97×10^{-1}	3.24	2.36×10^{3}
100	3.80×10^{-3}	2.84×10^{-1}	5.58×10^{-2}	6.63×10^{-2}	3.48	2.36×10^{3}
400	1.91×10^{-4}	9.03×10^{-1}	7.41×10^{-2}	4.99×10^{-2}	3.93	2.36×10^{3}
10^3	1.76×10^{-5}	2.29×10^{-3}	5.60×10^{-2}	4.15×10^{-2}	2.45	2.36×10^{3}
10^4	3.82×10^{-6}	1.46×10^{-4}	1.50×10^{-1}	0	1.21	2.60×10^{3}
2×10^4	3.58×10^{-1}	4.11×10^{-5}	1.85	0	8.31×10^{-1}	3.39×10^{3}
10^5	0	0	1.58×10	0	0	4.21×10^{3}

Table 3.2.8: Impedance of 10 km Tether shuttle System in 50 $\%H^+$ - 50% O^+ Plasma (unit:Ohms)

3.3 Factors Affecting Power Radiation and Radiation Impedance

The power radiated from a space structure can be written as

$$P_r = I^2 Z_r$$

so P_r is a function of total current I and radiation impedance Z_r. I is a given parameter in active radiation case. In passive radiation case, since I is determined by

$$I = \frac{\Phi'}{R + Z_r}$$

where $R = r_{load} + Z_{contactor} + R_{ohms}$ and $\Phi' = vBL_{22}$, I itself is a function of R and Z_r, the power radiated changes in accordance with Φ ,Z_r and R. For a given structure, Φ, R or I usually have been determined, so radiation impedance Z_r is the measure of power radiation.

From the calculations in last section, we saw that the impedance for different structures and in different environments can be very different. On examination of the radiation formula in Fourier space

$$P_r = P^+ + P^- = I^2 Z_r$$

$$P_r^{\pm} = \int |j_s \cdot k|^2 Q dk_1 dk_2 = I^2 Z_r^{\pm}$$

$$Z_r = Z_r^+ + Z_r^-$$

$$Z_r^{\pm} = \int (\frac{|\vec{j_s} \cdot \vec{k}|}{I})^2 Q dk_1 dk_2 \qquad (3.27)$$

we notice that when $\omega^* = 0$, (1) plasma property affects Z_r through radiation bands and term $Q = \frac{\pi^2}{cK_1^2\sqrt{\beta S}}$ and (2) the structure geometry and boundary

current flow pattern affects Z_r through term $|\vec{j}_s \cdot \vec{k}|/I$. When $\omega^* \neq 0$, Q and $|\vec{j}_s \cdot \vec{k}|/I$ are also functions of AC frequency w^* , so ω^* affect Z_r through both $|\vec{j}_s \cdot \vec{k}|/I$ and Q term.

Since the waves discussed here are excited by a moving conductor in a plasma medium, the radiation is the results of the interactions between the space structures and the environment. We are going to term $|\vec{j}_s \cdot \vec{k}|/I$ as "structure factor" , and Q together with radiation bands as "environment factor". When the whole structure- environment system is driven by ω^*, ω^* will affect both "structure factor" and "environment factor". It is not surprising that P_r and Z_r depends on, and only on, the coupled effect from structure and environment. So no matter in what function form P_r and Z_r are written, we can always regard P_r and $Z_r$as functions of environment, structure and AC frequency:$P_r = P_r(structure, environment, w^*)$ and $Z_r = Z_r(structure, environment, w^*)$.

Unfortunately, the relationship between Z_r and its variables is covered by the extremely complicated form of equation(3.27). Even for our simplified box structure model, the complexity still makes the analysis impossible in a general and analytical way. So in this section, we shall explore the implicit physics by conducting several "computational experiments". The dependence of Z_r on structure , environment and AC frequency will be discussed seperately on the basis of numerical results.

(I) Impedance vs. Structure

First we study the relations between Z_{rad} and the "structure factor". The

structure factor includes boundary current pattern and counductor geometry, therefor the impedance depends on both the boundary current pattern and the geometry dimensions. For the purpose of exploring these functional relations, first we investigate a thin tether with two cubic terminators. The boundary current density is taken to be uniform. In such a structure, the boundary current pattern effect is simplified to that of boundary current at different direction and the geometry effect is simplified to that of collecting surface area and direction.

To explore the relation between Z_r and boundary current pattern, we take a structure with the following dimension:

L_{21} =1 Km, L_{22} =1.002 Km, $d_{11} = d_{31}$ =1 cm, $d_{12} = d_{32}$ =1m

Each time we insulate some of the collecting surfaces so that the boundary current only flows at the desired direction. The radiation impedances are calculated in O^+ plasma. The following experimental cases are chosen:

1) Current only flows through surface A_1 and A_1'

$$P_{r1} = \int\int |\vec{j}_s \cdot \vec{k}|^2 Q dk_1 dk_2 = I_1^2 Z_1$$

2) Current only flows through surface A_2 and A_2'

$$P_{r2} = \int\int |\vec{j}_s \cdot \vec{k}|^2 Q dk_1 dk_2 = I_2^2 \cdot Z_2$$

3) Current only flows through surface A_3 and A_3'

$$P_{r3} = \int\int |\vec{j}_s \cdot \vec{k}|^2 Q dk_1 dk_2 = I_3^2 \cdot Z_3$$

4) Current only flows through surface A_4 and A_4'

$$P_{r4} = \int\int |\vec{j}_s \cdot \vec{k}|^2 Q dk_1 dk_2 = I_4^2 \cdot Z_4$$

5) Current flows through every surface

$$P_{ra} = \int\int |\vec{j}_s \cdot \vec{k}|^2 Q dk_1 dk_2 = I_a^2 \cdot Z_a$$

The radiation impedance formula is given in section 3.2. We assume same total current follows in each of the above system

$$I_a = I_1 = I_2 = I_3 = I_4$$

and compare the radiation impedance.

Shown in Fig 3.12 to Fig 3.14 are the radiation impedances Z_1, Z_2, Z_3, Z_4 and Z_a as functions of w^*.We found that for $w^* \neq 10^4$Hz, there always exists $Z_1 > Z_2 > Z_4 > Z_a > Z_3$ for this structure. For $w^* \sim 10^4$Hz, Z_2,Z_3,Z_4 and Z_a jump to a maximum value while Z_1 is still not very sensitive to w^*.

To explore the relation between Z_r and geometry, we still consider a 1 km tether ($d_{11} = d_{31} = 1cm$)with two cubic terminators. This time we change the size of terminators and calculate the impedances. The dimensions used are

a) $L_{21} = 1km$,$L_{22} = 1.002km$,$d_{12} = d_{32} = 1m$;

b) $L_{21} = 1km$,$L_{22} = 1.02km$,$d_{12} = d_{32} = 10m$;

c) $L_{21} = 1km$,$L_{22} = 1.1km$,$d_{12} = d_{32} = 50m$;

The impedances for different boundary current pattern Z_1,Z_2, Z_3,Z_4 and Z_a are calculated.The impedances of tethers with $L = L_{22}$, Z_t, are also calculated. Shown in the following table are total impedances for each structure evaluated at $w^* = 400$ Hz and $w^* = 20$ kHz.

$w^* = 400$	Z_t	Z_a	Z_1	Z_2	Z_3	Z_4
structure a	3.07×10^3	2.84×10	2.36×10^2	5.68×10	9.53	5.68×10
structure b	3.07×10^3	1.95	1.69×10	2.94×10^{-1}	6.94×10^{-3}	2.94×10^{-1}
structure c	3.07×10^3	1.57×10^{-1}	1.41	1.40×10^{-2}	$9.28 \times 1)^{-5}$	1.40×10^{-2}
$w^* = 20kHz$	Z_t	Z_a	Z_1	Z_2	Z_3	Z_4
structure a	3.39×10^3	1.17×10^2	1.72×10^2	5.71×10^2	1.52×10^2	5.7×10^2
structure b	3.39×10^3	1.71	1.08×10	3.75	1.92×10^{-1}	3.75
structure c	3.39×10^3	3.54×10^{-1}	3.18	5.70 $times 10^{-3}$	3.94×10^{-5}	5.70×10^{-3}

Examining the table, we found as collecting area increases, all the impedances Z_1,Z_2,Z_3,Z_4 and Z_a decrease. At each case, we always have

$$Z_t >> Z_1 > Z_2 \sim Z_4 > Z_3$$

and $Z_1 > Z_a > Z_3$.

So a few important conclusions can be drawn from our testing cases:

(1) The impedance increases as total collecting area decreasing for any given boundary current. (2) For system with the same current collecting area, if the current is collected only in $\vec{x}_3$ direction(surface $A_3 - A_3'$), we can get a minimum impedance; if the current is only collected in $\vec{x}_1$ direction(surface $A_1 - A_1'$), we get a maximum impedance. (This may not hold at $w^* \sim 10^4$.) If current is collected in every syrfaces, the impedance lies between Z_1 and Z_3. (3) A thin tether always has a much larger impedances than any other systems which is insensitive to w^*.

The reason can be understood as follows: since we are assuming the same current flows in each case, increasing the collecting area means decreasing the current density at interface, thus the wave intensity corresponding to this current

density decrease. So there will be less resistance. If Z_r is the only important resistance, then less energy will be radiated. If the collecting area are the same and assuming the same current density in every direction, since the plasma is a good conductor in the direction parallel to the magnetic field and a poor conductor in the perpendicula direction, it is much easier for the current to transfer along the magnetic field so we get the minimum resistance. As for $\vec{x}_2$ and $\vec{x}_3$ direction, the current transfers in a poor conductor. But since the induced field is $E' \sim \vec{V} \times \vec{B}$, this helps current component in $\vec{x}_2$ direction. Thus it is not to be surprised that we have $Z_3 < Z_2 < Z_1$ in our testing cases. Since Z_a depends on the superposition effects of current in every direction, we have $Z_3 < Z_a < Z_1$. For a tether with current flowing directly through the two ends, since the collecting area is so small, a very large boundary current density is required which corresponds to a large perturbation. The perturbation is so large that it always meets a large resistance from the environment. In other words,it is very hard for this wave to keep from damping with any finite amount of energy. Thus we always have a high impedance which almost reaches a kind of "saturation" value. So the impedance is a very weak dependence on w^* .

We shall now study the impedance of the space station and tether shuttle system. We are interested to see what will happen if we insulate some of the solar array or tether connector surfaces. Again we consider the above discussed case: (1) I_1 through $A_1 - A_1'$; (2) I_2 through $A_2 - A_2'$; (3)I_3 through $A_3 - A_3'$; (4)I_4 through $A_4 - A_4'$;(5)I_5 through $A_5 - A_4'$;(6) station without solar array or tether without connectors, I_t through two end surfaces. For each structure, the current flow in each case are assumed the same.The impedances for space station are compared in Fig 3.15 to Fig 3.17. The impedances for tether-shuttle system

are compared in Fig 3.18 to Fig 3.20. For tether shuttle system , we found

$$Z_t >> Z_1 > Z_a > Z_2 \sim Z_4 > Z_3 \quad (except\ at\ ; w^* \sim 10^4\ Hz)$$

For space station, we found

$$Z_1 > Z_4 > Z^{no\ array} > Z_2 > Z_5 > Z_3 \quad (except\ at\ ; w^* \sim 10^4\ Hz)$$

The comparison for space station turns out to be different from that for tether system. Obviously the flat plate shape of solar array amplifies the perturbation density from $A_1 - A_1'$,$A_2 - A_2'$ and $A_4 - A_4'$ surface while it decreases the perturbation density from $A_3 - A_3'$ surface. so it is more important for a space station to have large collecting surface facing x_3 direction and insulate other surfaces in order to have low radiation impedance.

The comparisons of radiation impedance do not represent the power radiated. For active power radiation: the radiation impedance measures the power radiation. For passive power radiation, the current I also depends on R and Z_r. The comparison of power radiated passively are shown in Fig 3.21 to Fig 3.23. Shown in Fig 3.21 are power loss from space station, where induced potential $V = 24$ volt and $R = 500$ ohms for each case. We found

$$P_1 > P_4 > P^{noarray} > P_2 > P_a > P_3$$

Shown in Fig 3.22 are power loss from a tether shuttle system where $V = 2410$ volt and $R = 100$ ohms for each case. We found

$$P_1 > P_{tether} > P_a > P_2 \sim P_4 > P_3$$

Shown in Fig 3.23 are power loss from a 1km tether system where $V = 240$ volt and $R = 50$ ohms for each case. We found

$$P_a > P_3 > P_1 > P_2 \sim P_4 > P_{tether}$$

Those results suggest that: since a thin tether or a tether subsatellite system with small collecting surfaces $A_1 - A_1'$ have a high impedance at all w^*, they are able to radiate large energy actively. So they are suitable for being used as antenna. For a space station, having a large collecting surface at x_3 direction and insulating other surfaces of solar array led to minimum power loss.

It should be noted that the above comparisons are under the assumption that the same total current flows for different systems and the same boundary current density at every direction. However, it could be possible that we have different total current for different system or different boundary current density at different directions. Then the relative values of power radiation could be quite different.

(II) Impedance vs. environment and w^*

We have found the impedances in different environment are very different. This is caused by the difference on $Q(w)$ function and radiation bands which vary with ion plasma frequencies. Since it is also found that the effect from environment is strongly coupled with that from AC frequency w^* (This will be pointed out at the end of this section), we discuss the dependence of impedance on multi-ion plasma environment and on AC frequency jointly .

For simplicity, we investigate a two-ion species plasma. The ion species are chosen to be those of very different mass. Without loss of generality, we consider a plasma composed of O^+ and H^+. We change the number density of O^+ and H^+, but always keep $n_{O+} + n_{H+} = n_e$. The radiation impedance will be studied as a function of n_{O+}/n_{H+}.

In $H^+ - O^+$ plasma environment, the radiation bands are:

$$bands\ I \quad 0 < w < \Omega_{iO+}$$

$$bands\ II \quad w_{lh_1} < w < \Omega_{iH+}$$

$$bands\ III \quad w_{lh_2} < w < \Omega_e$$

Where $\Omega_{iO+} = 1.977 \times 10^2$Hz,$\Omega_{iH+} = 3.163 \times 10^3$ Hz and $\Omega_e = 5.808 \times 10^6$Hz. Shown in the table are w_{lh_1} and w_{lh_2} in different $H^+ - O^+$ plasma.

n_{H+}/n_e	n_{O+}/n_e	w_{lh_1}	w_{lh_2}
0.1	0.9	1.902×10^3	5.229×10^4
0.2	0.8	1.424×10^3	6.414×10^4
1/3	2/3	1.070×10^3	8.099×10^4
0.5	0.5	7.905×10^2	9.638×10^4
2/3	1/3	5.839×10^2	1.096×10^5
0.8	0.2	4.386×10^2	1.191×10^5
0.9	0.1	3.283×10^2	1.257×10^5

When $n_{H+}/n_e = 1$ or $n_{O+}/n_e = 1$ the environment comes back to single ion plasma. The radiation bands in H^+ plasma and O^+ plasma are:

n_{H^+}/n_e	n_{O^+}/n_e	w_{lh}	band I	band II
0	1	3.302×10^4	$0\text{-}1.977 \times 10^2$	$3.302 \times 10^4 - 5.808 \times 10^6$
1	0	1.32×10^5	$0 - 3.163 \times 10^2$	$1.320 \times 10^5 - 5.808 \times 10^6$

From the above tables, we see that in an originally O^+ plasma, as long as there is a new ion species, say H^+, appearing, a new radiation frequency band will be forced to open. As n_{H^+} increases (n_{O^+} decreases), w_{lh_1} decreases and w_{lh_2} increases. So the width of the new band —$|\Omega_{iH} - w_{lh_1}|$ becomes larger and larger and the width of band III —$|\Omega_e - w_{lh_2}|$ becomes smaller and smaller. This result can be extented to an arbitary two-ion species plasma. In a plasma originally composed of single heavy ion species, when light ion species are added , the original band$\left|\Omega_e - w_{lh}^{heavy}\right|$ will divide into two bands:$\left|w_{lh_1} - \Omega_i^{light}\right|$ and $|w_{lh_2} - \Omega_e|$. As n_{light} increases, the new band II extends from Ω_i^{light} to low frequency (but $w_{lh_1} > \Omega_i^{heavy}$ always) and the new band III shortens its width towards Ω_e. When $n_{light} = n_e$ ($n_{heavy} = 0$), band I and band II combine to one band $\left|0 - \Omega_i^{light}\right|$ and band III becomes $\left|w_{lh}^{light} - \Omega_e\right|$. It is noticed, in the above process, there always exists

$$\Omega^{heavy} < w_{lh_1} < w_{lh}^{heavy} < \Omega^{light} < w_{lh_2} < w_{lh}^{light} < \Omega_e$$

It is interesting to see how the radiation impedances response to a change in the surrounding plasma, so we calculate the impedance of a space station and a tether shuttle system as function of n_{H^+}/n_{O^+} at a given w. The dimensions and current pattern are the same as that in section 3.2 .

The impedances of space station with and without solar array at $w^* = 400$ Hz and $w^* = 20$ kHz are shown in Fig 3.24 through Fig 3.27. These two frequencies

are chosen because they are typical frequencies for space power system. Fig 3.24 and Fig 3. 26 show the impedances from each bands in $H^+ - O^+$ plasma with n_{H+}/n_e changing from 0.1 to 0.9 (n_{O+}/n_e changing from 0.9 to 0.1). Fig 3.25 and Fig 3.27 show the total impeadances responding to the process of the environment gradually changing from single O^+ plasma, to $H^+ - O^+$ plasma and finally to H^+ plasma. The impedance of a tether shuttle system and a tether at $w^* = 400$Hz and $w^* = 20$kHz are shown in Fig 3.28 through Fig 3.31. The impedances from each bands in $H^+ - O^+$ plasma are shown in Fig 3.28 and Fig 3.30. The total impedances are shown in Fig 3.29 and Fig 3.31.

From those results, we notice that:

(1) At $w^* = 400$ Hz, for all the structures calculated, the impedances from band I always slightly decrease as n_{H+}/n_e increase. As to the total impedance, for space station with solar array and tether shuttle system, when there is a very small amount of H^+ added into single O^+ plasma, the impedances jump to their maximum values. But when n_{H+}/n_e increases, the impedance decreases. When $n_{H+} = n_e$ ($n_{O+} = 0$), we find the impedance in single H^+ plasma bigger than that in single O^+ plasma.

(2) At $w^* = 20$ kHz, for all structures, the impedances from band I slightly increase and the impedances from band II slightly decrease as n_{H+}/n_e increase. But the impedances from band III behaves in a very complicated way. It seems for a given structure, there exist some particular values of n_{H+}/n_e at which Z_{III}'s take their minimum values. Since the total impedance is dominated by the impedance from band III, it is hard to generalize the behaviour of the impedance.

But one conclusion can be drawn: for space station and tether shuttle system we have:

$$Z^{H^+-O^+} >> Z^{H^+} > Z^{O^+}$$

where $Z^{H^+-O^+}$— total impedance in $H^+ - O^+$ plasma, Z^{H^+} —impedance in H^+ plasma and Z^{O^+}— impedance in O^+ lasma.

(3) For a tether without end connectors, at both $w^* = 400$ Hz and $w* = 20$ kHz, the impedance is a weak dependence on the environment. As n_{H^+}/n_e increases, impedance simply decreases very slightly ($w^* = 400Hz : Z^{O^+} \simeq 3 \times 10^3$ *ohms*, $Z^{H^+} \simeq 2 \times 10^3$ *ohms*. $w^* = 20$ *kHz* : $Z^{O^+} \simeq 3.5 \times 10^3$ *ohms*, $Z^{H^+} \simeq 3.2 \times 10^3$ *ohms*).

The above results apply only to the cases $w^* = 400Hz$ and $w^* = 20kHz$. To include the effect from the AC frequency, from Fig 3.32 to Fig 3.35 we compare the total impedances for a space station and a tether shuttle system as functions of w^* in the following typical environments:

(1) O^+ plasma;

(2) H^+ plasma;

(3) $H_2O^+ - O^+$ plasma: $\frac{n_{H_2O^+}}{n_e} = 0.9$ $\frac{n_{O^+}}{n_e} = 0.1$;

(4) $H^+ - O^+$ plasma: $\frac{n_{H^+}}{n_e} = 0.5$ $\frac{n_{O^+}}{n_e} = 0.5$.

The number density of electrons n_e and other plasma parameter are the same. For the space station and the tether shuttle system we found:

(1) when $10^3 < w^* < 10^4$(Hz), the impedances in H_2O^+ and O^+ plasma go up to their maximum and the impedances in H^+ and $H^+ - O^+$ plasma go down to their minimum. For this frequency range there exist

$$Z^{H_2O^+} \sim Z^{O^+} >> Z^{H^+} \sim Z^{O^+-H^+}$$

(2) when $w^* > 10^4$(Hz), the impedances in H^+ and $H^+ - O^+$ plasma go up to their maximum and the impedances in H_2O^+ and O^+ plasma decay quickly.

$$Z^{H^+-O^+} >> Z^{H^+} > Z^{H_2O^+} \sim Z^{O^+}$$

(3)The impedances of some other kind of structures are also calculated. The results show that for different structures, the resulting effects from environment and w^* are not always consistent. Especially for $w^* < 10^2$Hz, it seems each structure has it's own "most favorable" environment in which it will have a bigger or smaller impedance. But the differences are usually not very large.

4)For a long tether, the impedance almost does not change in the whole w^* range in $H_2O^+ - O^+$ and O^+ plasma. It also does not change for $w^* < 10^4$Hz in $H^+ - O^+$ and H^+ plasma. We find the high impedance of a tether is hardly affected by either environment or w^*. For the space station, if we insulate almost the whole solar array but leave a very tiny conducting area, we shall also get a very high impedance which acts like that of a tether.

In order to understand the interactions between wave and environment, here

we present a hypothesis which seems able to explain the above effects.

We assume the environment could be modeled as a medium composed of millions of damped oscillators. Those oscillators are excited to oscillation if there are perturbations. Whenever there is a wave propagating through this medium ,the energy carried by the wave will be transfered to those oscillators to overcome the inside damping. Thus radiation impedance can be represented by the total energy consumed by all the damped oscillators.

A single ion species plasma, such as H^+ and O^+ plasma, could be modeled by a set of simple oscillators. Their characteristic frequencies would be $w_0^{H^+} \sim \sqrt{K/m^{H^+}}$ and $w_0^{O^+} \sim \sqrt{K/m^{O^+}}$ by analogy to a harmonic oscillator. A multi-ion plasma, such as $H_2O^+ - O^+$ and $H^+ - O^+$ plasma, could be modeled by a set of coupled oscillators. There are two characteristic frequencies w_{01} and w_{02} for a coupled oscillator[11]. For 90 % H_2O^+– 10 % O^+ plasma, we might consider there is only weak coupling. Using results from classical mechanics, its characteristic frequencies would be: $w_{01}^{H_2O^+-O^+} \sim w^{O^+}(1+\epsilon)$ and $w_{02}^{H_2O^+-O^+} \sim w^{O^+}(1-\epsilon)$ where $\epsilon << 1$. Thus we have $w_{01}^{H_2O^+-O^+} \sim w_{02}^{H_2O^+-O^+} \sim w^{O^+}$. But for 50 % H^+ – 50 % O^+ plasma, strong coupling could be expected and $w_{01}^{H^+-O^+}$ and $w_{02}^{H^+-O^+}$ would be very different.

If w^* is very low, the wave propagation is determined mainly by the properties of the environment. If the perturbation of the structure matches the natural wave length scale in this environment, then the wave will propagate very easily so we get a low radiation impedance. It is not surprising that each structure has its own "nature" environment in which the perturbation propagates most easily.

When w^* increases, all oscillators in the medimum are driven to "oscillate" at the same frequency. Since the oscillation of heavier oscillators consumes more energy then lighter oscillators, the propagation of a wave with same amplitude will meet a larger "damping" force in heavier ion plasma, so we get a larger impedance. When $w^* \sim 10^4$ Hz, it seems that $w_0^{O^+}$ is about this value, a "resonances" is set up in an O^+ plasma. Since $w_{01}^{H_2O^+-O^+} \sim w_{02}^{H_2O^+-O^+} \sim w^{O^+}$, a resonance also happen in a $H_2O^+ - O^+$ plasma. At resonance the damped oscillators consume a much greater amount of energy due to resonance oscillating motion so we get a peak value of impedance. This is the reason at $10^3 < w^* < 10^4(\text{Hz})$, $Z^{H_2O^+-O^+}$ and Z^{O^+} increase to the maximum while $Z^{H^+-O^+}$ and Z^{H^+} decrease to the minimum. If we further increase w^*, since fewer and fewer heavier particle can follow the external driven frequency,the total "damping force" decreases. We get a smaller impedance because less energy is consumed by "damping force" in plasma composed of heavy ion species. (The other reason is warm plasma effects.) So $Z^{H_2O^+-O^+}$ and Z^{O^+} decrease after $w^* > 10^4 Hz$. Since $m_{O^+}/m_{H^+} = 16$ results $w_0^{H^+}/w_0^{O^+} \sim 4$, resonance happenes in H^+ plasma at $w^* \sim 4 \times 10^4$. So Z^{H^+} gets its peak value there. As to $H^+ - O^+$ plasma, it seems that $w_{01}^{H^+-O^+}$ and $w_{02}^{H^+-O^+}$ is in the range of 2×10^4 Hz to 1×10^5 Hz, thus we get very large impedances in $H^+ - O^+$ plasma for $w^* \sim 2 \times 10^4 Hz$ and $w^* \sim 10^5$Hz. For a tether or a solar array which is insulated almost completely, because of the very small conducting area, the local electron flux density required will be so high that no environment can be matched by the perturbation. A great amount of energy is always needed from the souce to support the perturbation propagation. Therefor any kind of environment is like a same barrier which is difficult to be overcome. A great amount of energy is always needed from the source to support the perturbation propagation. So we get a staturation radiation impedance which is almost the same in any plasma environment and

is hardly changed by w^* .

To summarize the discussion on the multi-ion species environmental effects:

(1)For system with very low AC frequency ($w^* < 100\ Hz$) , the major effect from multi-ion environment will be only on the wave radiation bands. Different structures may have their own "nature" environment within which the impedance is a little smaller.

(2)For system with high AC frequency, since the appearence of a new kind ion species will change the "characteristic frequencies", the impedance will be affected due to "resonance".

The power radiated in passive state by space station and tether shuttle system in (1) O^+ plasma (2) H^+ plasma (3) $90\%H_2O^+ - -10\%O^+$ plasma (4) $50\%H^+ - -50\%O^+$ plasma are compared from Fig 3. 36 to Fig 3. 39.

Though the physics of the effects from structure and environment is still not fully understood, from the results and discussions in this section, we can obtain a few general rules to help the design of large space structures:

(1) For a space structure with low AC current frequency, ($w^* < 10^2 Hz$) , the effect of environment is not very significant though for each structure there exists its own "nature" environment. In order to get a lower impedance, we can increase the total current collecting area or insulate the conducting surfaces at

$\vec{x_1}$ direction to force more current flow through the surfaces at $\vec{x_3}$ direction. In order to get a higher impedance, we decrease the total current collecting area or insulate the conducting surface at $\vec{x_3}$ direction to force more current to flow through surfaces $A_1 - A_1'$

(2) For space structure with AC current in the frequency range $10^2 < w^* < 10^4(Hz)$, we can still change the impedance by changing the collecting area or collecting surfaces in the above mentioned way. The impedance can also be changed by changing the surrounding environment.Usualy a plasma composed of heavier ion species can result in higher impedance while plasma composed of lighter ion species can result in lower impedances.

(3) For space structure with AC current at $w^* > 10^3$Hz, since a kind of "characteristic frequencies" for LEO environment are usually in this same region, impedances could jump to peak values at some AC frequencies. For O^+ and 90 % H_2O^+- 10 % O^+ plasma, this value is about 10^4 Hz. A space station with driven AC current of the same frequency could radiate a great amount of energy. For space structures with AC current of $w^* > 10^3$ Hz, we may avoid the occurrence of this maximum impedance for a fixed w^* by changing the environment . But changing the surrounding plasma from single-ion species to multi-ion species always results in more "resonances" frequencies .

(4) If we want a high, stable impedance at any w^* and in any environment, a thin tether with current flow directly through the two ends is the best choice.

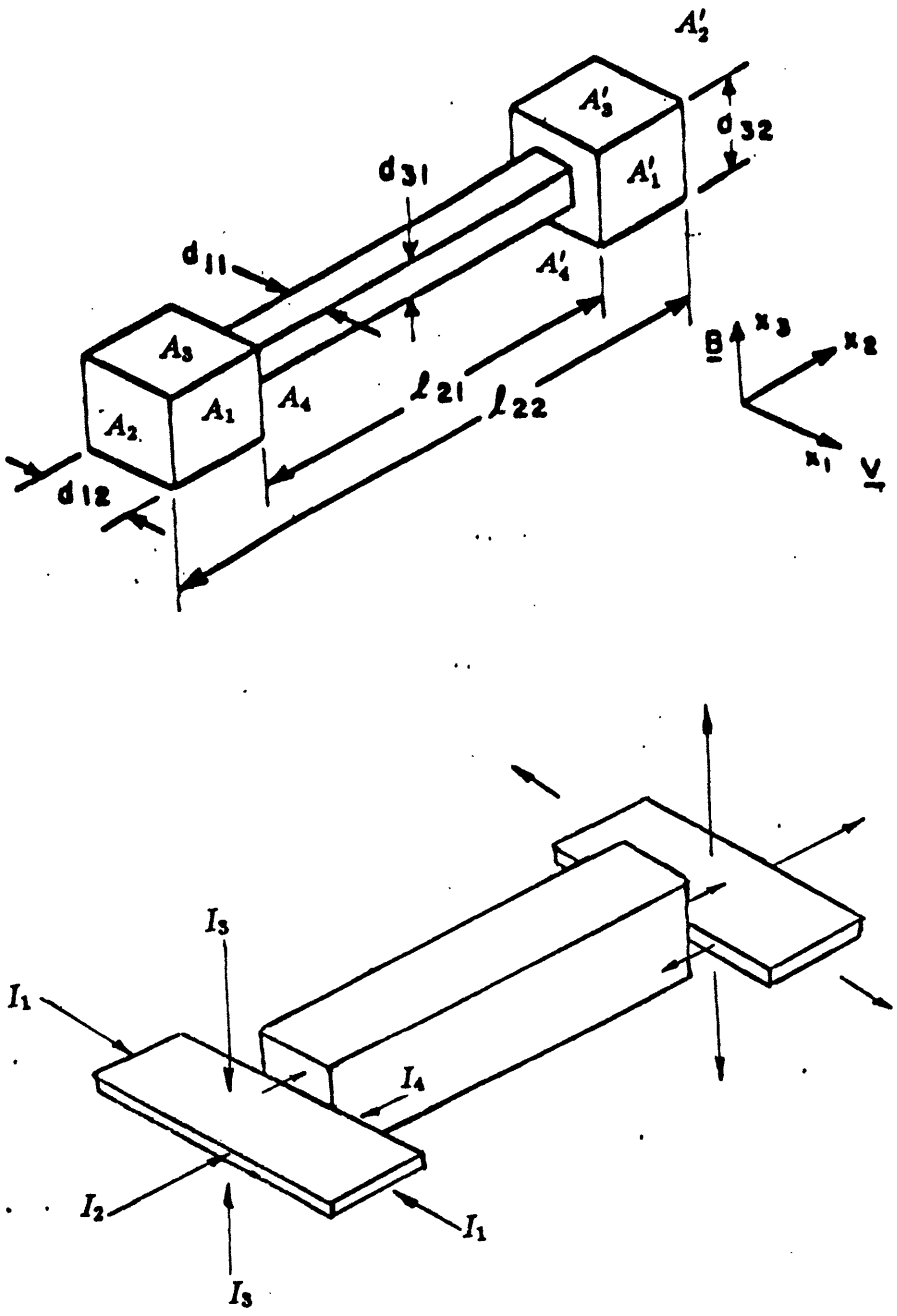

Figure 3.1: Generalized box structure model

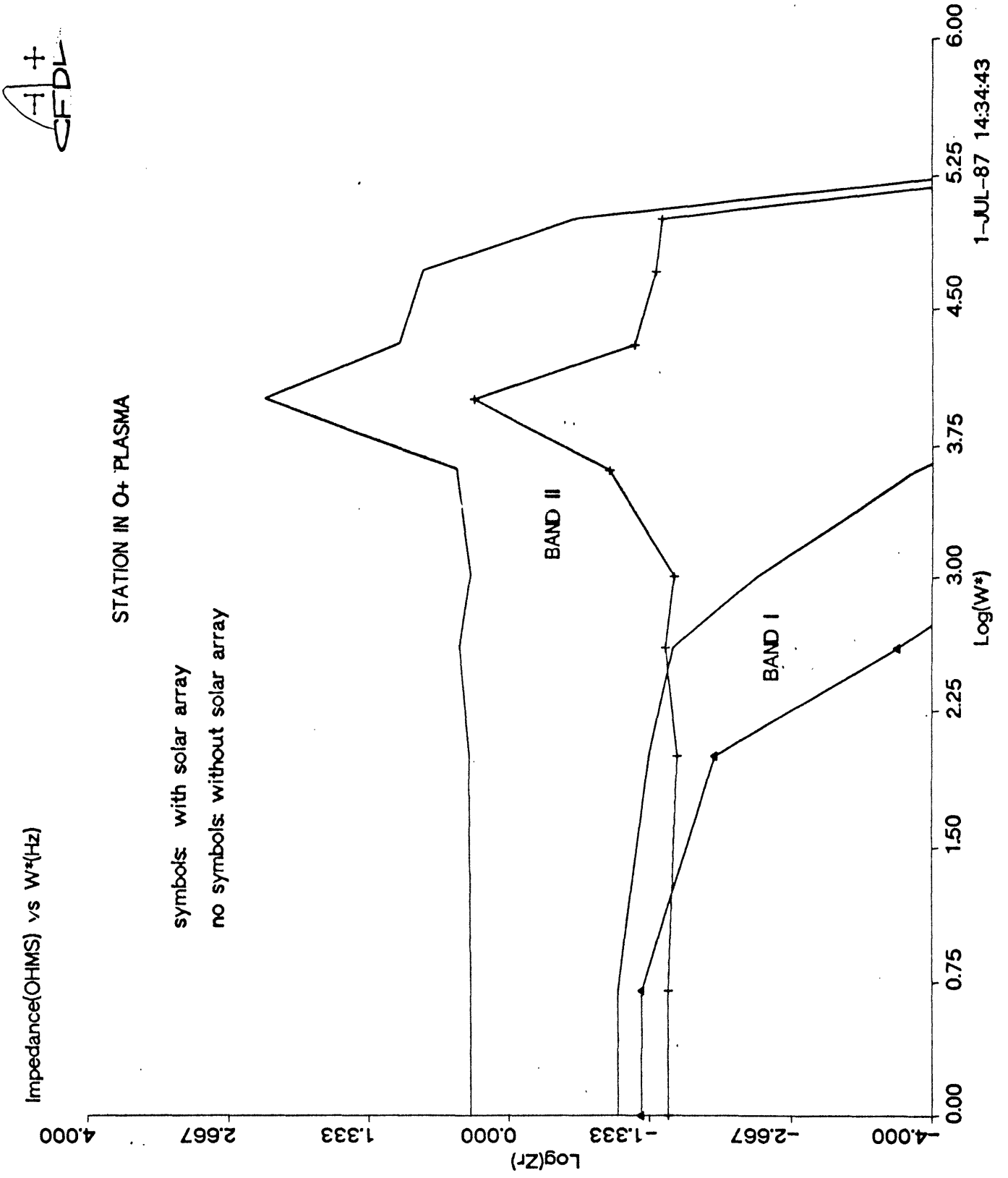

Figure 3.2: Impedance of Space Station in O^+ Plasma

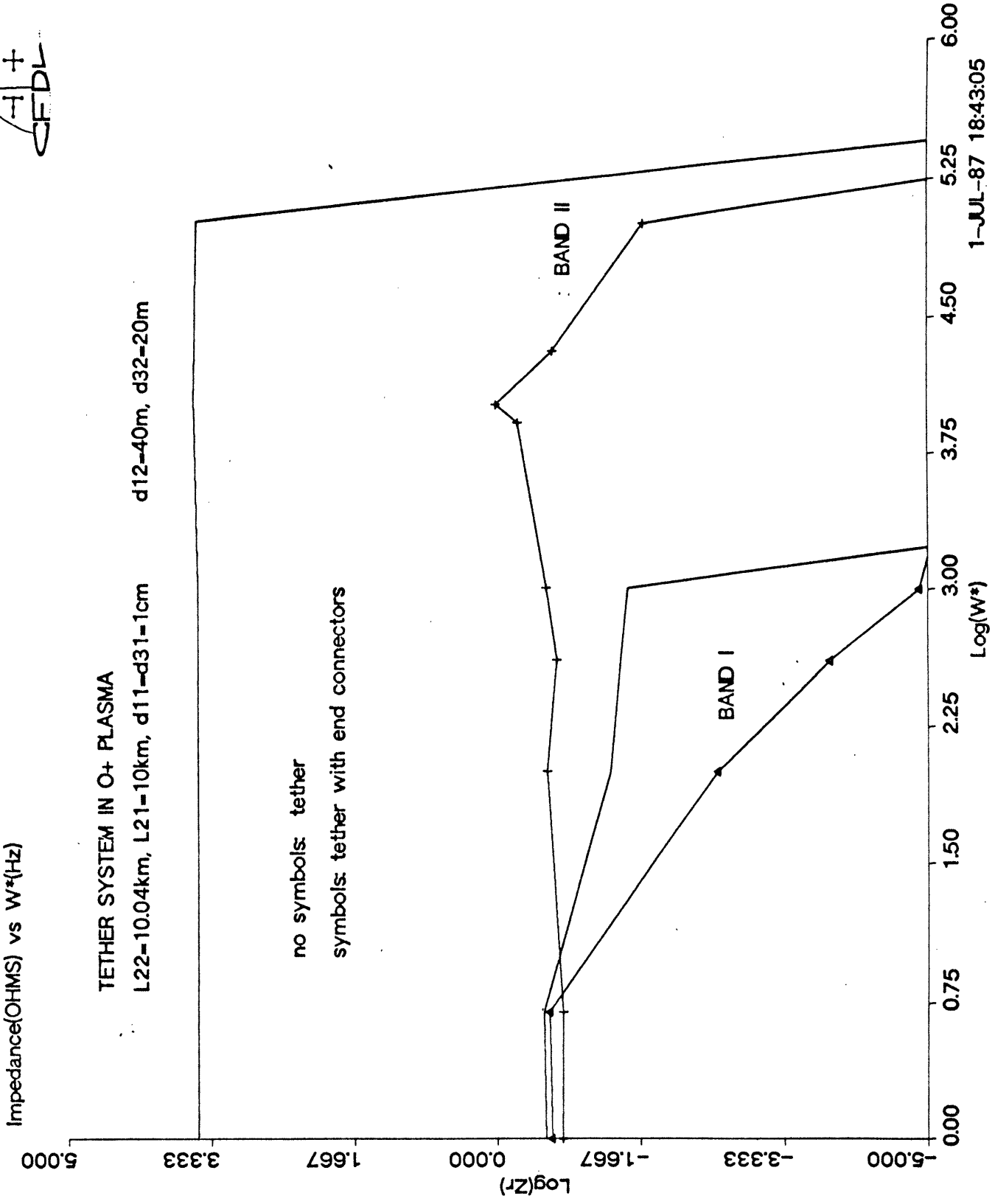

Figure 3.3: Impedance of Shuttle-Tether in O^+ Plasma

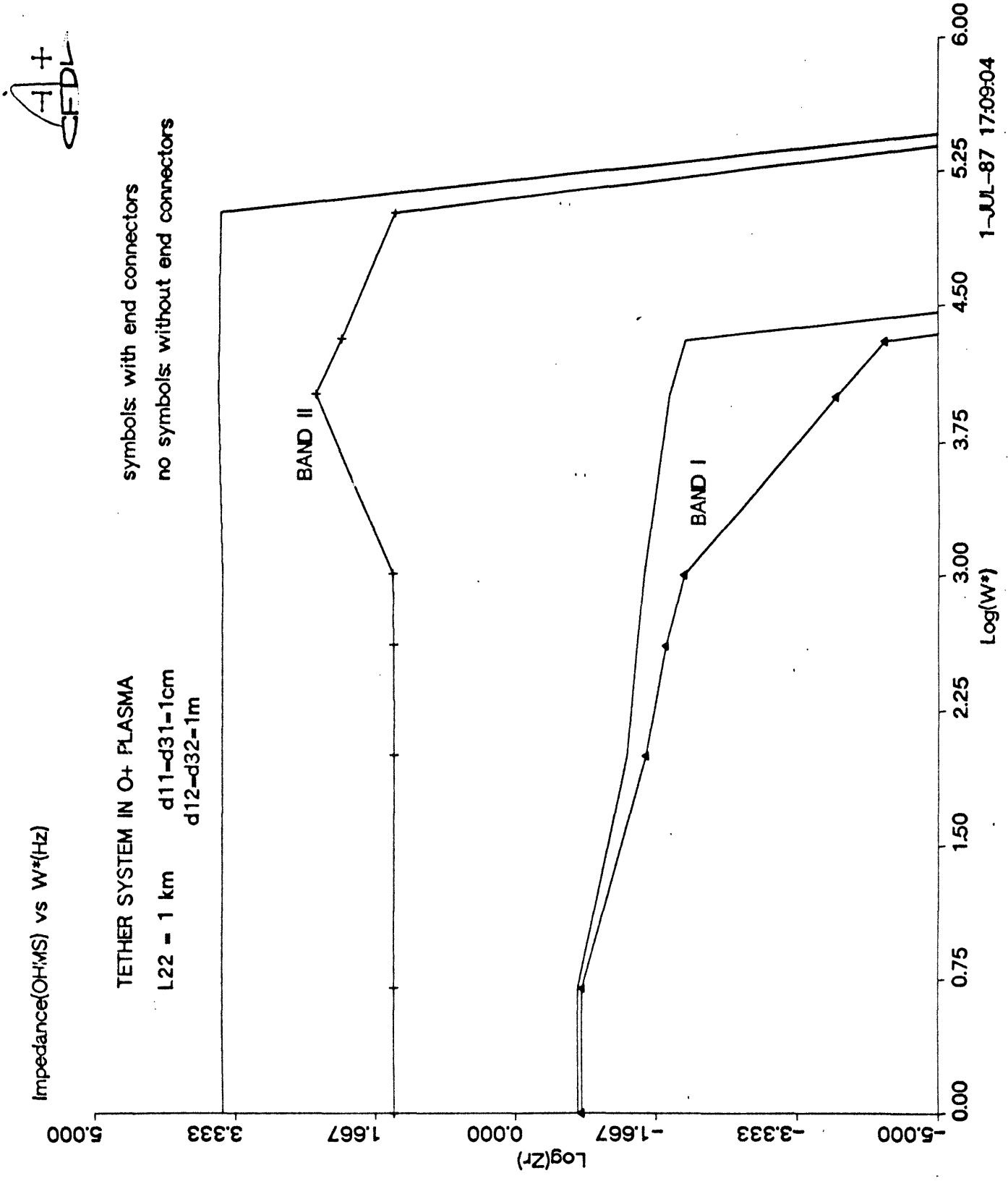

Figure 3.4: Impedance of 1 km tether–1 m terminator system in O^+ Plasma

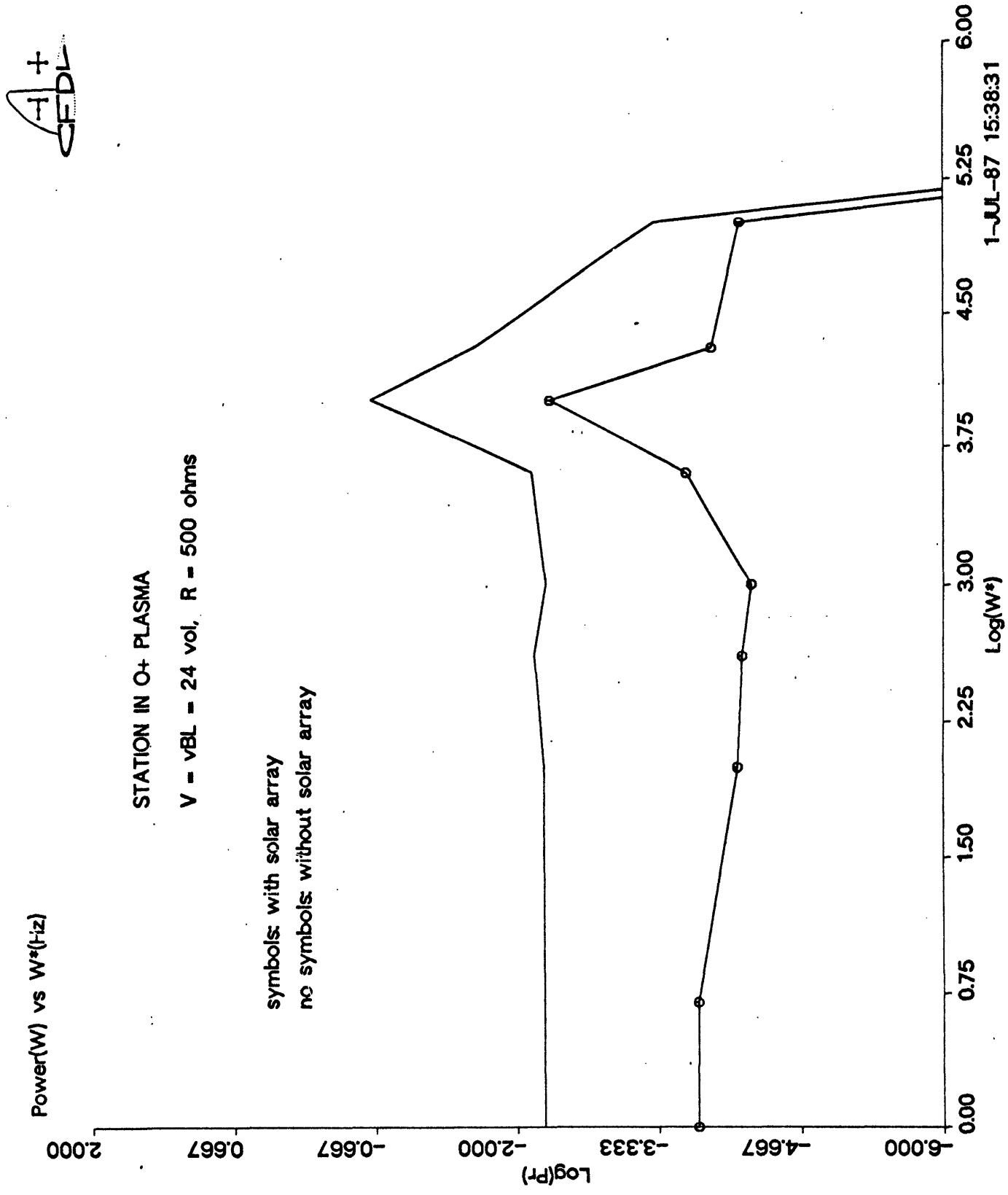

Figure 3.5: Passive Power Radiation in O^+ Plasma from Space Station

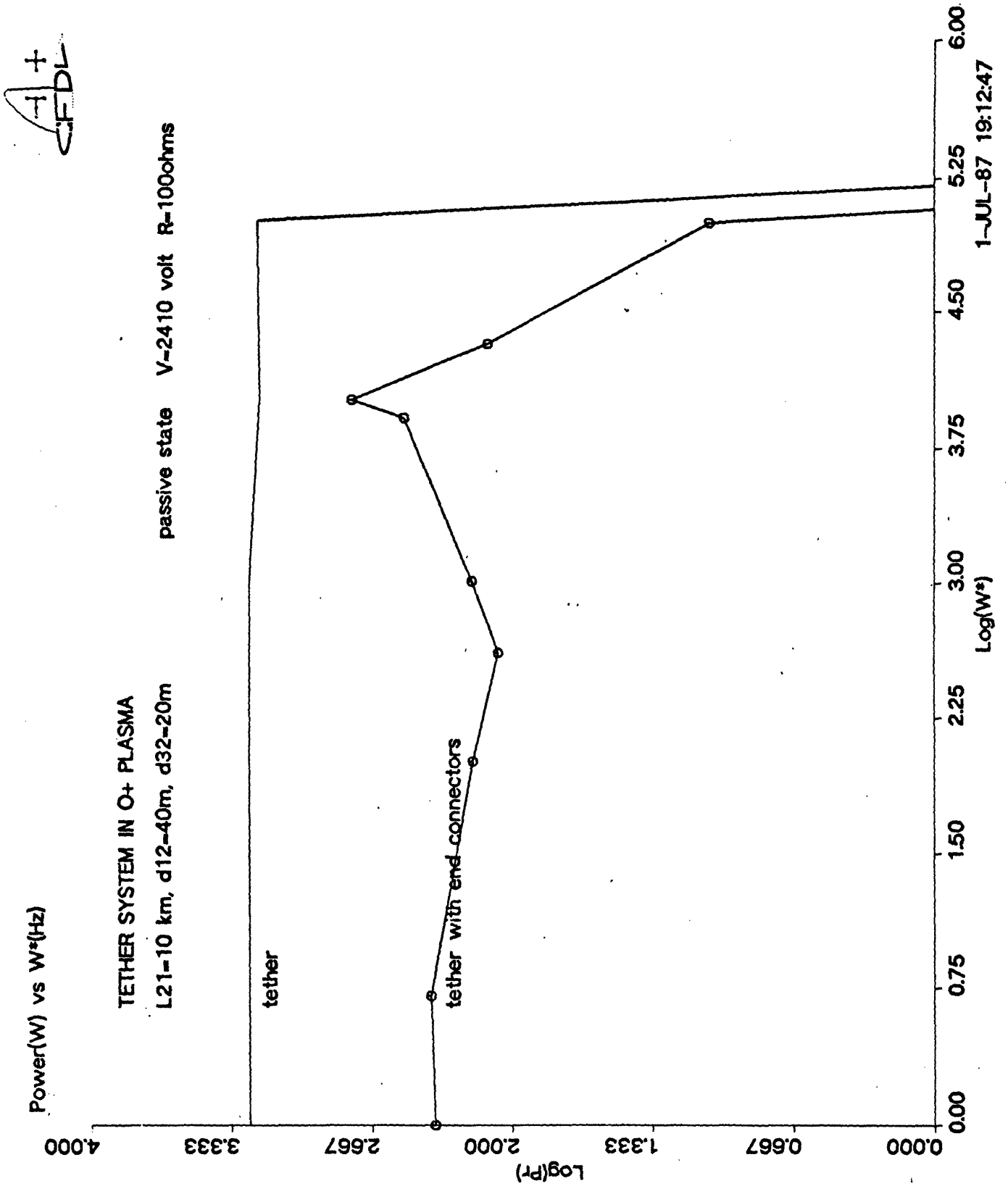

Figure 3.6: Passive Power Radiation in O^+ Plasma from Shuttle-Tether System

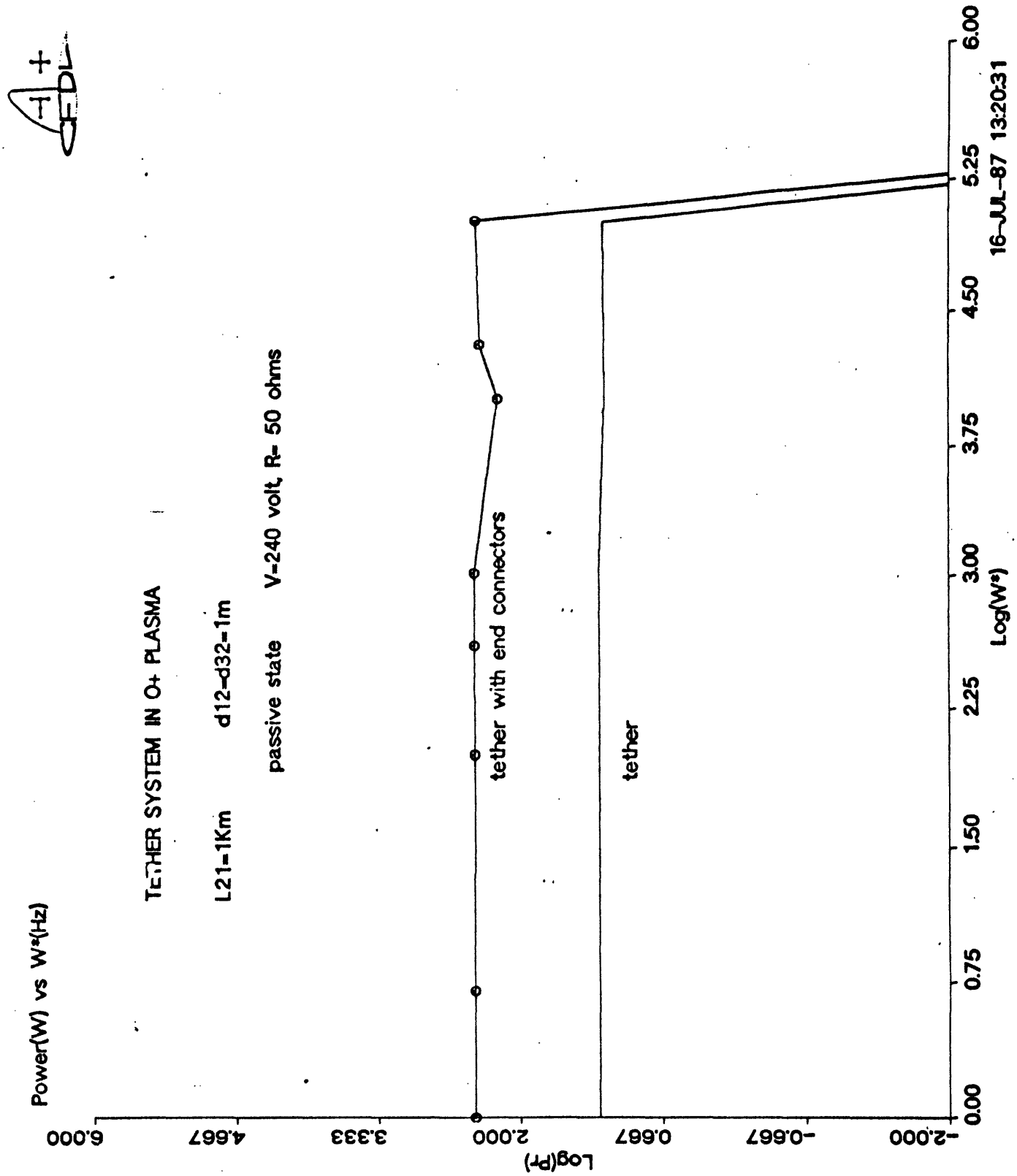

Figure 3.7: Passive Power Radiation in O^+ Plasma from 1 km tether–1 m terminator System

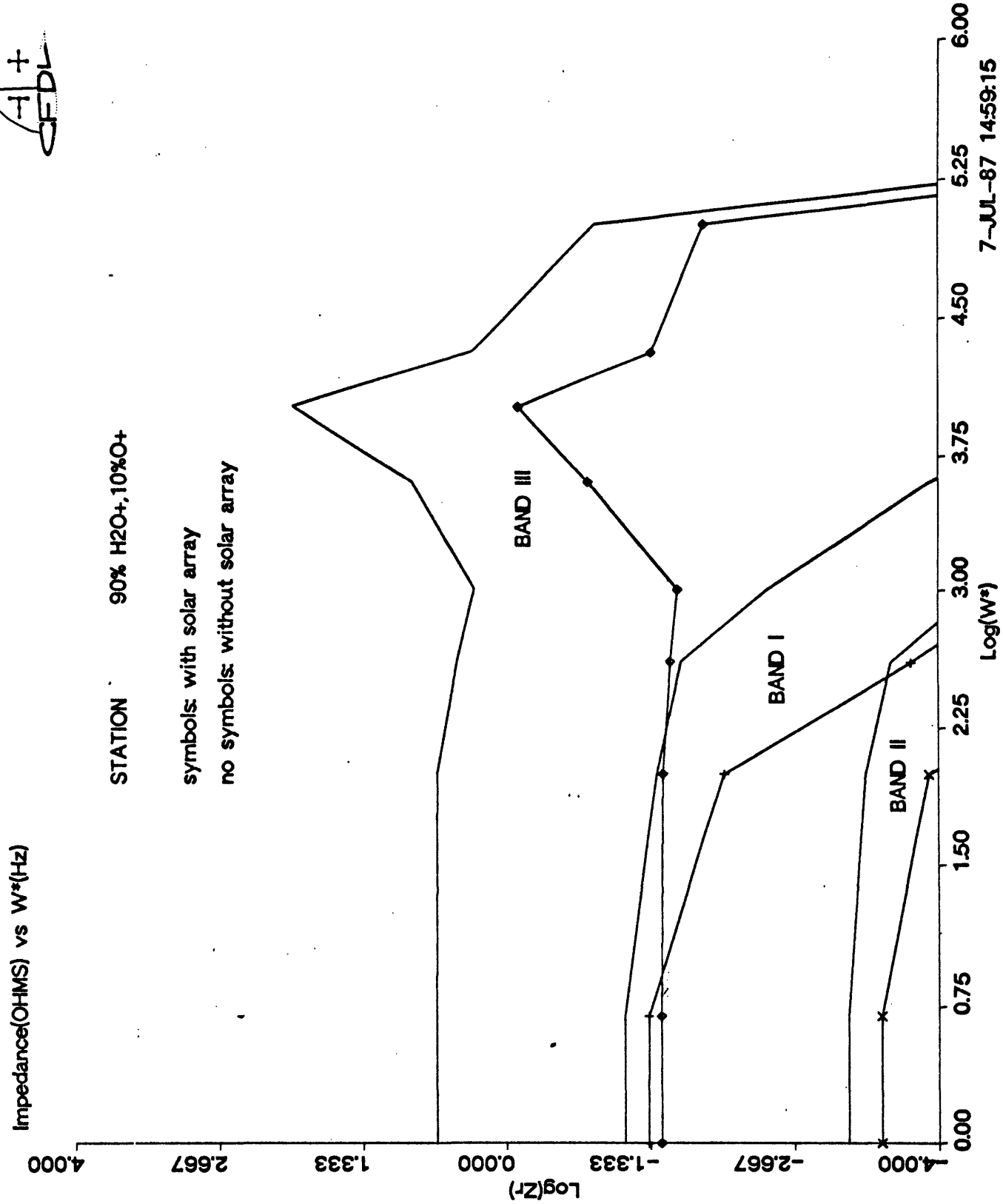

Figure 3.8: Impedance of Space station in $90\%H_2O^+ - 10\%O^+$ Plasma

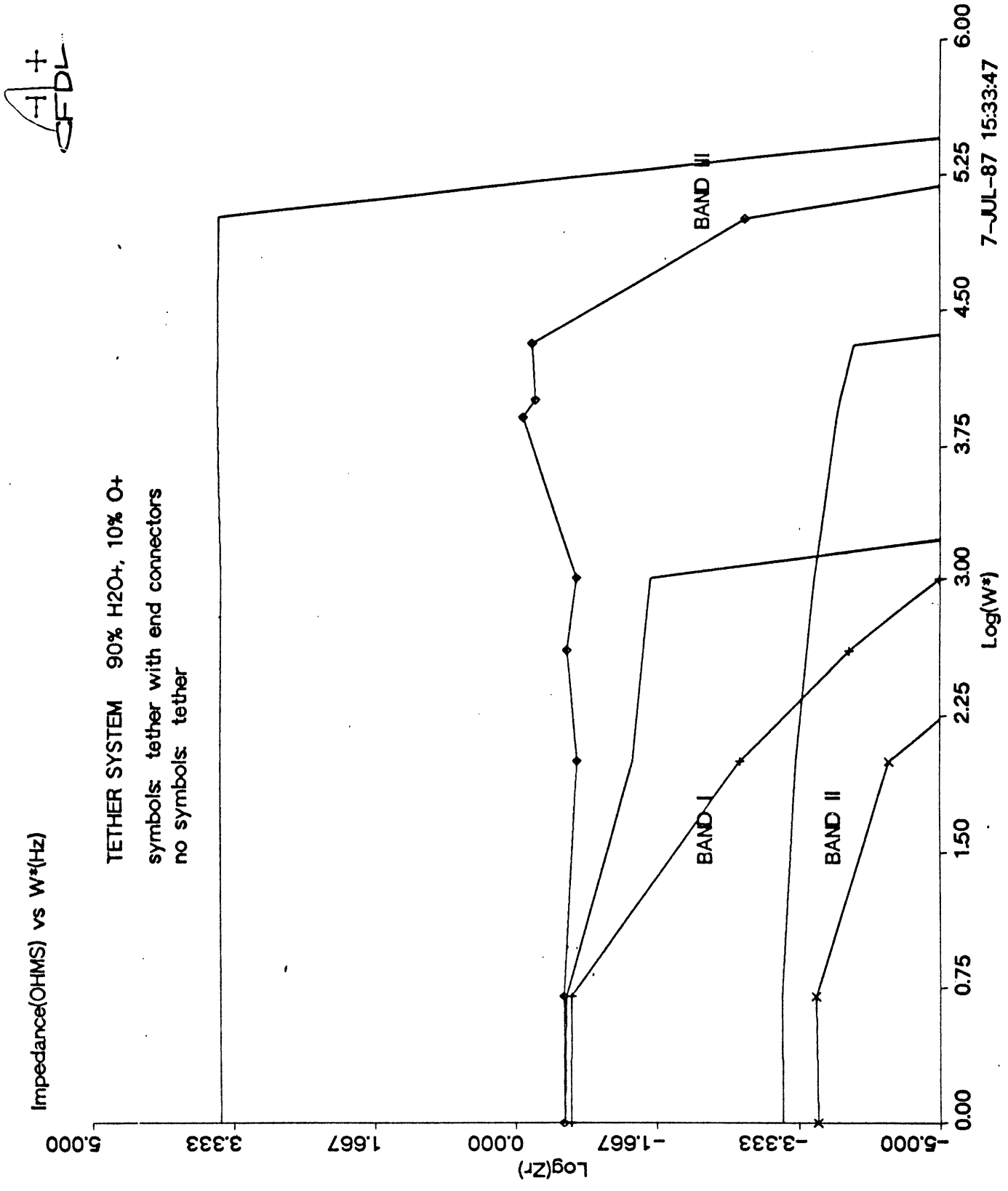

Figure 3.9: Impedance of Shuttle-Tether System in $90\%H_2O^+ - 10\%O^+$ Plasma

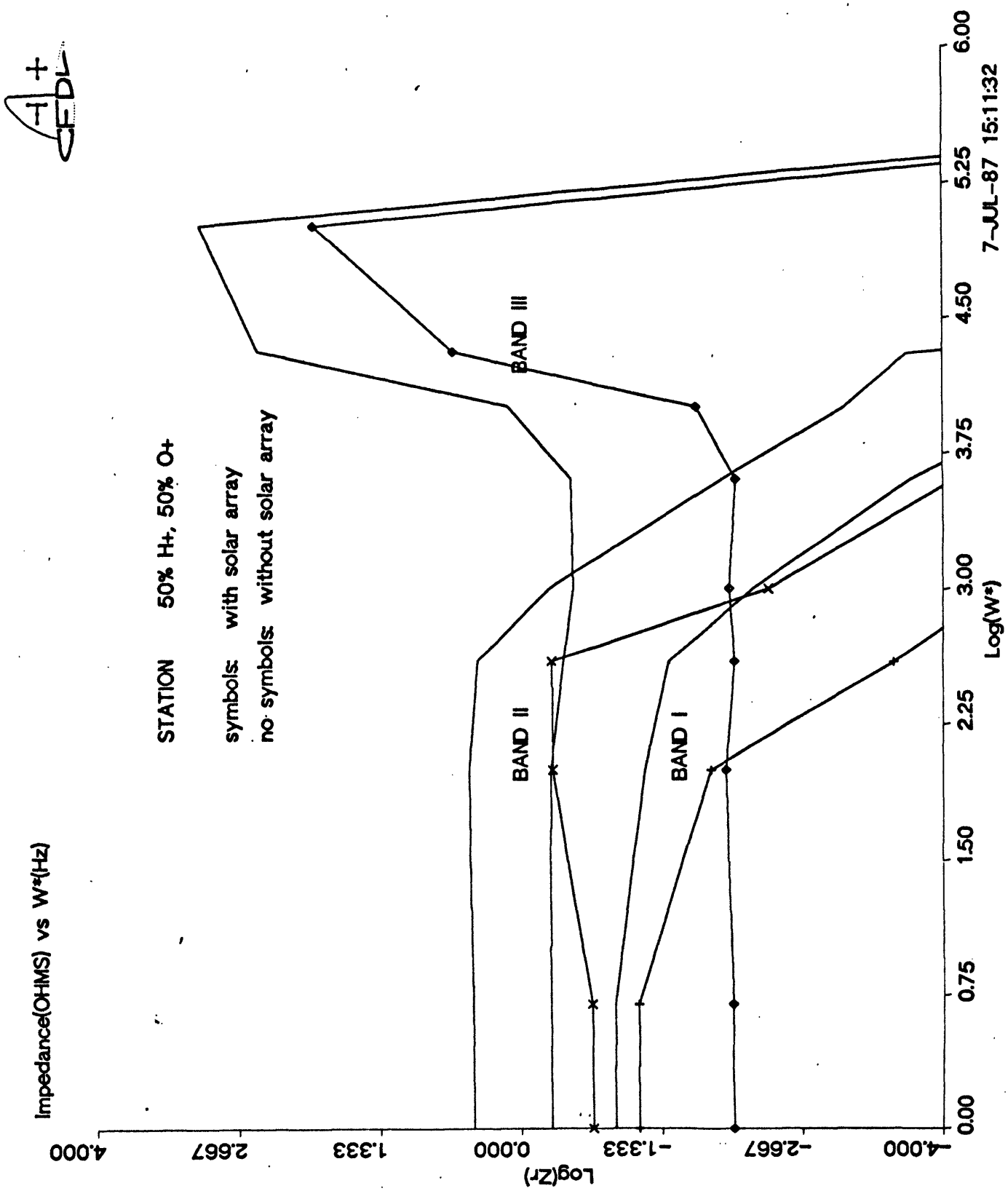

Figure 3.10: Impedance of Space station in $50\%H^+ - 50\%O^+$ Plasma

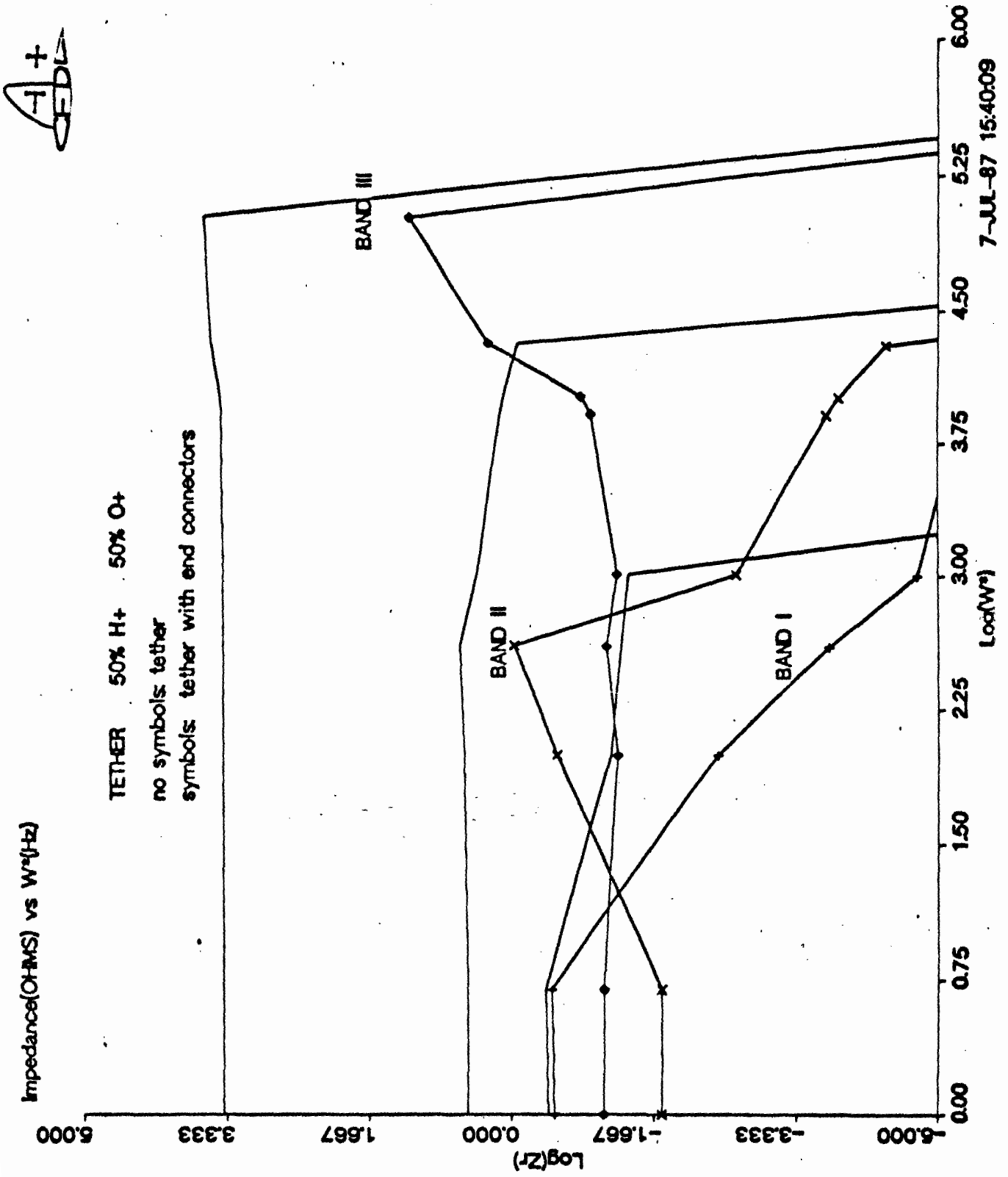

Figure 3.11: Impedance of Shuttle-Tether System in $50\%H^+ - 50\%O^+$ Plasma

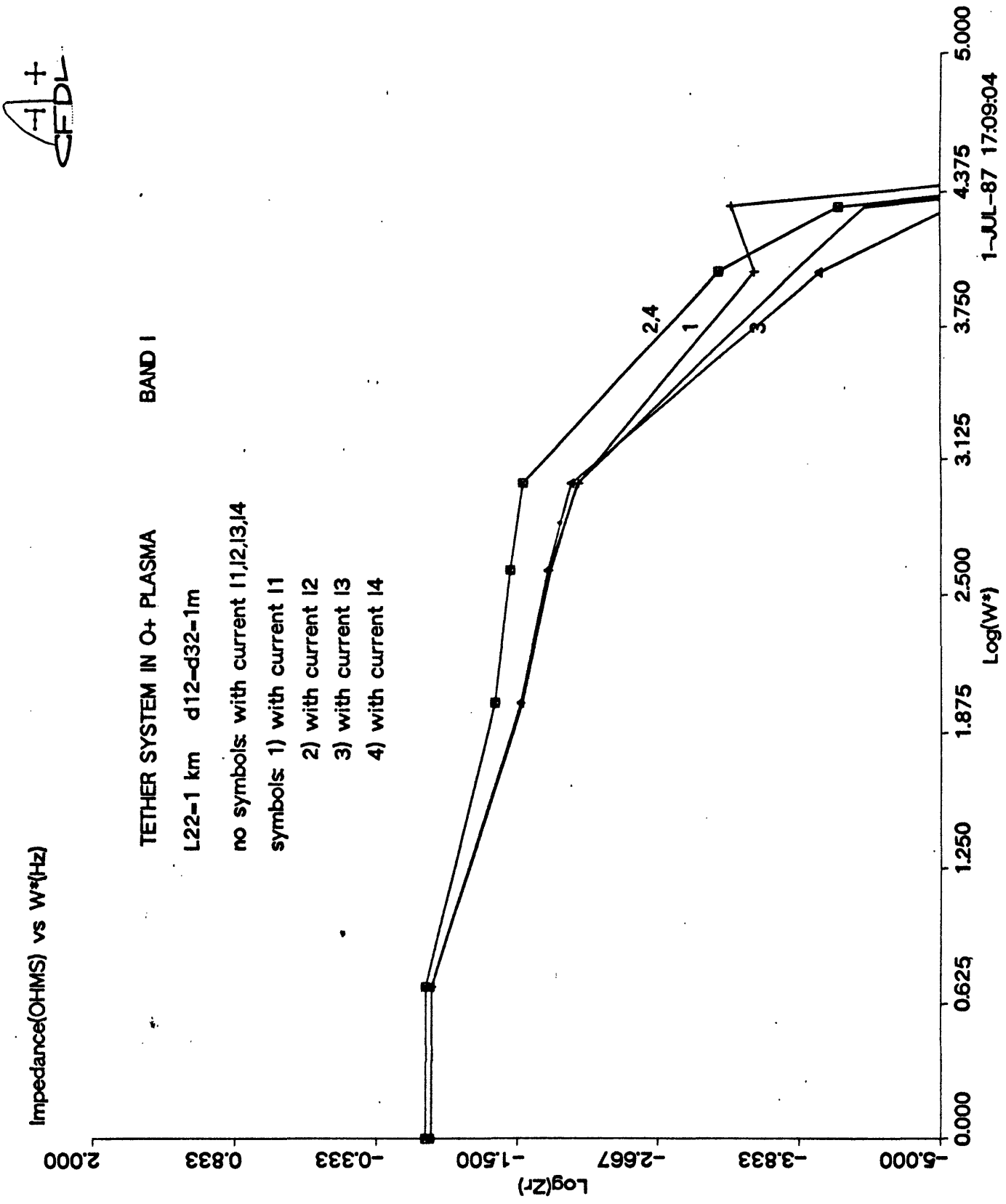

Figure 3.12: 1 km tether–1 m terminator system with different boundary current pattern: impedance–band I

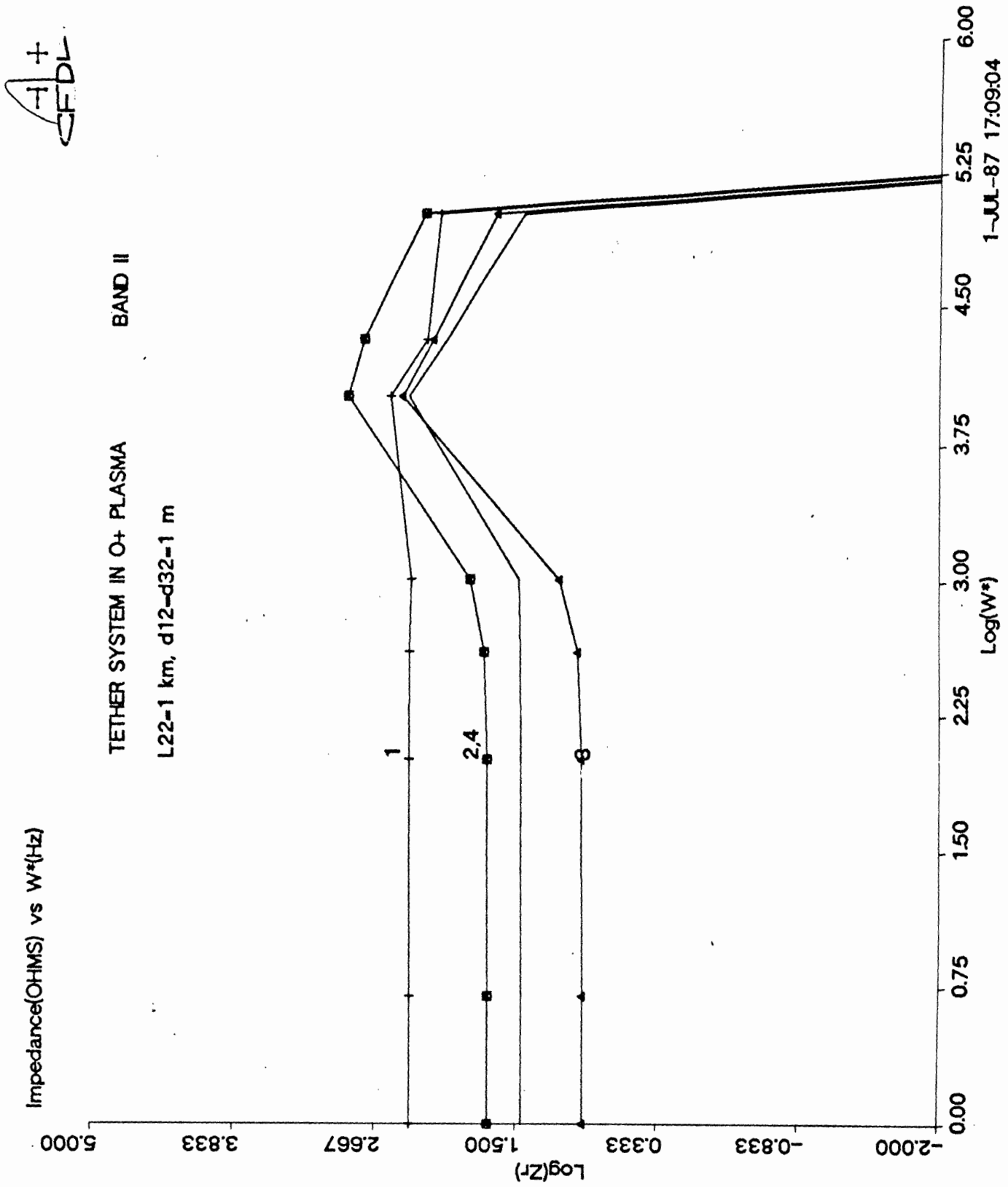

Figure 3.13: 1 km tether–1 m terminator system with different boundary current pattern: impedance–band II

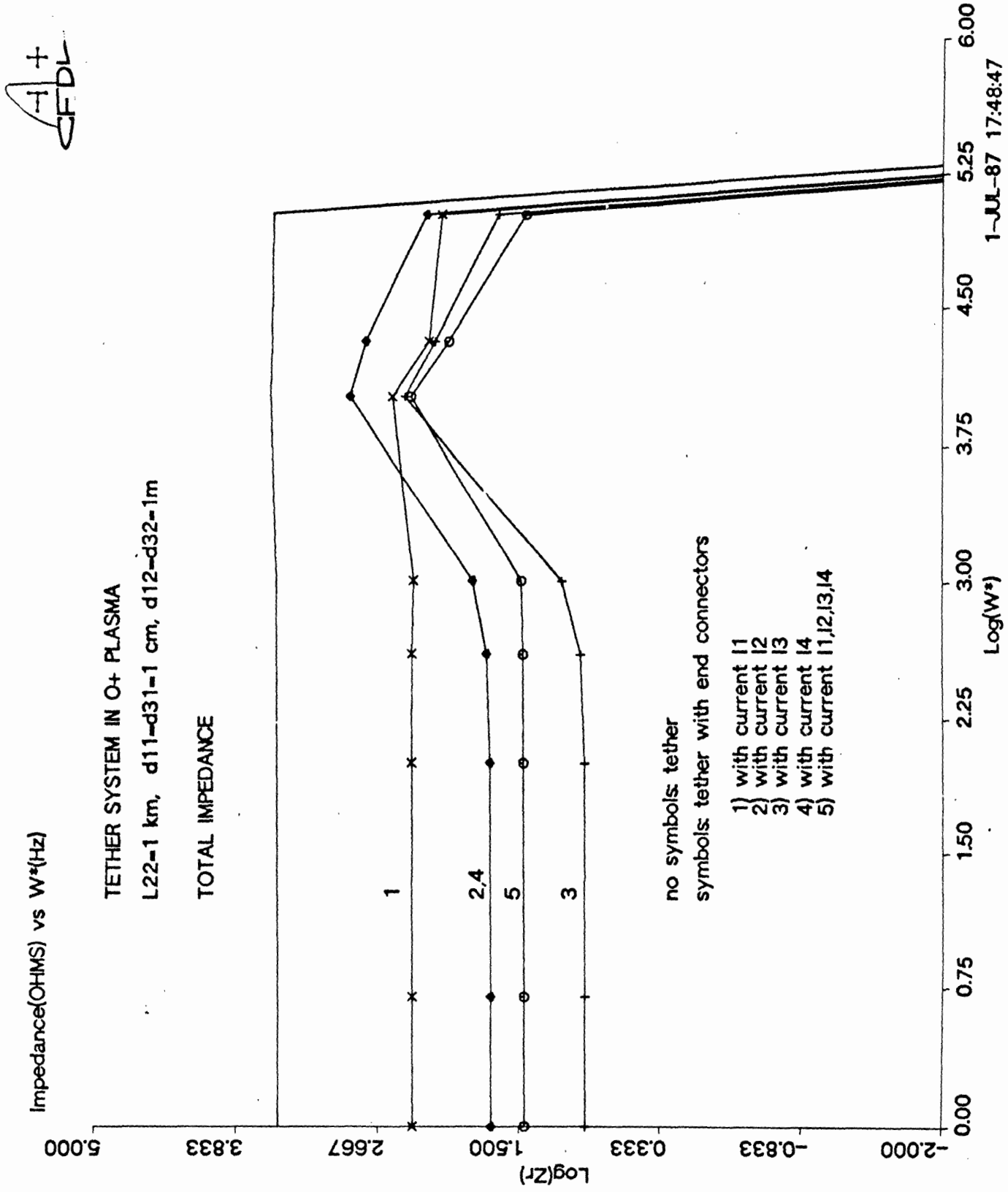

Figure 3.14: 1 km tether–1 m terminator system with different boundary current pattern: total impedance

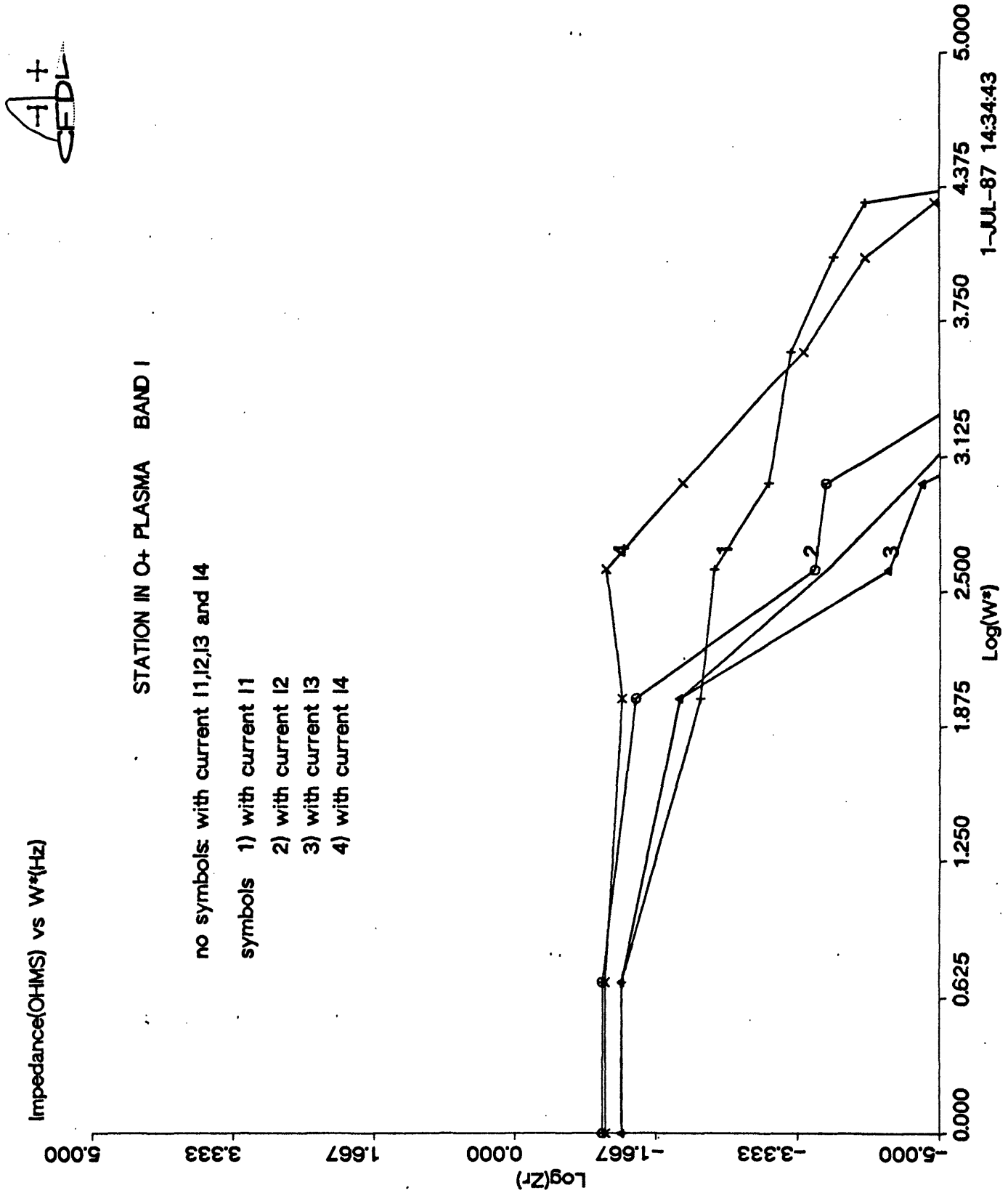

Figure 3.15: Space station with different boundary current pattern: impedance–band I

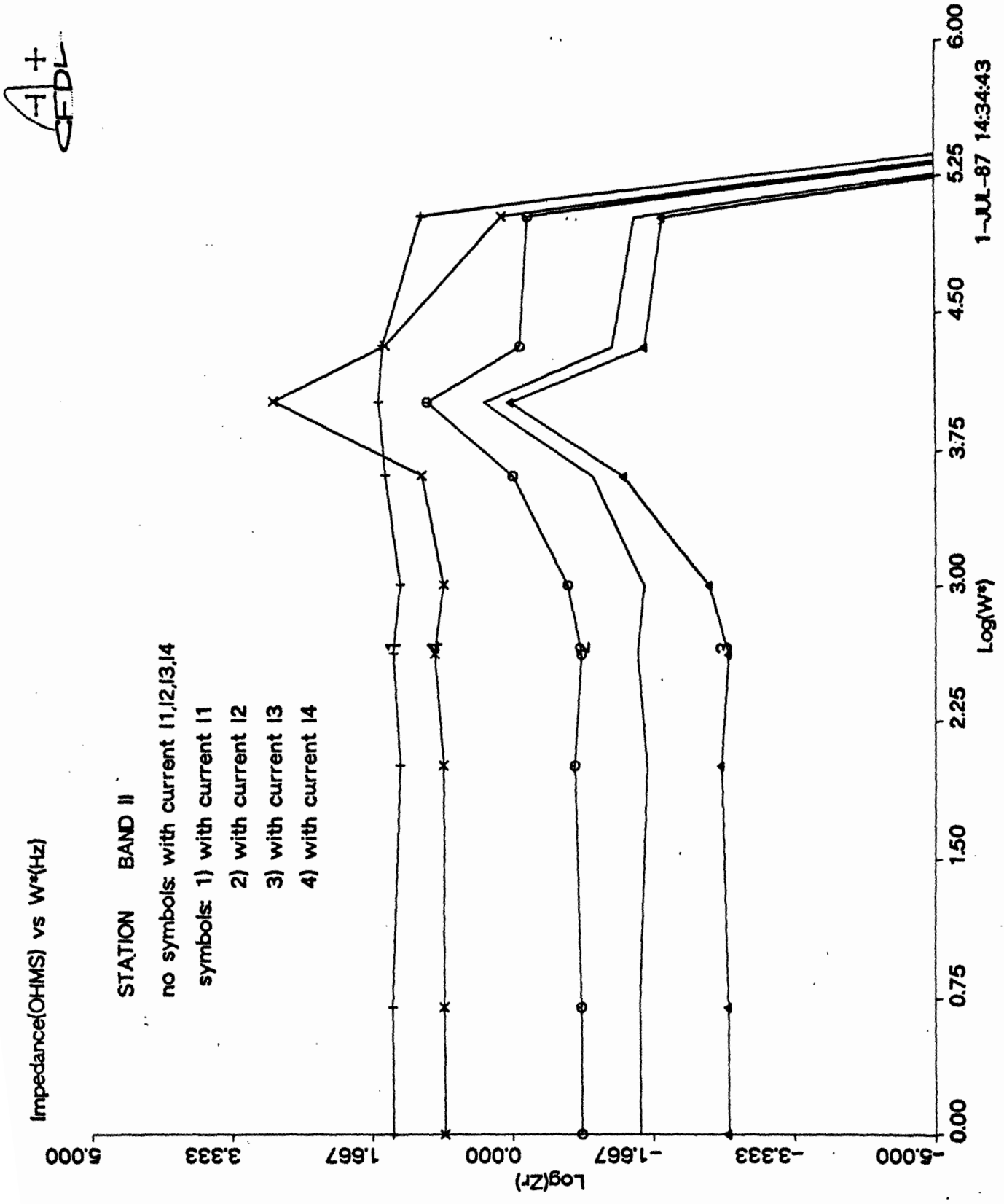

Figure 3.16: Space station with different boundary current pattern: impedance–band II

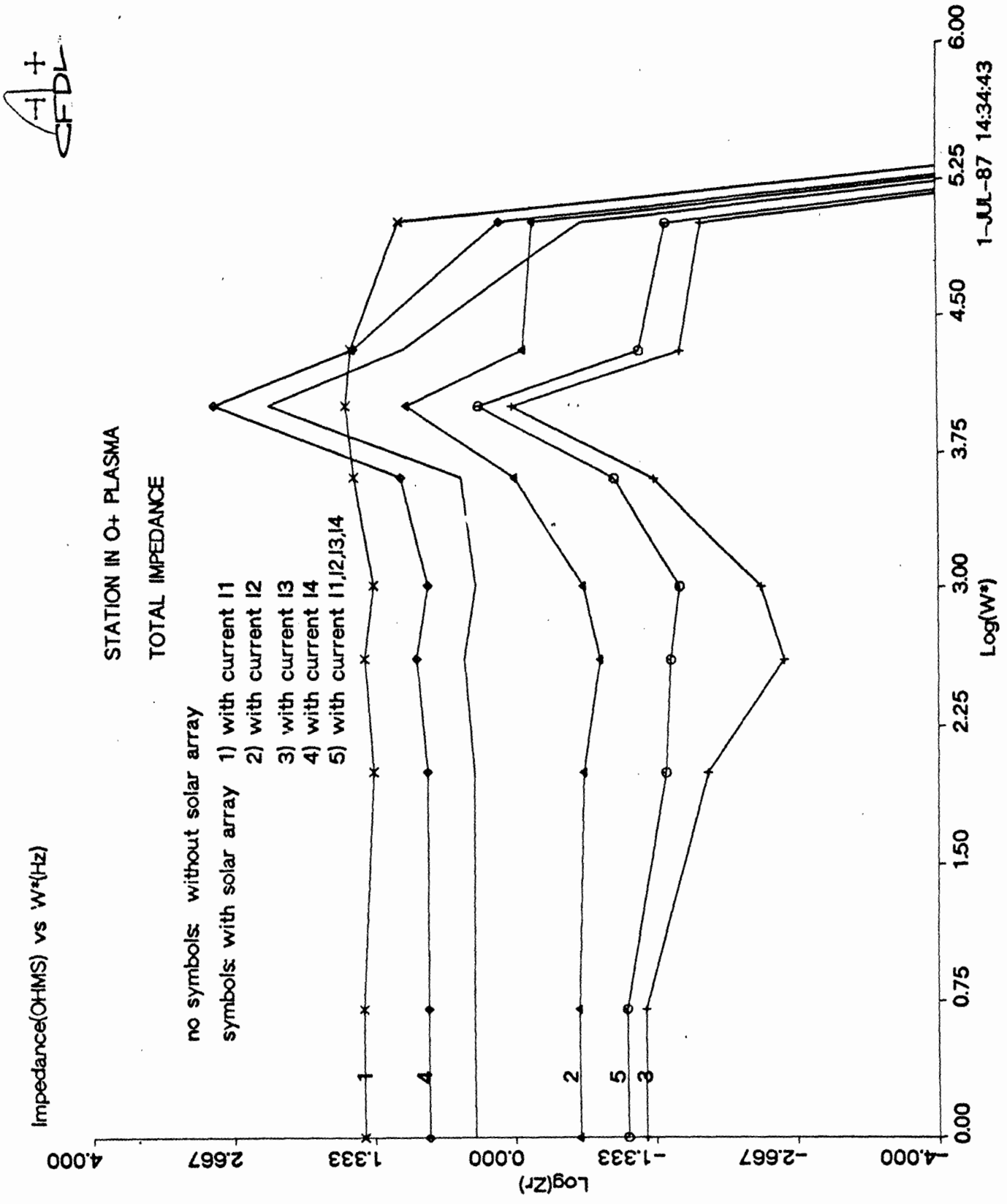

Figure 3.17: Space station with different boundary current pattern: total impedance

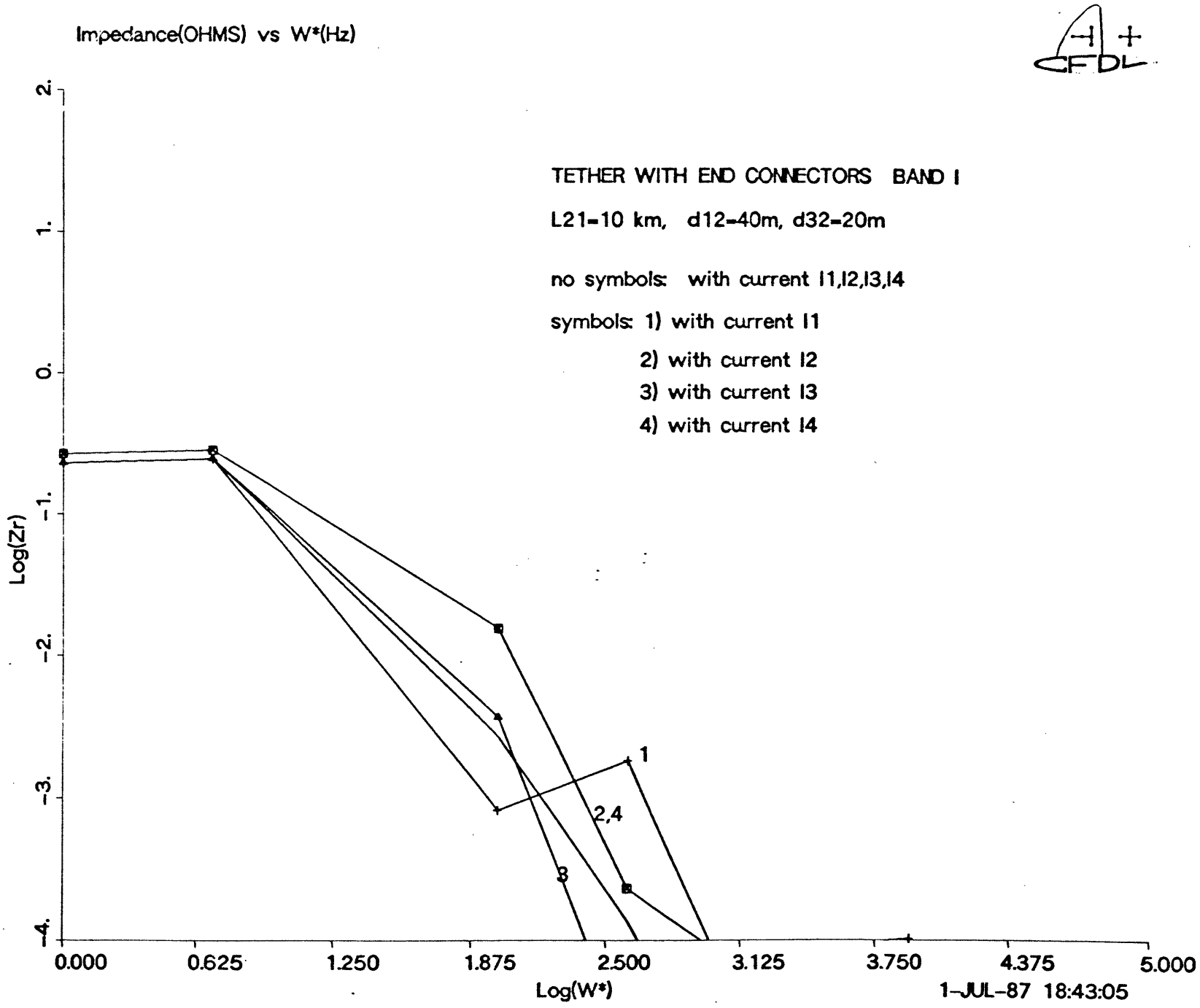

Figure 3.18: Shuttle-tether system with different boundary current pattern: impedance–band I

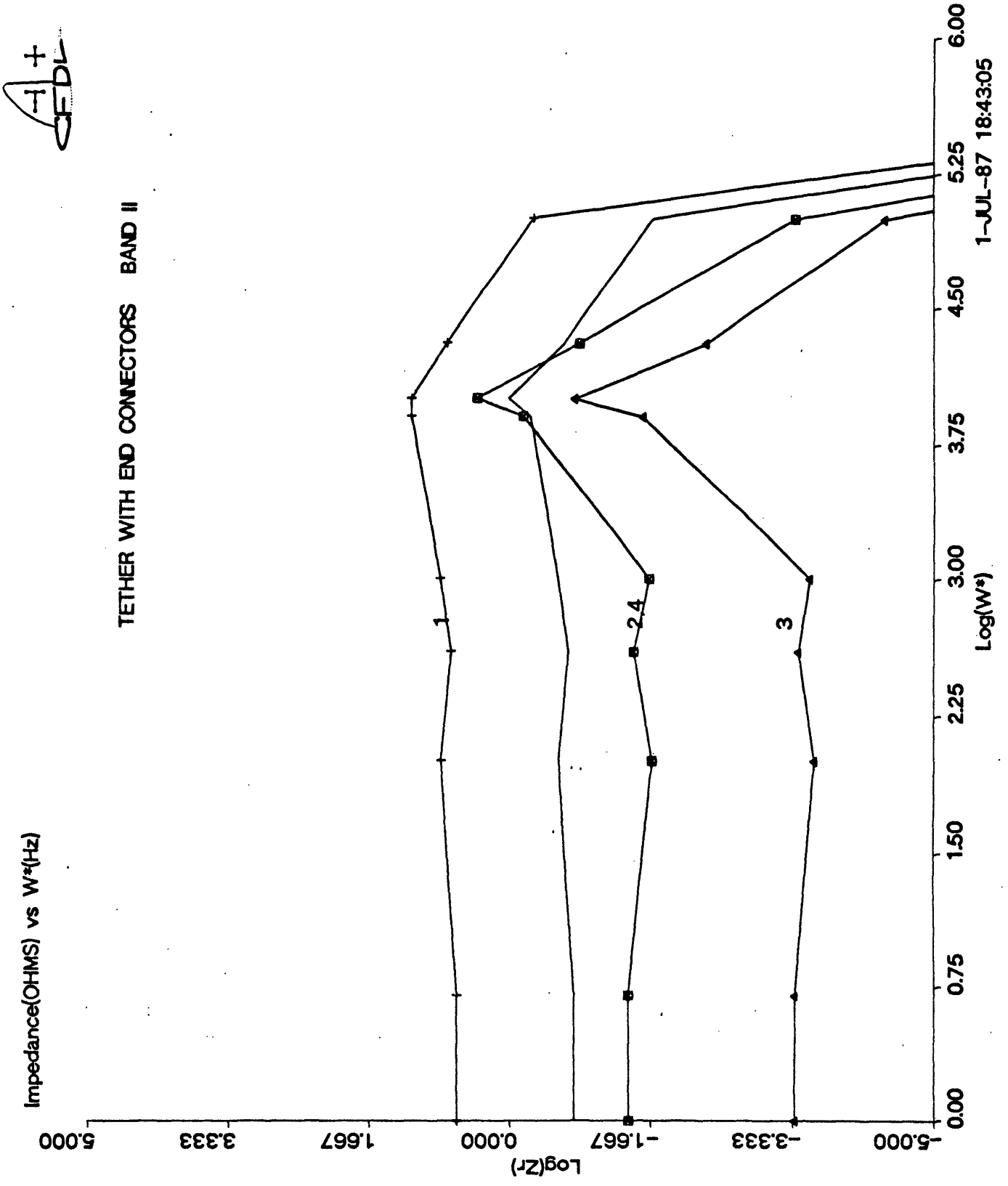

Figure 3.19: Shuttle-tether system with different boundary current pattern: impedance–band II

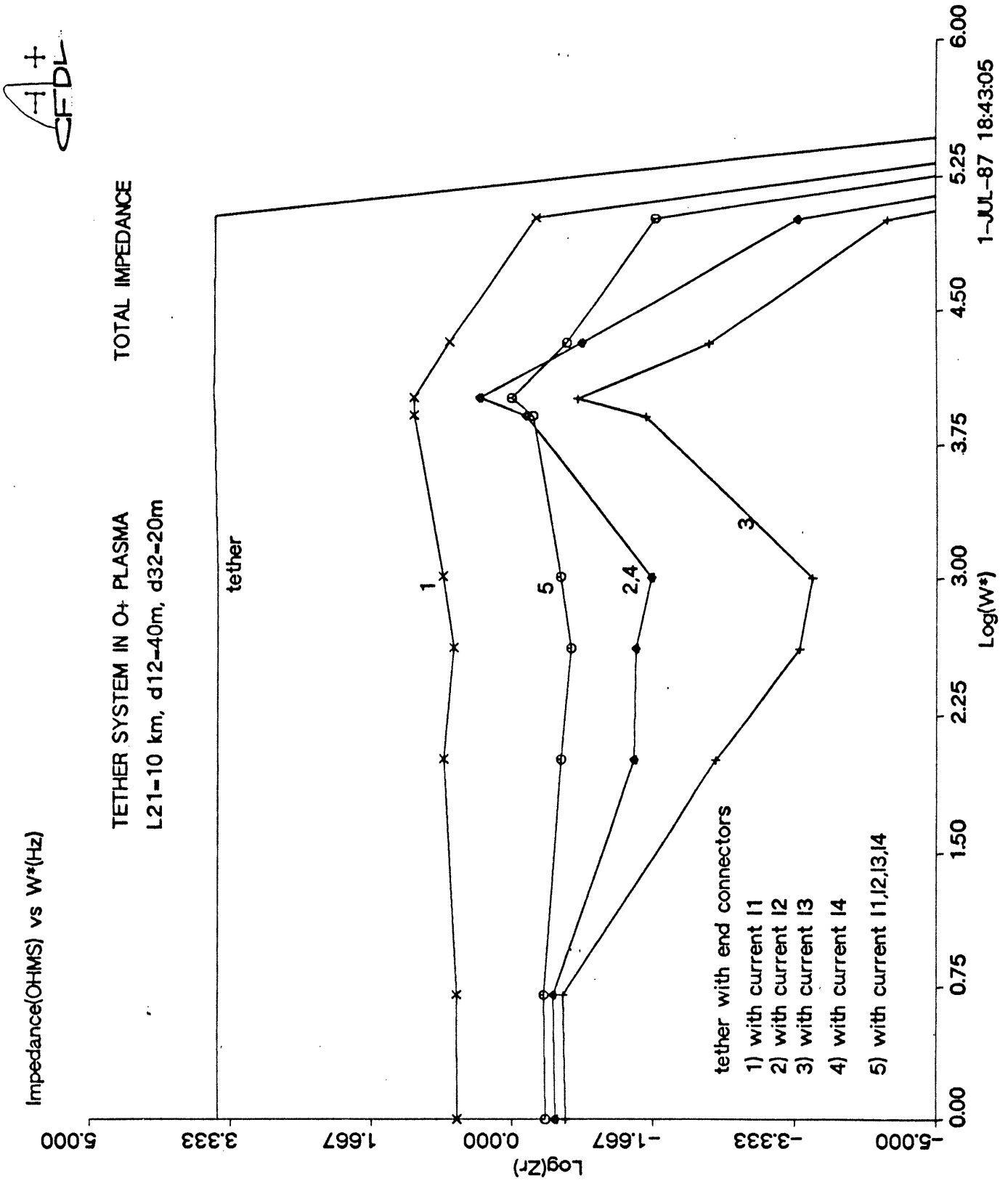

Figure 3.20: Shuttle-tether system with different boundary current pattern: total impedance

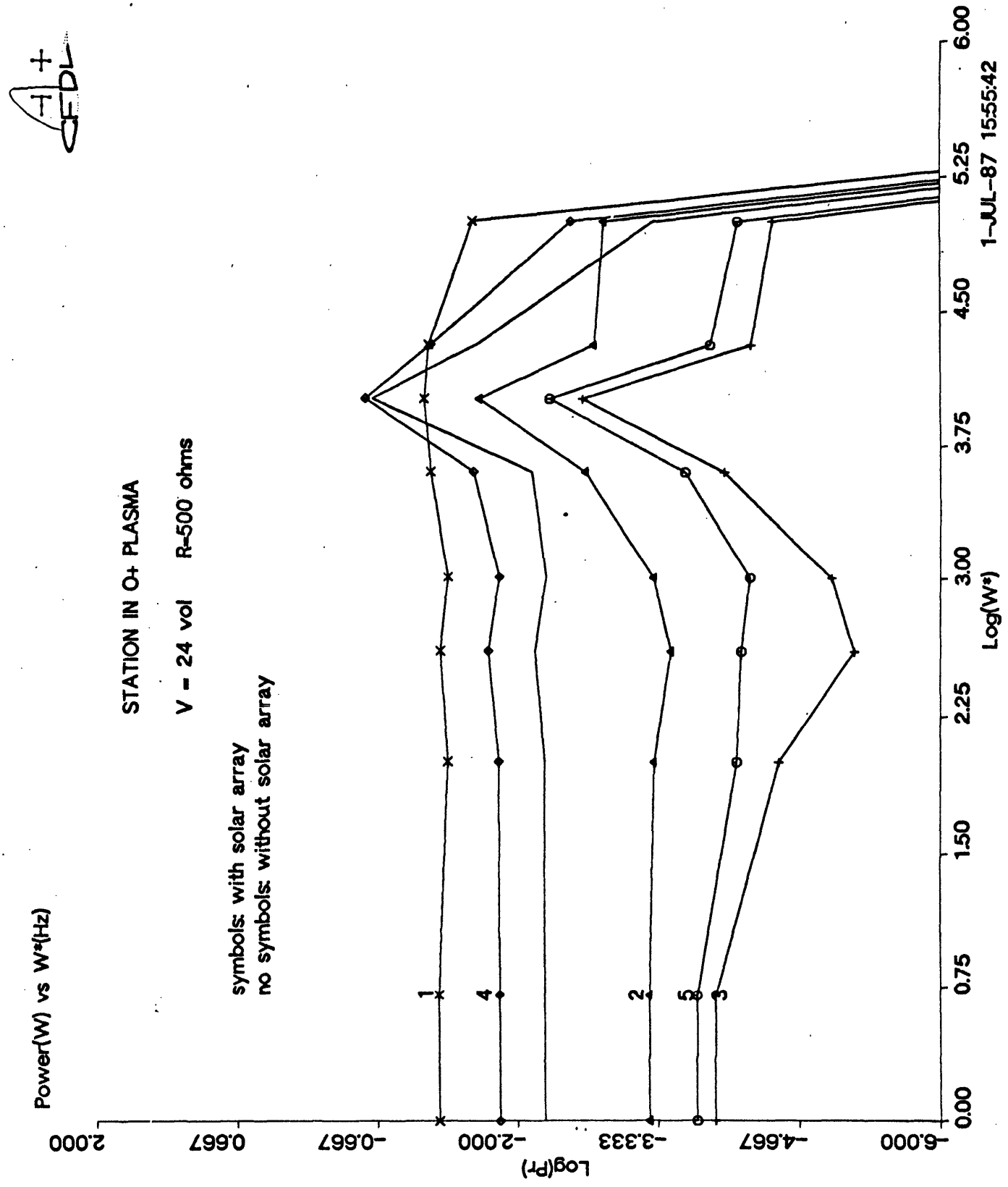

Figure 3.21: Space station with different boundary current pattern: power radiated

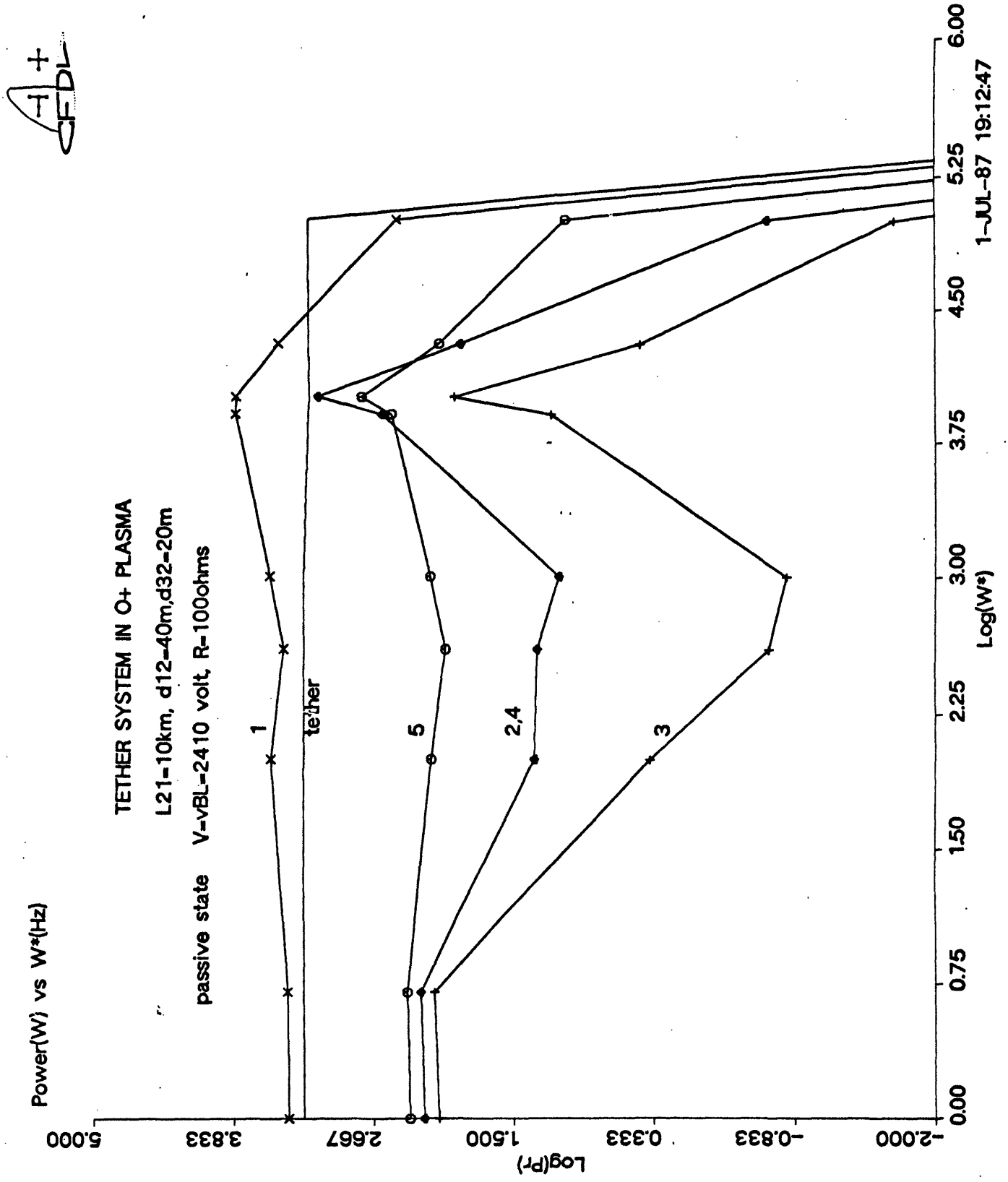

Figure 3.22: Shuttle-tether system with different boundary current pattern: power radiated

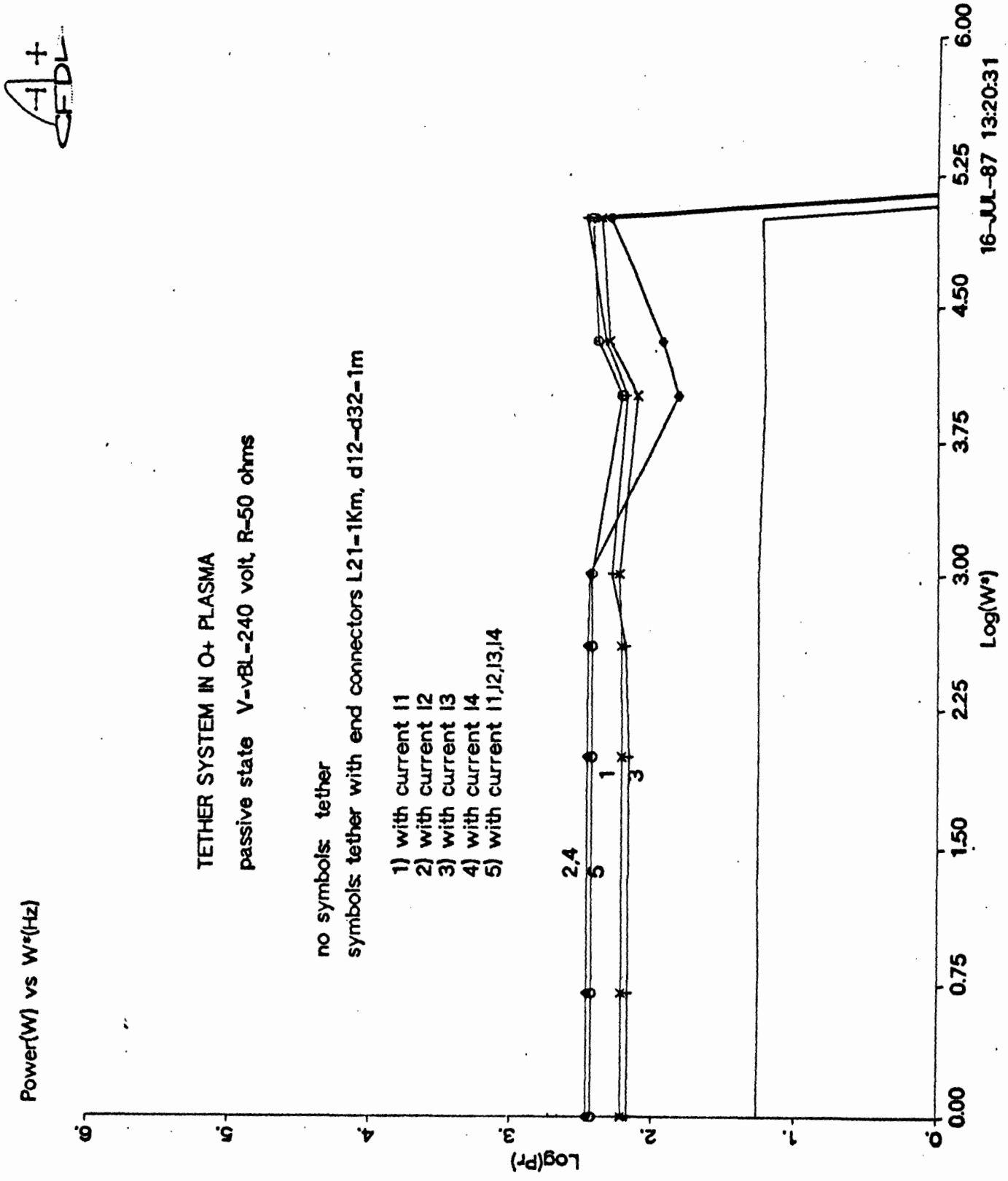

Figure 3.23: 1 km tether–1 m terminator system with different boundary current pattern: power radiated

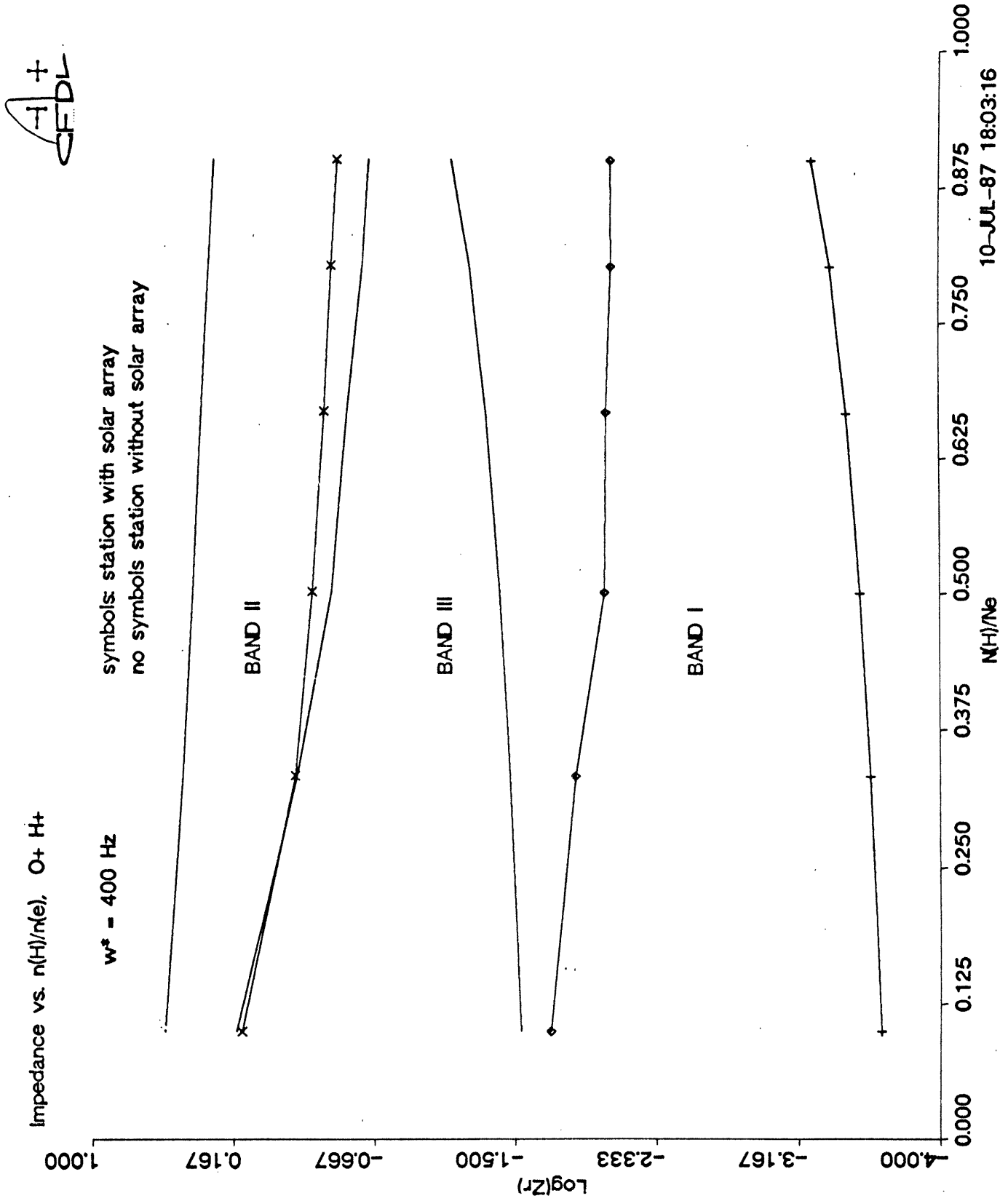

Figure 3.24: Effect of multi-ion spacies: impedance of space station associated with each band (w^*=400 Hz)

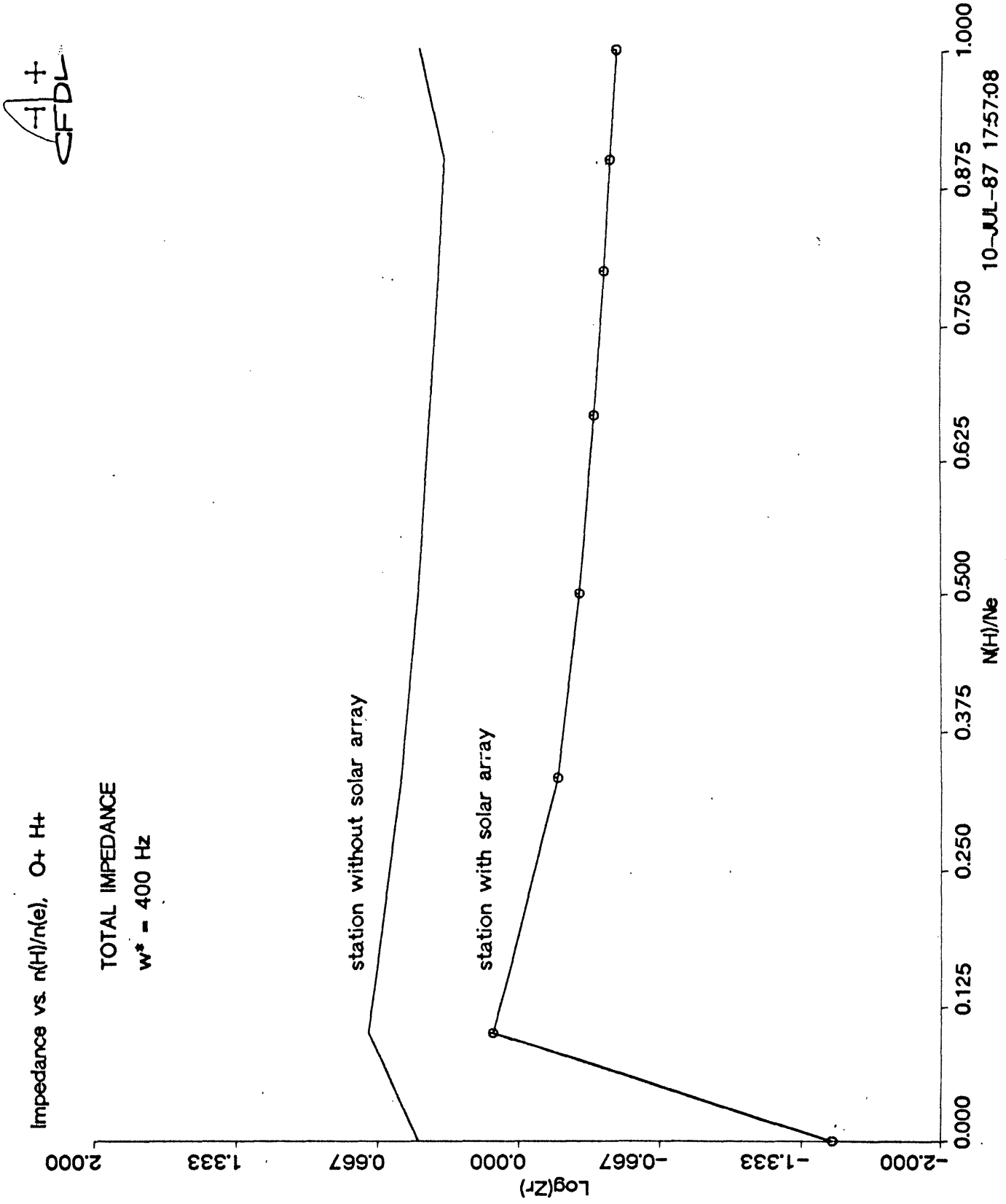

Figure 3.25: Effect of multi-ion spacies: total impedance of space station (w^*=400 Hz)

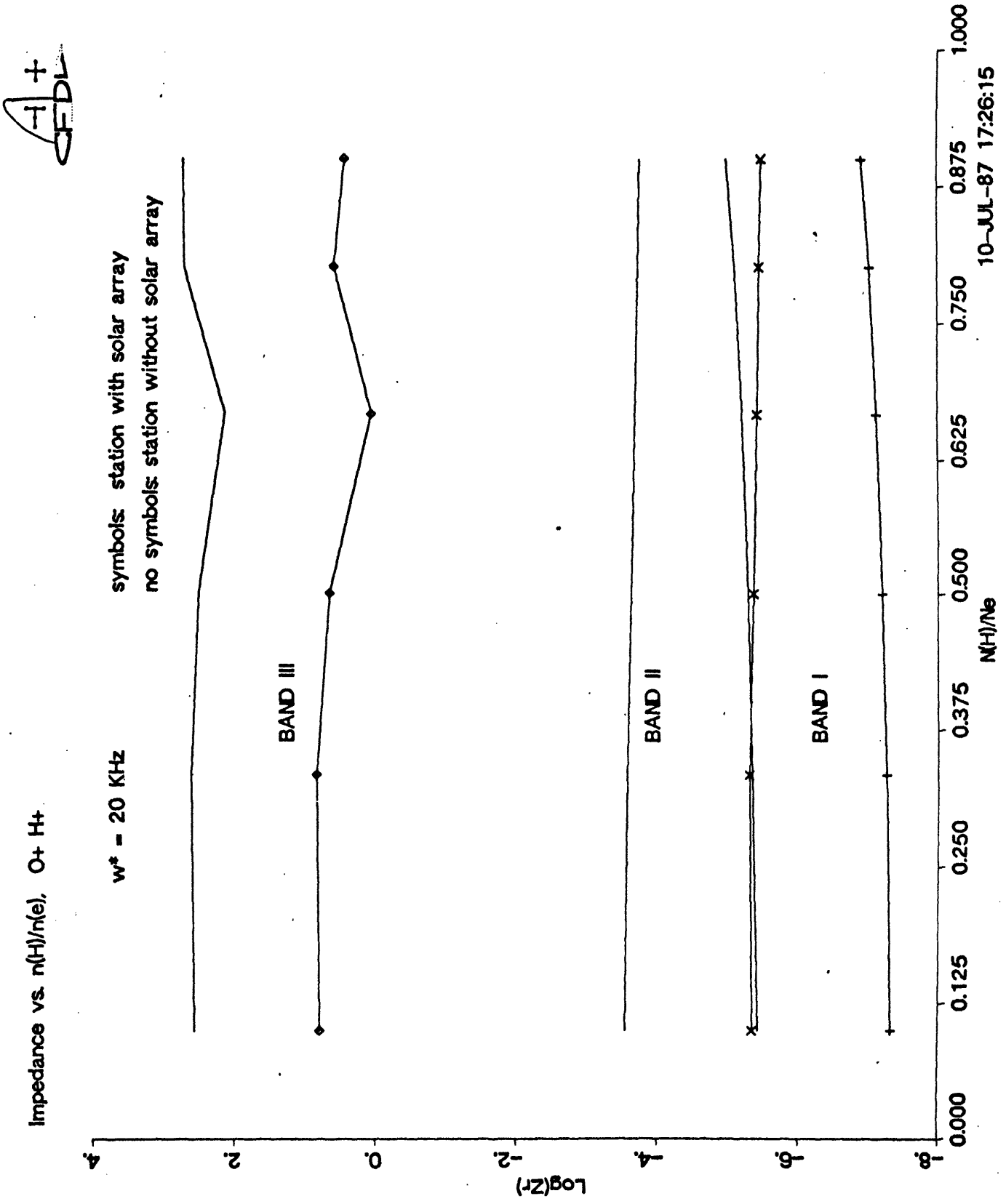

Figure 3.26: Effect of multi-ion spacies: impedance of space station associated with each band (w^*=20 kHz)

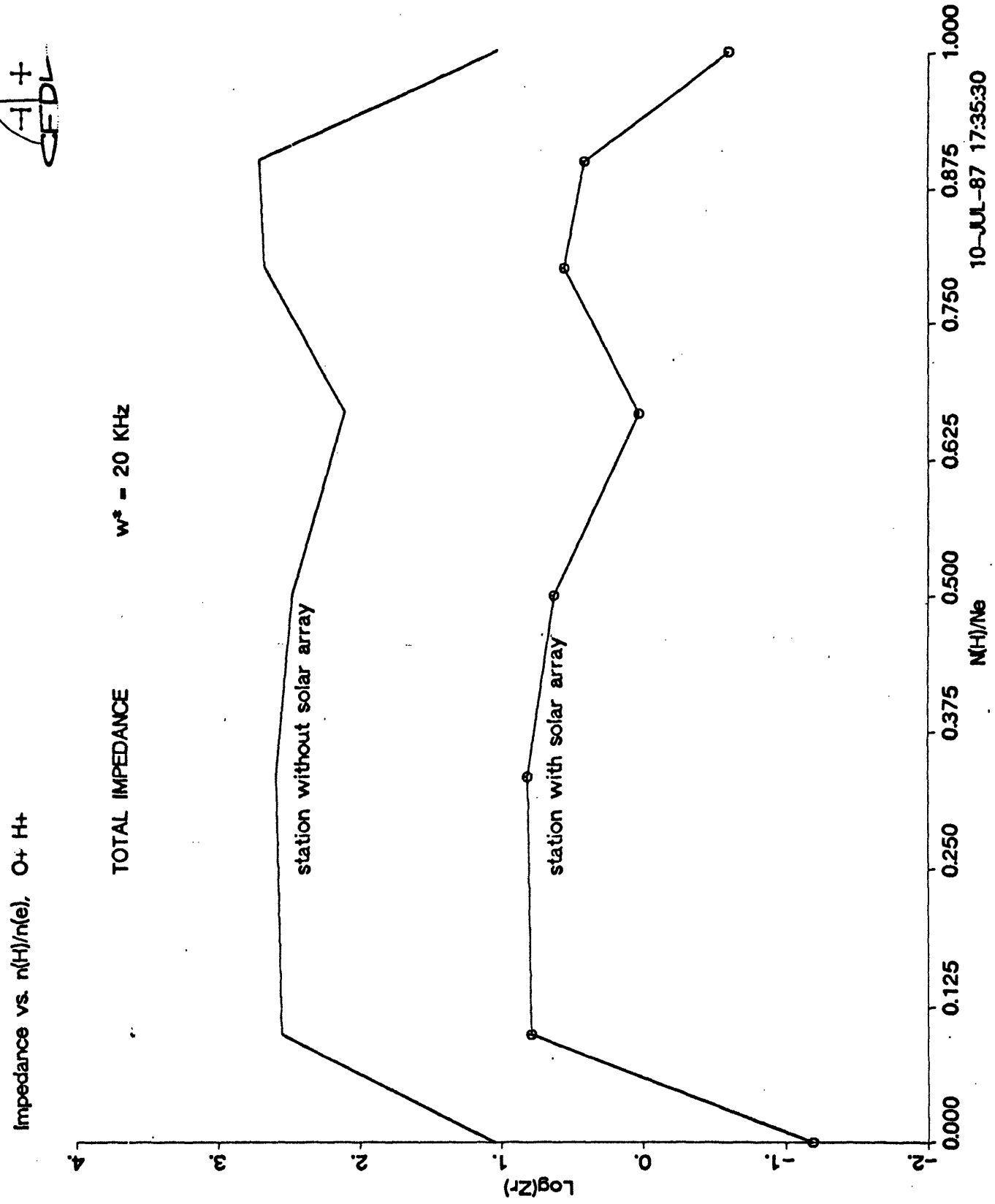

Figure 3.27: Effect of multi-ion spacies: total impedance of space station (w^*=20 kHz)

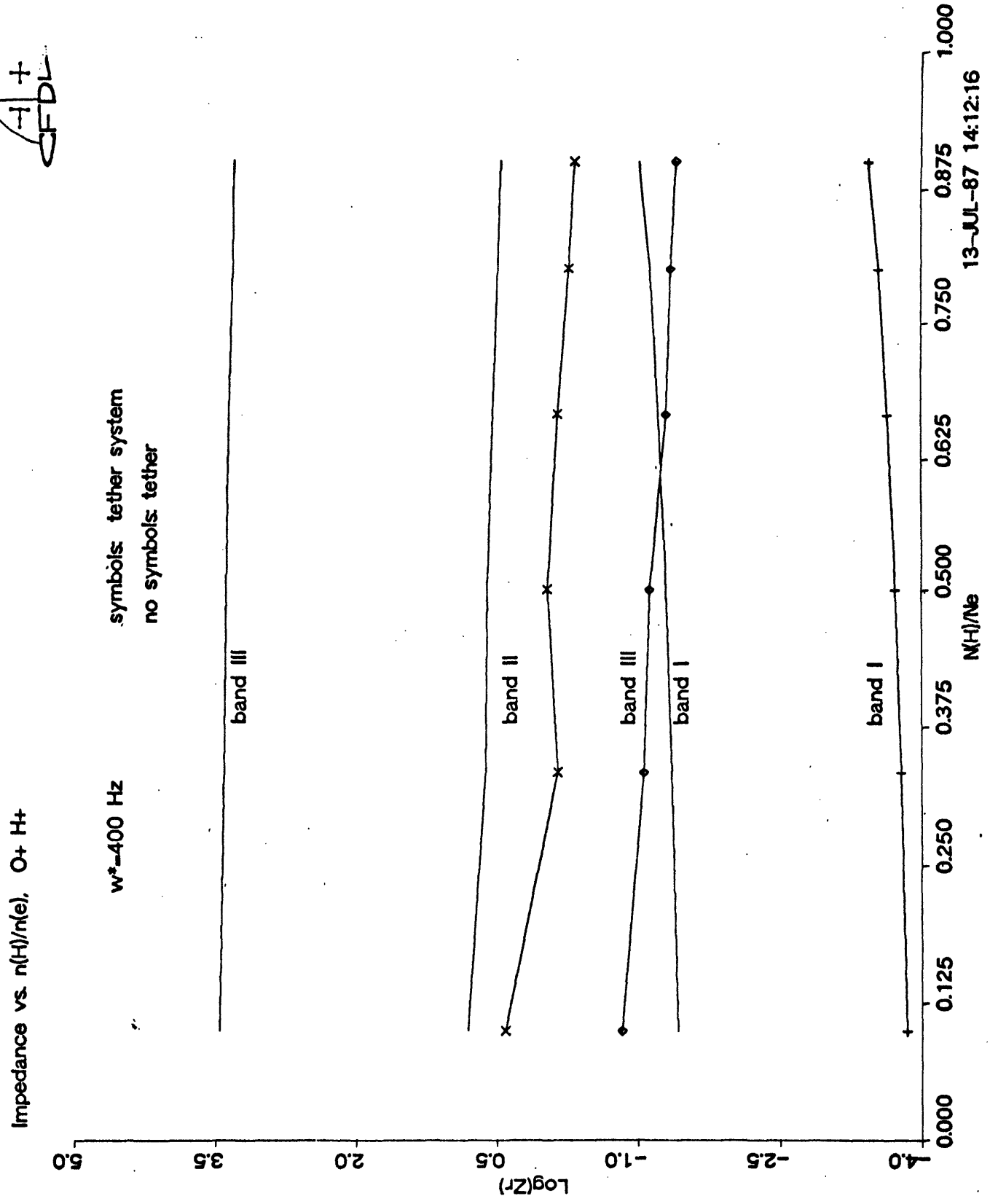

Figure 3.28: Effect of multi-ion spacies: impedance of shuttle-tether system associated with each band (w^*=400 Hz)

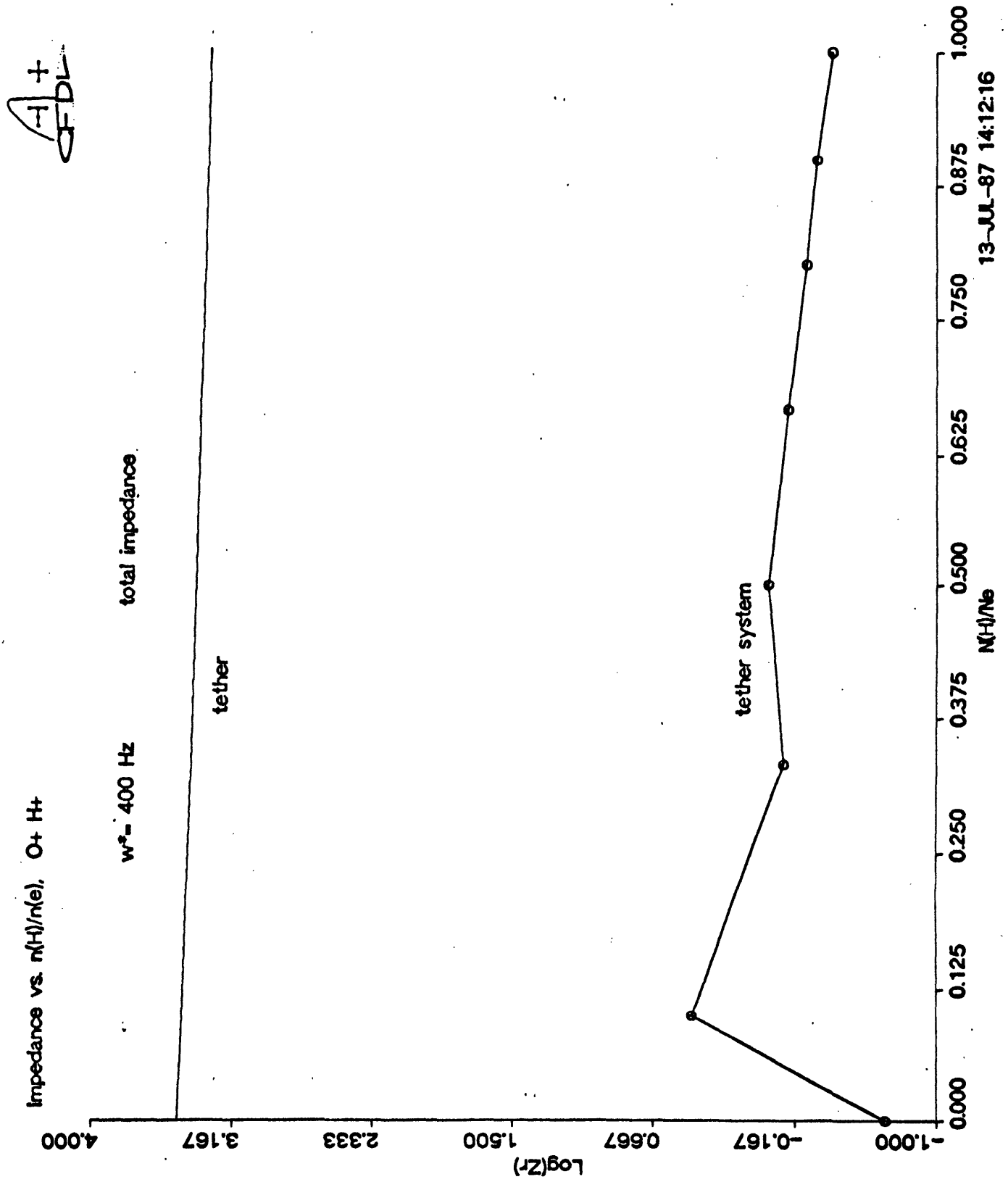

Figure 3.29: Effect of multi-ion spacies: total impedance of shuttle-tether system (w^*=400 Hz)

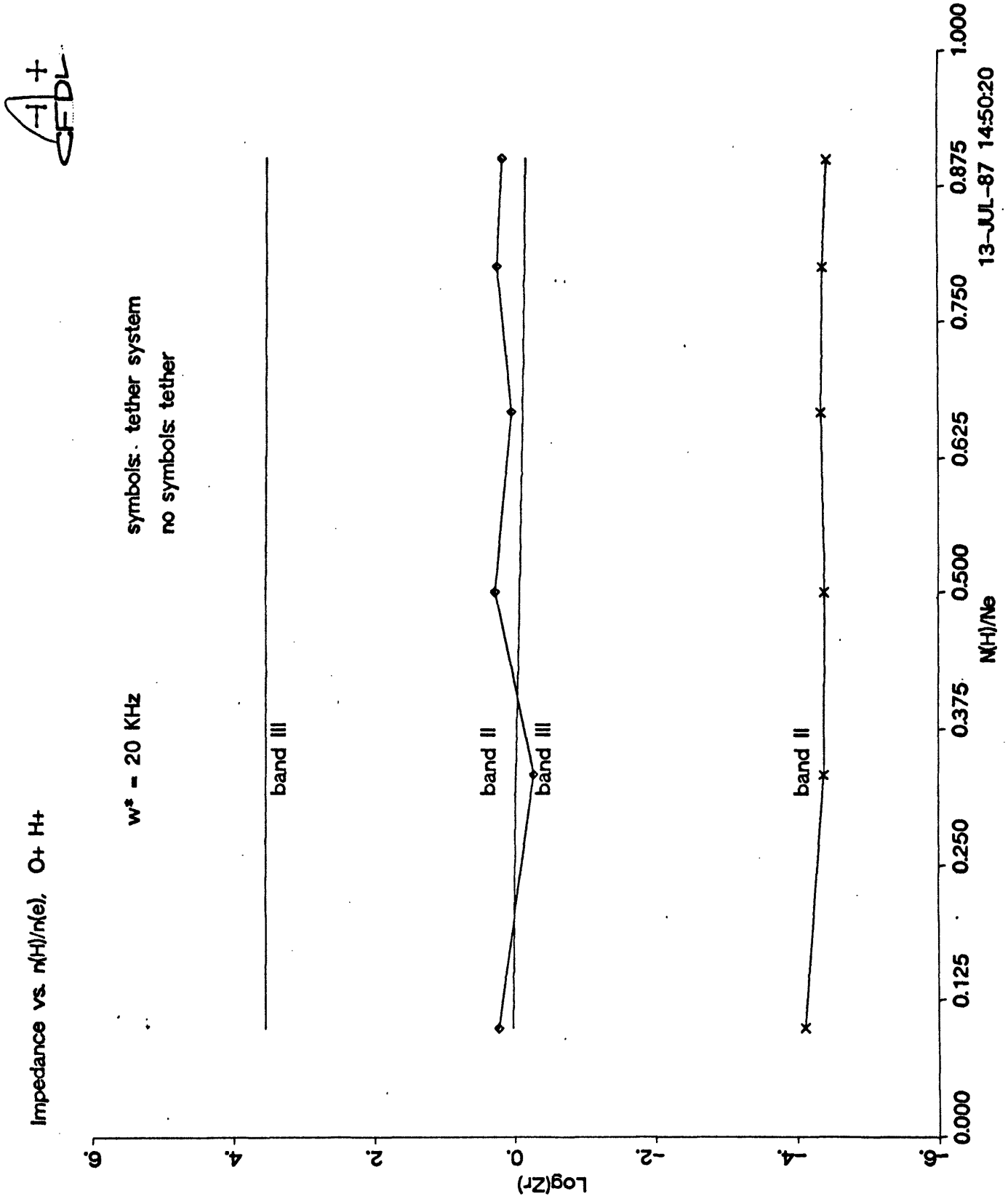

Figure 3.30: Effect of multi-ion spacies: impedance of shuttle-tether system associated with each band (w^*=20 kHz)

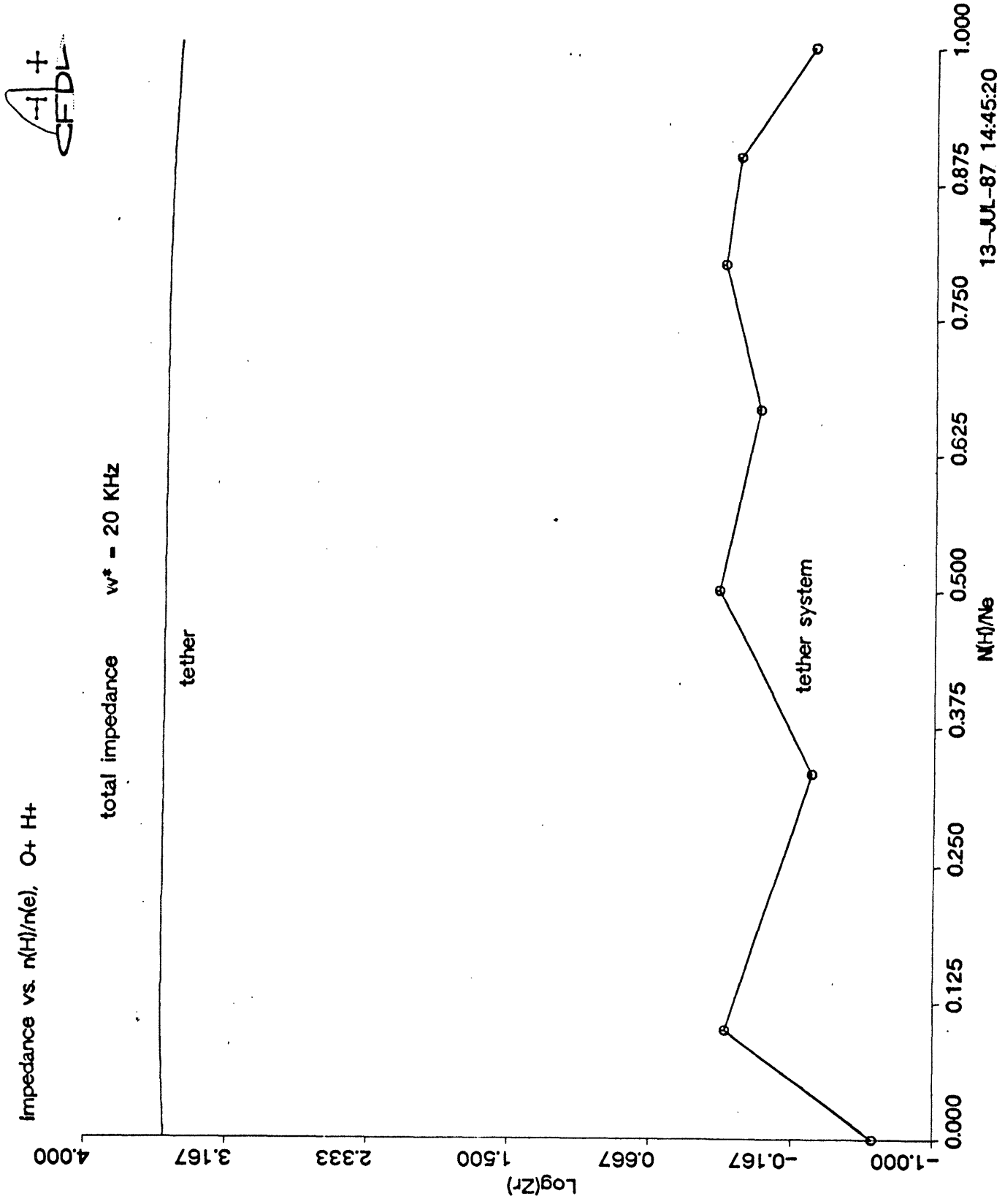

Figure 3.31: Effect of multi-ion spacies: total impedance of shuttle-tether system (w^*=20 kHz)

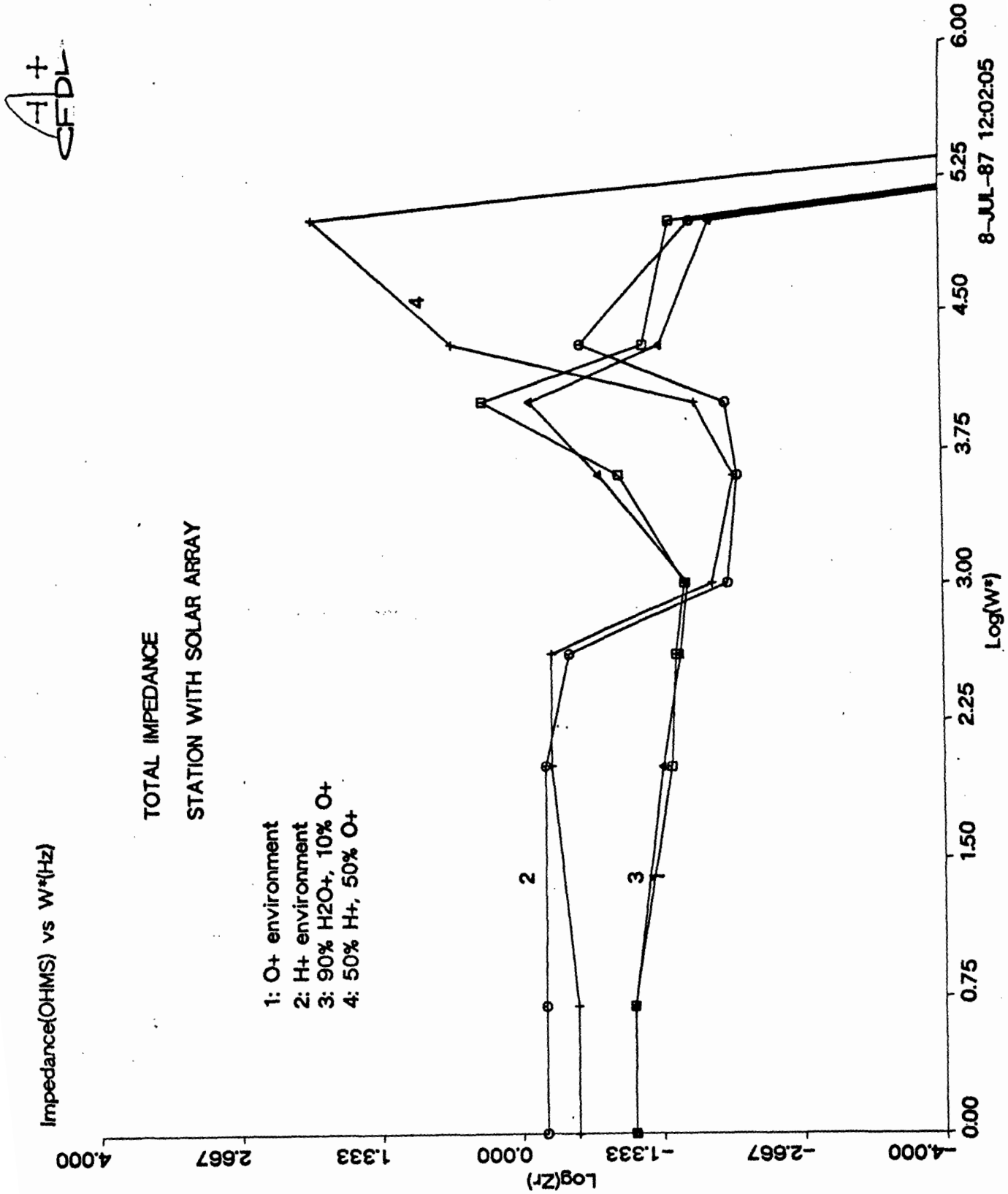

Figure 3.32: Total impedance in different environments — space station

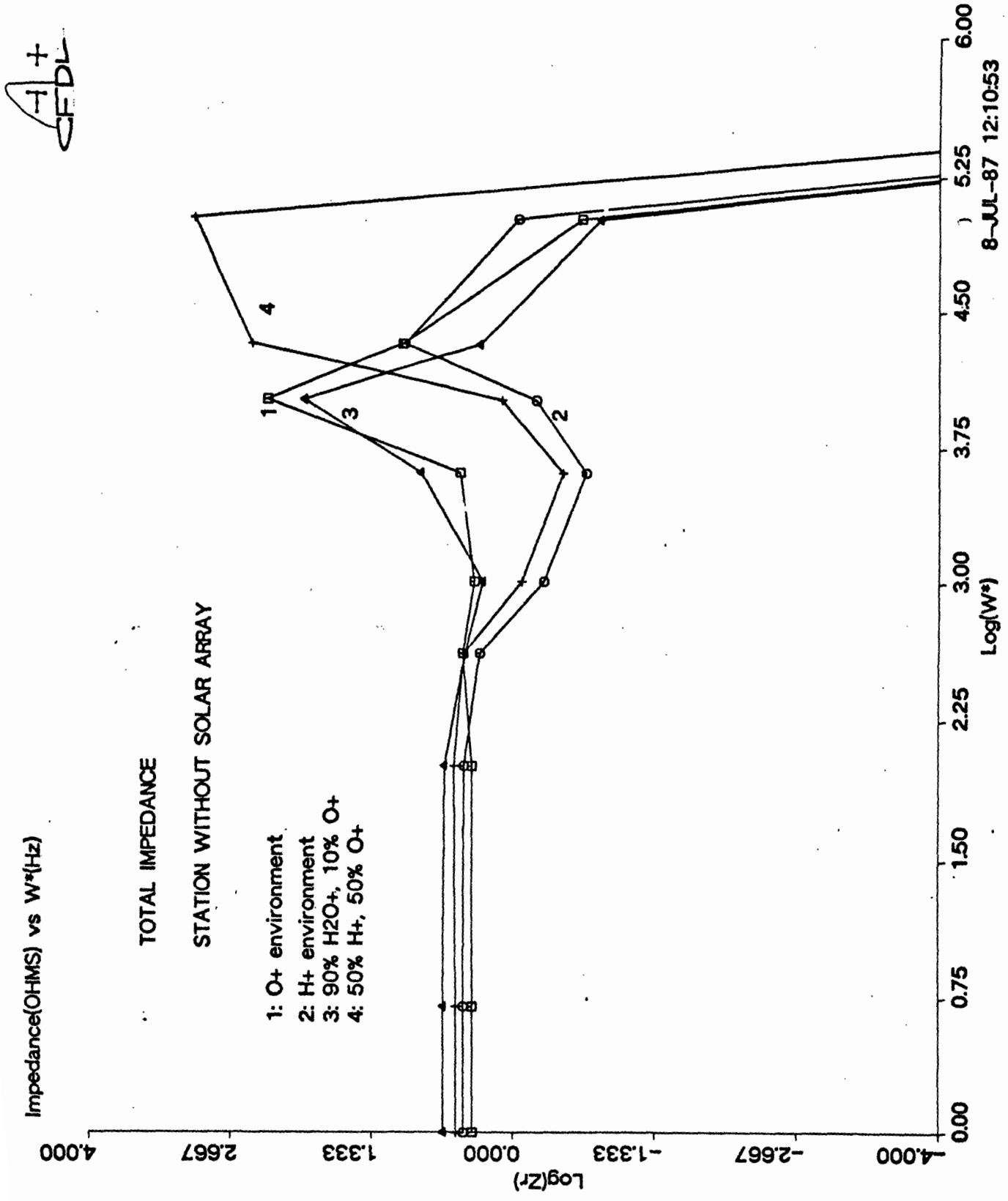

Figure 3.33: Total impedance in different environments — space station without solar array

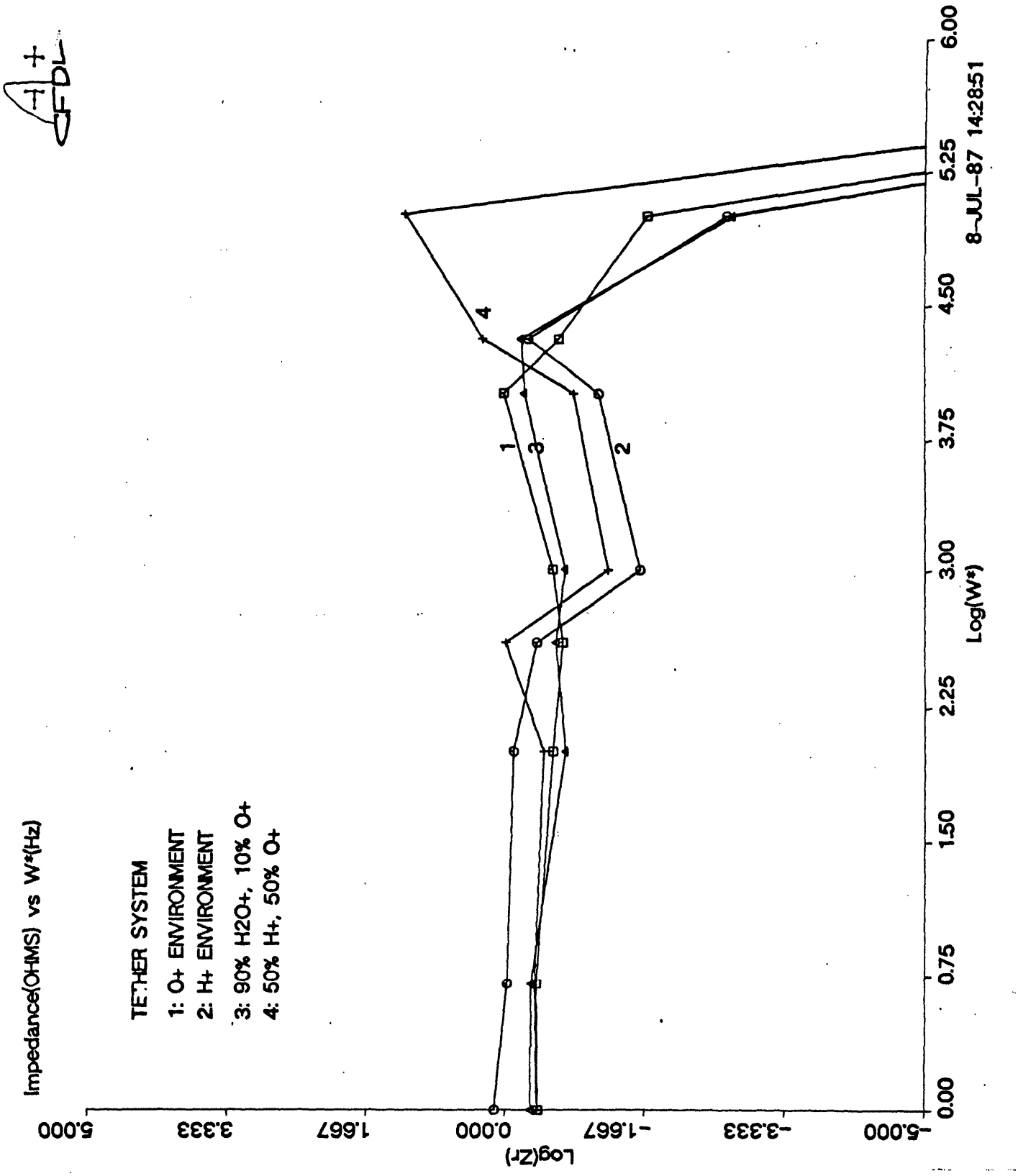

Figure 3.34: Total impedance in different environments — shuttle-tether system

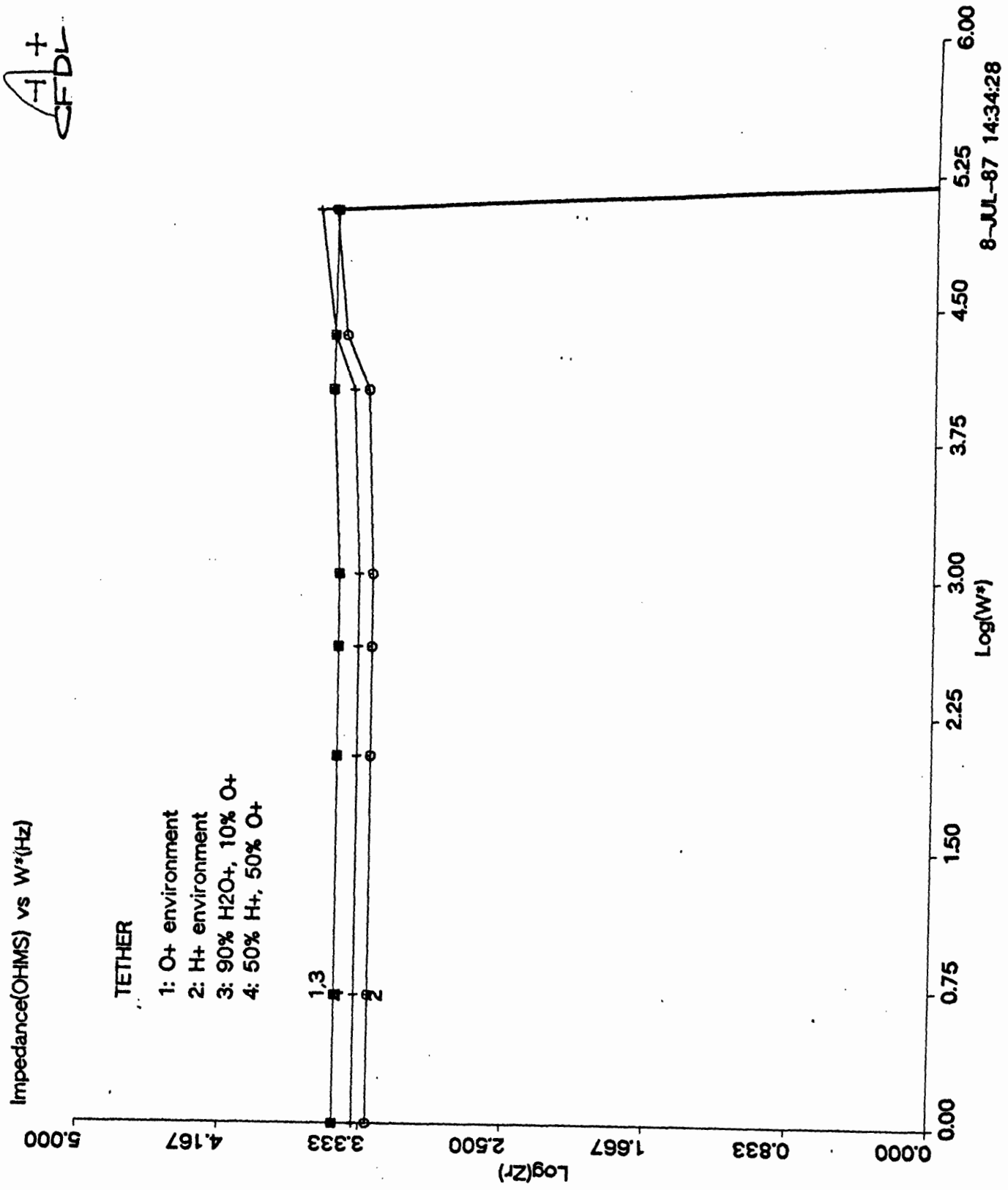

Figure 3.35: Total impedance in different environments — 10 km tether

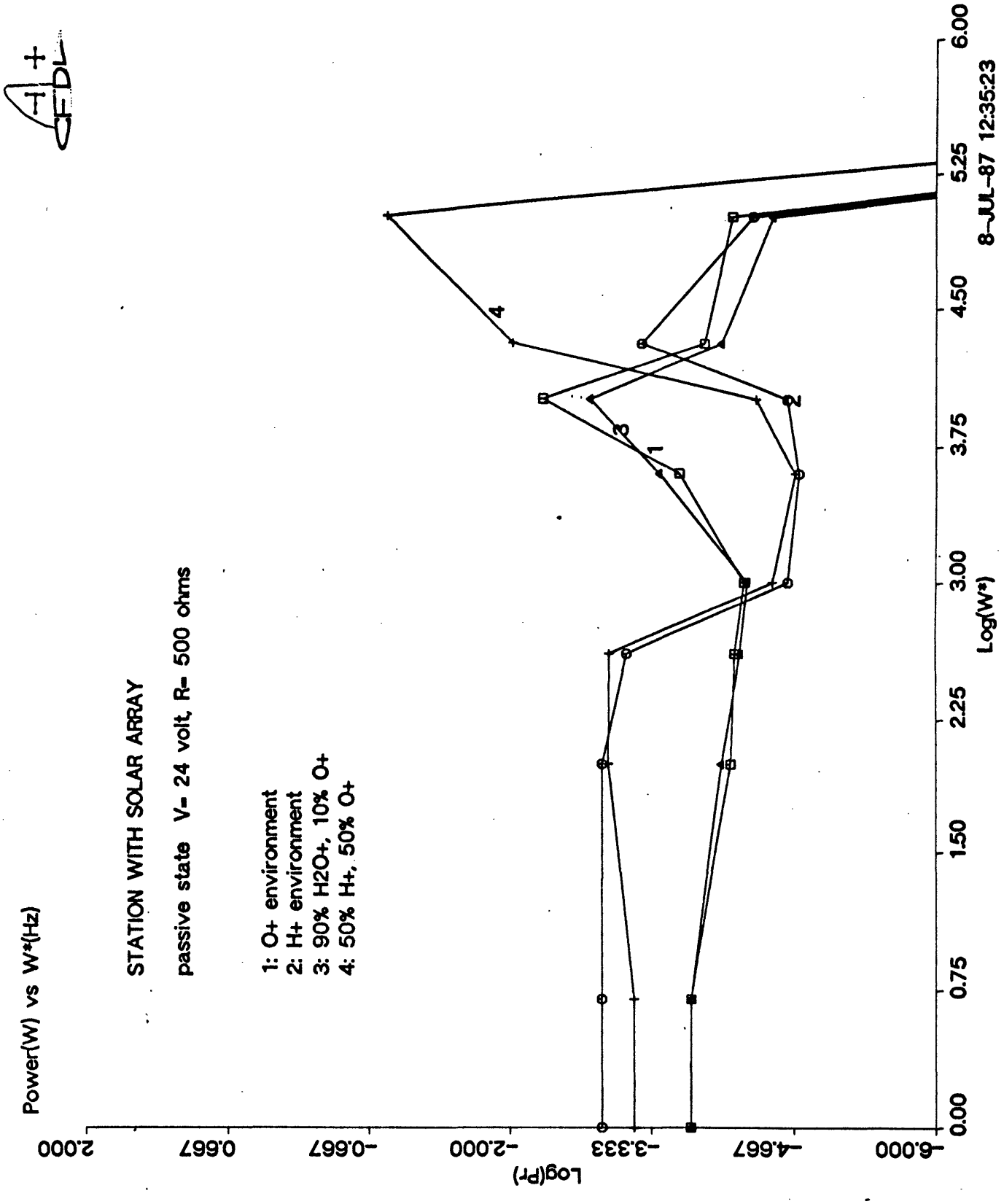

Figure 3.36: Power radiated in different environments — space station

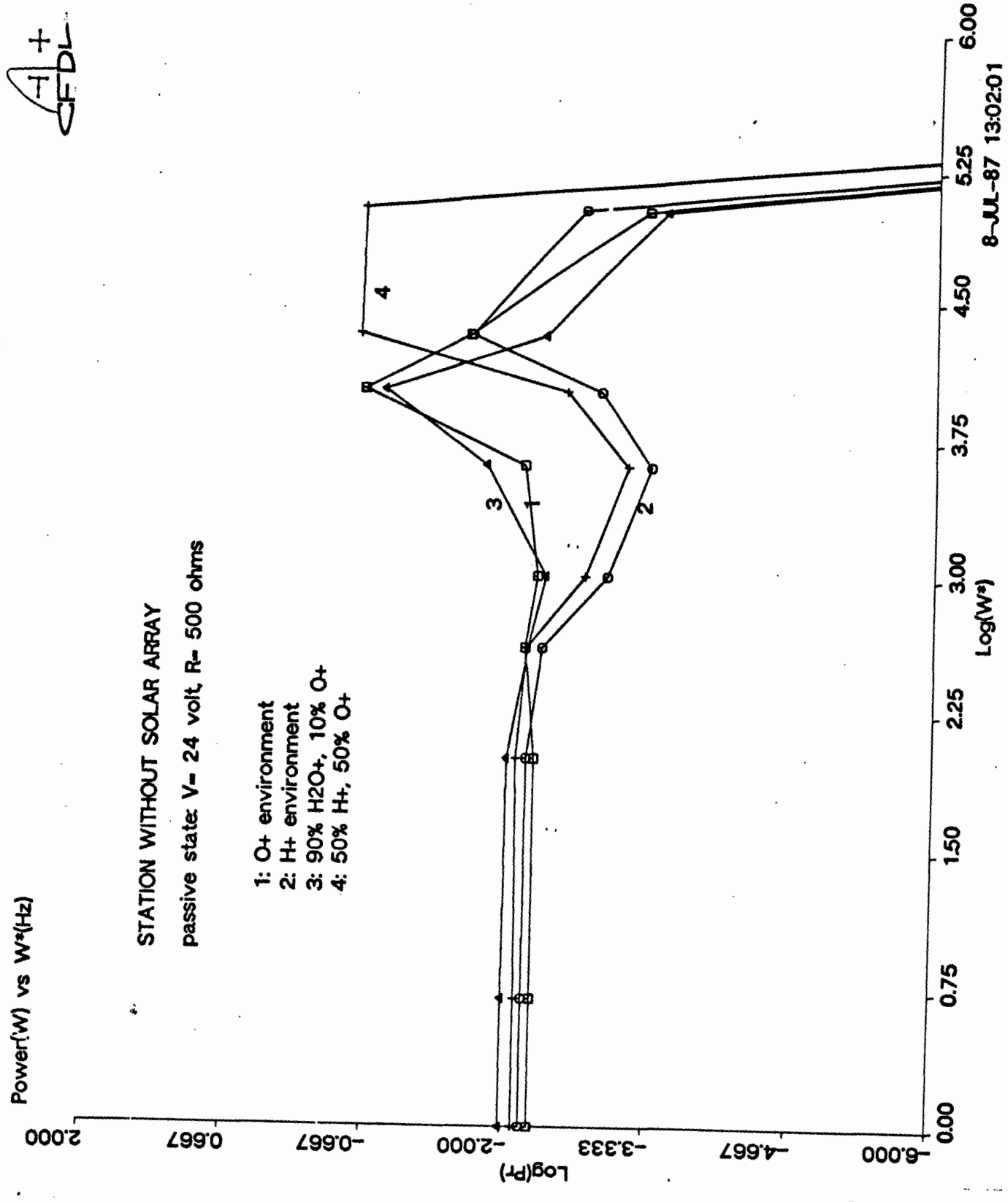

Figure 3.37: Power radiated in different environments — space station without solar array

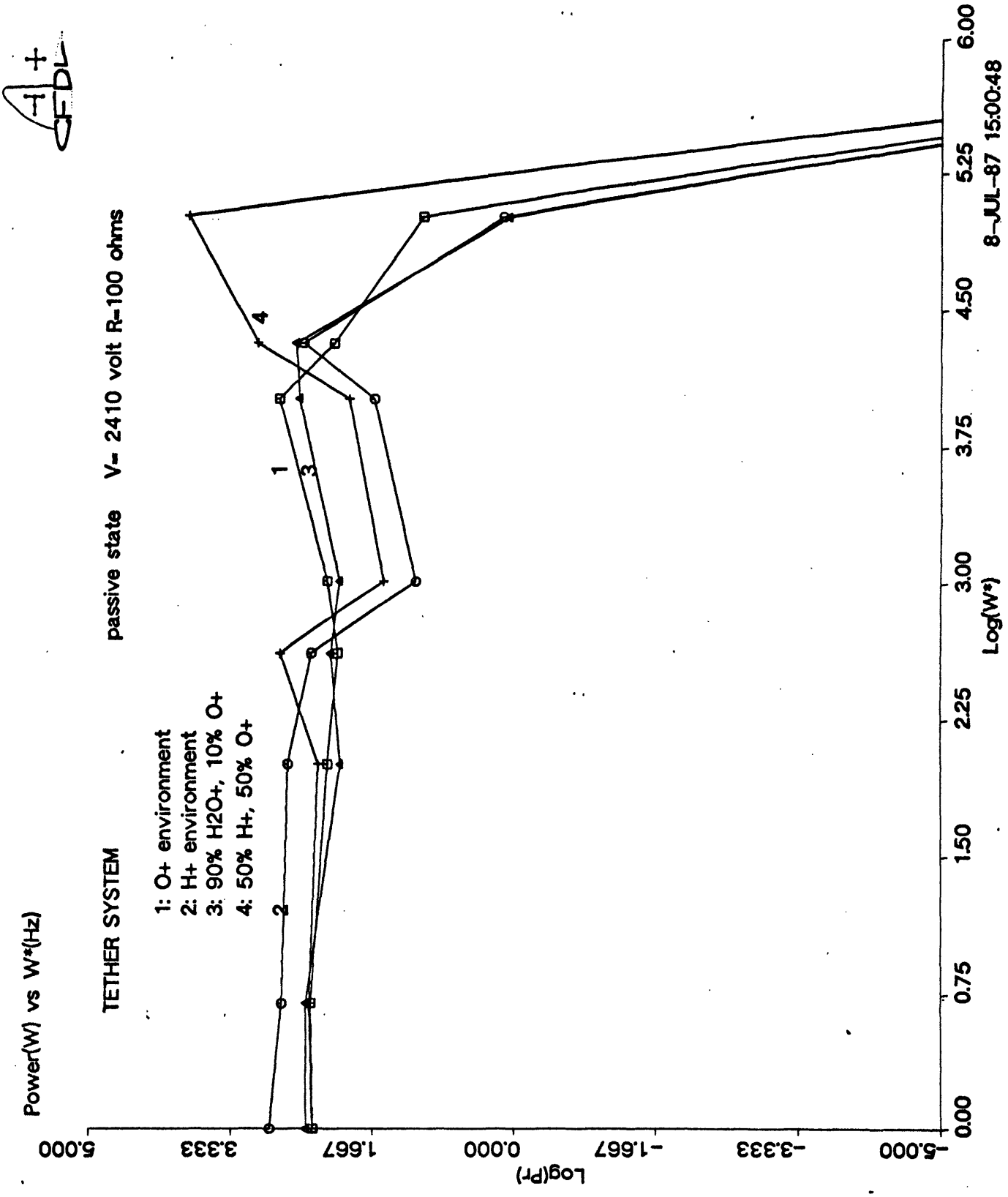

Figure 3.38: Power radiated in different environments — shuttle tether system

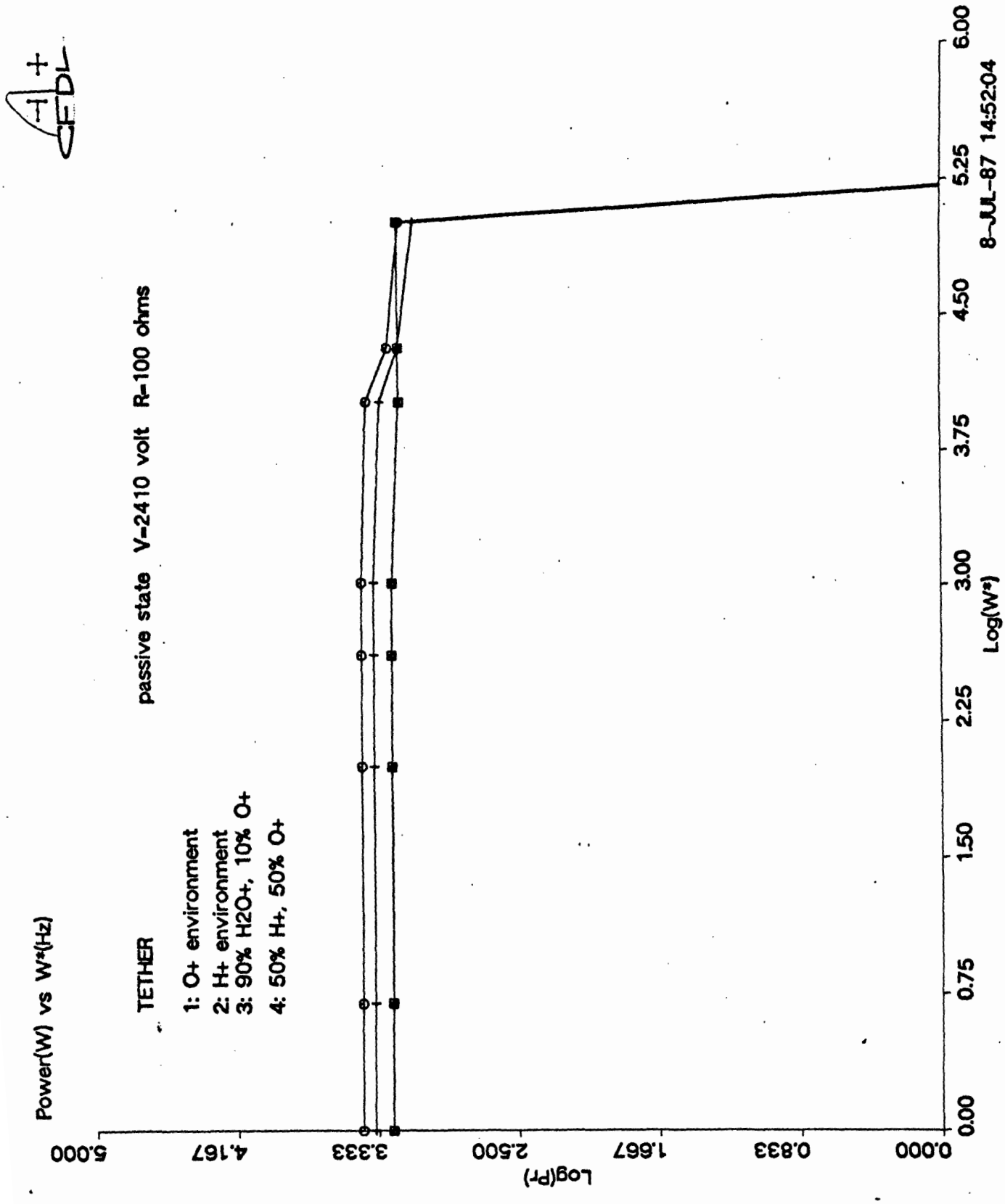

Figure 3.39: Power radiated in different environments — 1 km tether

Chapter 4
Summary and Conclusion

We have presented a linear theory of plasma wave radiation by a conductor with AC current moving through a magnetized plasma. The properties of non-evanescent waves in multi-ion plasma are discussed and the power radiation is studied. This theory is applied to large space structures at low earth orbit. The space structure is modeled by a generalized box structure with current driven into the terminators in every direction. A general power radiation formula is derived and a computation code is developed.

The radiation impedance and power radiation have been calculated for space structures of different shapes and dimensions in several single and muliti-ion plasma enviornments. The radiation impedance is studied as a function of AC frequency,structure and environment. The implicit relationship between them have been discussed.

We found that generally the radiation impedance can be changed in the following way: (1) increasing total collecting area can decrease the total impedance and vice versa. (2) For a fixed geometry shape,the system with boundary current mainly flowing in the direction of the magnetic field has the minimum impedance while the system with boundary current mainly flowing in the di-

rection of motion has the maximum impedance. (this is not always true at $w^* \sim 10^4 Hz$) (3) For structures with AC current at $w^* = 10^3 - 10^4 Hz$, those in a plasma of lighter average ion mass have smaller impedance and those in a plasma of heavier average ion mass have larger impedance. For structures with AC current at $w^* > 10^4 Hz$, usually those in a plasma of heavy-light have a much larger impedance than those in plasma of other kind. (4) For structures almost insulated entirely or a thin tether , the impedance can be very high. The higher the impedance, the more weakly it depends on w^*,structure and enviornment.

The numerical results and physics regulations obtained here can be applied directly to the design of space structures. For instance, while designing a space station, in order to minimize the power loss, we want to make the value of radiation impedance Z_r far away from the sum value of other resistances R. The radiation impedance can be changed by modifing the dimension, shape or current collecting surface of a structure in the above mentioned way. If the structure is fixed, creating an artifical surrounding environment can also change the impedance. If neither structure nor environment can be changed, then we need to adjust the value of R based on the value of Z_r.

We must caution the reader against interpreting our results too literally. The results are obtained under several approximations and restrictions. One restriction is that we only consider the far field and the power radiated is integrated on a closed surface at infinity. In a recent study by Rasmussen et al, it was shown that the far field criteria in free space are not applicable to anisotropic media[16]. From this arose concerns that the far field assumption may not be satisfied everywhere when considering very large objects such as our space struc-

ture. If this turns out to be true in reality, the details of near field which we have complectly neglected here could be very important. The other thing is: we simulate the warm plasma effect by merely cutting off the k_2 integration. This may oversimplify the warm plasma effects. There is recent research showing that: for $k > \frac{1}{\rho_e}$, though the electron plasma waves are heavily damped, the source still loses energy into plasma by exciting those damped waves [12]. The details of the boundary current pattern also need further investigation. We assume the same current density at every collecting surfaces and the total current is determined by the dimensions in $\vec{V} \times \vec{B}$ direction and R. The solution to the real current pattern depends on more understanding of the physics of plasma contactor. If the current pattern turns out to be very different from what we have assumed, the results presented here certainly need to be modified.

Reference

1. P.M.Banks, P.R.Williamson,and K.-I. Oyama. Electrical behavior of a shuttle electrodynamic tether system(SETS). *Planet and Space Science*, 29:139 - 147, 1981.

2. A. Barnett. In situ measurements of the bulk plasma velocity near the IO flux tube. *Journal of Geophysical Research*, 91:3011, 1986.

3. A. Barnett and S. Olbert. Radiation of plasma waves by a conducting body moving through a magnetized plasma. *Journal of Geophysical Research*, 91:10117- 10135, 1986.

4. V. Belcastro, P.Veltri, and M. Dobrownoly. Radiation from long conducting tethers moving in the near-earth environment. *Nuovo Cimento* , 5:537- 560, 1982.

5. H.G.Booker. *Cold Plasma Waves*, Martinus Nijhoff Publishers, Dordrecht (1984).

6. M.Dobrownoly and P.Veltri. MHD power radiated by a large conductor in motion through a magnetoplasma. *Nuovo Cimento* ,9:27-38, 1986.

7. S.D.Drell, H.M.Foley , and M.A. Ruderman. Drag and propulsion in the ionosphere: an Alfven engine in space. *Journal of Geophysical Research*, 70:3131, 1965.

8. R.D.Estes. Alfven waves from an electrodynamic tethered satellite system. 1987. submitted to *Journal of Geophysical Research.*

9. D.E.Hastings, A. Barnett, and S.Olbert. Radiation from large space structures in low earth orbit with induced ac current. 1987. submitted to *Journal of Geophysical Research.*

10. B.D.Green, G.E.Caledonia, and T.D.Wilkerson. The shuttle environment: gases, particulates and glow. *Journal of Spacecraft and Rockets*, 22:500-511,1985.

11. J.B.Marion. *Classical Dynamics of Particles and Systems*, Academic Press, Orlando (1970).

12. Nicole Meyer-Vernet. Power loss of a conductor moving through a warm plasma: electron plasma wave contribution. 1987. To be published in *Astronomy and Astrophysics.*

13. S.Olbert. private communication. 1987.

14. C.E.Rasmussen and P.M.Banks. Theory of the electrodynamic tethers. COSPAR proceedings *Advances in Space Research.* In press.

15. C.E.Rasmussen, P.M.Banks, and K.J. Harker. The excitation of plasma waves by a current source moving in a magnetized plasma: the MHD approximation. *Journal of Geophysical Research*, 90:505-515,1985.

16. C.E.Rasmussen, P.M.Banks, and K.J. Harker. The minimum distance to the far field in a magnetized plasma. *Radio Science*, Vol.21, Number 6, pp. 920-928, November-December 1986.

17. T.H.Stix. *Theory of Plasma Waves*,McGraw-Hill,New York(1962).

Appendix A
Appendices

A.1 Derivation of The Radiation Impedance Formula

a) A tether with I_t flowing in and out through the two end surfaces in the $\vec{x}_2$ direction.

$$\vec{J}_c = -J_t\vec{x}_2 \quad x_2 = -L_{22}/2$$

$$\vec{J}_c = J_t\vec{x}_2 \quad x_2 = L_{22}/2$$

$$J_t = I_t/A_t$$

$$A_t = d_{11}d_{31}$$

$$\vec{j}\cdot\vec{k} = \frac{1}{(2\pi)^{3/2}i}\int \vec{n}\cdot\vec{J}_n da$$

$$\int \vec{n}\cdot\vec{J}_n da = J_t \int_{-d_{11}/2}^{d_{11}/2} dx_1 \int_{-d_{31}/2}^{d_{31}/2} dx_3$$

$$\left\{-e^{-i(k_1x_1+k_3x_3)+ik_2L_{22}/2} + e^{-i(k_1x_1+k_3x_3)-ik_2L_{22}/2}\right\}$$

$$= J_t \int_{-d_{11}/2}^{d_{11}/2} e^{-ik_1x_1}dx_1 \int_{-d_{31}/2}^{d_{31}/2} e^{-ik_3x_3}dx_3[-e^{ik_2L_{22}/2} + e^{-ik_2L_{22}/2}]$$

$$= J_t\left\{\frac{e^{-ik_1x_1}}{-ik_1}\Big|_{-d_{11}/2}^{d_{11}/2} \frac{e^{-ik_3x_3}}{-ik_3}\Big|_{-d_{31}/2}^{d_{31}/2} [-2i\sin(k_2L_{22}/2)]\right\}$$

Therefore:

$$|\vec{j}_s\cdot\vec{k}| = \frac{2J_t}{(2\pi)^{3/2}}\frac{\sin(k_1d_{11}/2)}{k_1/2}\frac{\sin(k_3d_{31}/2)}{k_3/2}\sin(k_2L_{22}/2)$$

$$= \frac{I_t}{A_t}\frac{2}{(2\pi)^{3/2}}[(d_{11}d_{31}\frac{\sin(k_1 d_{11}/2)}{k_1 d_{11}/2}\frac{\sin(k_3 d_{31}/2)}{k_3 d_{31}/2}\sin(k_2 L_{22}/2)]$$

Hence the power radiation formula can be writen as:

$$P_r = P_r^+ + P_r^-$$

$$P_r^\pm = \int |\vec{j_s}\cdot\vec{k}|^2 Q dk_1 dk_2$$

$$P_r = J_t^2 S_t = I_t^2 Z_t.$$

and the radiation impedance is:

$$Z_t = Z_t^+ + Z_t^-$$

$$Z_t^\pm = Z_0\frac{c}{c_A}\frac{1}{(d_{11}d_{31})^2}\int \frac{2}{(2\pi)^{3/2}}(d_{11}d_{31}\frac{\sin(k_1 d_{11}/2)}{k_1 d_{11}/2})^2\frac{1}{\sqrt{S(w)}}\frac{L_{22}dw}{V}[f_4(0)-f_4(1)] \tag{A.1}$$

$$k_1 = \frac{w \pm w^*}{V}$$

b)For a box structure with current I_2 flowing in and out only through the surfaces A_2 and A_2' (other surfaces are insulated):

$$\vec{J_c} = -J_2\vec{x}_2 \qquad x_2 = -L_{22}/2$$

$$\vec{J_c} = J_2\vec{x}_2 \qquad x_2 = L_{22}/2$$

$$J_t = I_2/A_2$$

$$A_2 = A_2' = d_{12}d_{32}$$

Similar to the derivation in a), we can get

$$|\vec{j_s}\cdot\vec{k}| = \frac{2J_2}{(2\pi)^{3/2}}\frac{\sin(k_1 d_{12}/2)}{k_1/2}\frac{\sin(k_3 d_{32}/2)}{k_3/2}\sin(k_2 L_{22}/2)$$

$$= \frac{I_2}{A_2}\frac{2}{(2\pi)^{3/2}}[d_{12}d_{32}\frac{\sin(k_1 d_{12}/2)}{k_1 d_{12}/2}\frac{\sin(k_3 d_{32}/2)}{k_3 d_{32}/2}\sin(k_2 L_{22}/2)]$$

Therefore the power radiation formula:

$$P_r = P_r^+ + P_r^-$$

$$P_r = J_2^2 S_2 = I_2^2 Z_2.$$

and the radiation impedance:

$$Z_2 = Z_2^+ + Z_2^-$$

$$Z_2^{\pm} = Z_0 \frac{c}{c_A} \frac{1}{(d_{12}d_{32})^2} \int \frac{2}{(2\pi)^{3/2}} (d_{12}d_{32} \frac{\sin(k_1 d_{12}/2)}{k_1 d_{12}/2})^2 \frac{1}{\sqrt{S(w)}} \frac{L_{22}dw}{V} [f_2(0) - f_2(1)] \tag{A.2}$$

$$k_1 = \frac{w \pm w^*}{V}$$

c) For a box structure with current I_4 flowing in and out only through the surfaces A_4 and A_4':

$$\vec{J}_c = -J_4 \vec{x}_2 \qquad x_2 = -L_{21}/2$$

$$\vec{J}_c = J_4 \vec{x}_2 \qquad x_2 = L_{21}/2$$

$$J_4 = I_4/A_4$$

$$A_4 = A_4' = d_{12}d_{32} - d_{11}d_{31}$$

Since:

$$\int_{A_4} \vec{n} \cdot \vec{J}_n da = \int_{A_4 + A_t} \vec{n} \cdot \vec{J}_n da - \int_{A_t} \vec{n} \cdot \vec{J}_n da$$

where:

$$\int_{A_4+A_t} \vec{n} \cdot \vec{J}_n da = \frac{I_4}{A_4} \frac{\sin(k_1 d_{12}/2)}{k_1/2} \frac{\sin(k_3 d_{32}/2)}{k_3/2} \sin(k_2 L_{21}/2)$$

$$\int_{A_t} \vec{n} \cdot \vec{J}_n da = \frac{I_4}{A_4} \frac{\sin(k_1 d_{11}/2)}{k_1/2} \frac{\sin(k_3 d_{31}/2)}{k_3/2} \sin(k_2 L_{21}/2)$$

Therefore:

$$|\vec{j_s}\cdot\vec{k}| = \frac{2J_2}{(2\pi)^{3/2}}\{\frac{\sin(k_1d_{12}/2)}{k_1/2}\frac{\sin(k_3d_{32}/2)}{k_3/2}$$
$$-\frac{\sin(k_1d_{11}/2)}{k_1/2}\frac{\sin(k_3d_{31}/2)}{k_3/2}]\sin(k_2L_{21}/2)\}$$
$$= \frac{2}{(2\pi)^{3/2}}\frac{I_4}{A_4}\{(d_{12}d_{32})\frac{\sin(k_1d_{12}/2)}{k_1d_{12}/2}\frac{\sin(k_3d_{32}/2)}{k_3d_{32}/2}$$
$$-(d_{11}d_{31})\frac{\sin(k_1d_{11}/2)}{k_1d_{11}/2}\frac{\sin(k_3d_{31}/2)}{k_3d_{31}/2}]\sin(k_2L_{21}/2)\}$$

Hence the power radiation formula is:

$$P_r = P_r^+ + P_r^-$$

$$P_r = J_4^2 S_4 = I_4^2 Z_4.$$

and the radiation impedance:

$$Z_4 = Z_4^+ + Z_4^-$$

$$Z_4^{\pm} = Z_0\frac{c}{c_A}\frac{1}{A_4}\int dw\frac{2}{(2\pi)^{3/2}}\frac{1}{\sqrt{S(w)}}\frac{L_{22}}{V} \quad (A.3)$$
$$\{(d_{12}d_{32}\frac{\sin(k_1d_{12}/2)}{k_1d_{12}/2})^2[f_2(0) - f_2(L_{21}/L_{22})] \quad (A.4)$$
$$+(d_{11}d_{31}\frac{\sin(k_1d_{11}/2)}{k_1d_{11}/2})^2[f_4(0) - f_4(L_{21}/L_{22})] \quad (A.5)$$
$$-2(d_{12}d_{32}\frac{\sin(k_1d_{12}/2)}{k_1d_{12}/2})(d_{11}d_{31}\frac{\sin(k_1d_{11}/2)}{k_1d_{11}/2})[f_{42}(0) - f_{42}(L_{21}/L_{22})]\} \quad (A.6)$$
$$k_1 = \frac{w \pm w^*}{V}$$

d) For a box structure with current I_1 flowing in and out only through surfaces A_1 and A_1' in the $\vec{x}_1$ direction:

$$\vec{J_c} = \begin{cases} -J_1\vec{x}_1 & x_1 = d_{12}/2, \quad -L_{22}/2 < x_2 < -L_{21}/2, \quad -d_{32}/2 < x_3 < d_{32}/2 \\ -J_1\vec{x}_1 & x_1 = -d_{12}/2, \quad L_{21}/2 < x_2 < L_{22}/2, \quad -d_{32}/2 < x_3 < d_{32}/2 \\ J_1\vec{x}_1 & x_1 = -d_{12}/2, \quad -L_{22}/2 < x_2 < -L_{21}/2, \quad -d_{32}/2 < x_3 < d_{32}/2 \\ J_1\vec{x}_1 & x_1 = d_{12}/2, \quad L_{21}/2 < x_2 < L_{22}/2, \quad -d_{32}/2 < x_3 < d_{32}/2 \\ 0 & \vec{x} \ at \quad elsewhere \end{cases}$$

$$J_1 = I_1/A_1$$

$$A_1 = (\frac{L_{22} - L_{21}}{2})d_{32}$$

Thus

$$\int \vec{n} \cdot \vec{J}_n da = J_1 \int_{-L_{22}/2}^{-L_{21}/2} dx_2 \int_{-d_{32}/2}^{d_{32}/2} dx_3$$

$$\left\{ -e^{-i(k_2x_2+k_3x_3)+ik_1d_{12}/2} - e^{-i(k_2x_2+k_3x_3)-ik_1d_{12}/2} \right\}$$

$$+ \int_{L_{21}/2}^{L_{22}/2} dx_2 \int_{-d_{32}/2}^{d_{32}/2} dx_3 \left\{ e^{-i(k_2x_2+k_3x_3)+ik_1d_{12}/2} \right.$$

$$\left. + e^{-i(k_2x_2+k_3x_3)-ik_1d_{12}/2} \right\}$$

$$= J_1[e^{ik_1d_{12}/2} + e^{-ik_1d_{12}/2}] \left\{ \int_{-d_{32}/2}^{d_{32}/2} e^{-ik_3x_3} dx_3 \right.$$

$$\left. [\int_{-L_{22}/2}^{-L_{21}/2} -e^{-ik_2x_2} dx_2 + \int_{L_{21}/2}^{L_{22}/2} e^{-ik_2x_2} dx_2] \right\}$$

Therefore:

$$|\vec{j}_s \cdot \vec{k}| = \frac{2J_1}{(2\pi)^{3/2}} \cos(k_1d_{12}/2) \frac{\sin(k_3d_{32}/2)}{k_3/2}$$

$$\frac{2\sin(k_2(L_{22} - L_{21})/)4}{k_2/2} \sin k_2(L_{22} + L_{21})/4$$

$$= \frac{I_1}{A_1} \frac{2}{(2\pi)^{3/2}} [2d_{32} \frac{(L_{22} - L_{21})}{2}][\frac{\sin(k_2(L_{22} - L_{21})/4)}{k_2(L_{22} - L_{21})/4}]$$

$$\cos(k_1d_{12}/2) \frac{\sin(k_3d_{32}/2)}{k_3d_{32}/2} \sin k_2(L_{22} + L_{21})/4$$

Therefore the power radiation formula is:

$$P_r = P_r^+ + P_r^-$$

$$P_r = J_1^2 S_1 = I_1^2 Z_1.$$

and

$$Z_4^{\pm} = Z_0 \frac{c}{c_A} \int (\frac{2}{(2\pi)^{3/2}} \frac{1}{\sqrt{S(w)}} \frac{L_{22}dw}{V}$$

$$(\frac{1}{2d_{32}(L_{22} - L_{21})/2} \cos(k_1d_{12}/2))^2 [f_1(0) - f_1(\frac{1 + L_{21}/L_{22}}{2})] \qquad \text{(A.7)}$$

e) For a box structure with current I_3 flowing in and out only through surfaces A_3 and A_3' in the $\vec{x}_3$ direction:

$$\vec{J}_c = \begin{cases} -J_3\vec{x}_3 & x_3 = d_{32}/2, \quad -L_{22}/2 < x_2 < -L_{21}/2, & -d_{12}/2 < x_1 < d_{12}/2 \\ -J_3\vec{x}_3 & x_3 = -d_{32}/2, \quad L_{21}/2 < x_2 < L_{22}/2, & -d_{12}/2 < x_1 < d_{12}/2 \\ J_3\vec{x}_3 & x_1 = -d_{32}/2, \quad -L_{22}/2 < x_2 < -L_{21}/2, & -d_{12}/2 < x_1 < d_{12}/2 \\ J_3\vec{x}_3 & x_3 = d_{12}/2, \quad L_{21}/2 < x_2 < L_{22}/2. & -d_{12}/2 < x_1 < d_{12}/2 \\ 0 & \vec{x}\ at & elsewhere \end{cases}$$

$$J_3 = I_3/A_3$$

$$A_3 = (\frac{L_{22} - L_{21}}{2})d_{12}$$

Therefore:

$$\int \vec{n} \cdot \vec{J}_n da = J_3 \int_{-L_{22}/2}^{-L_{21}/2} dx_2 \int_{-d_{12}/2}^{d_{12}/2} dx_1$$
$$\left\{ -e^{-i(k_2x_2+k_1x_1)+ik_3d_{32}/2} - e^{-i(k_2x_2+k_1x_1)-ik_3d_{32}/2} \right\}$$
$$+ \int_{L_{21}/2}^{L_{22}/2} dx_2 \int_{-d_{12}/2}^{d_{12}/2} dx_1 \left\{ e^{-i(k_2x_2+k_1x_1)+ik_3d_{32}/2} + e^{-i(k_2x_2+k_1x_1)-ik_3d_{32}/2} \right\}$$
$$= J_3[e^{ik_3d_{32}/2} + e^{-ik_3d_{32}/2}] \left\{ \int_{-d_{12}/2}^{d_{12}/2} e^{-ik_1x_1} dx_1 \right.$$
$$\left. [\int_{-L_{22}/2}^{-L_{21}/2} -e^{-ik_2x_2} dx_2 + \int_{L_{21}/2}^{L_{22}/2} e^{-ik_2x_2} dx_2] \right\}$$

Hence:

$$|\vec{j}_s \cdot \vec{k}| = \frac{2J_1}{(2\pi)^{3/2}} \cos(k_3d_{32}/2) \frac{\sin(k_1d_{12}/2)}{k_1/2}$$
$$\frac{2\sin(k_2(L_{22} - L_{21})/4)}{k_2/2} \sin(k_2(L_{22} + L_{21})/4)$$
$$= \frac{I_3}{A_3} \frac{2}{(2\pi)^{3/2}} [2d_{12} \frac{(L_{22} - L_{21})}{2}] [\frac{\sin k_2(L_{22} - L_{21})/4}{k_2(L_{22} - L_{21})/4}]$$
$$\cos(k_3d_{32}/2) \frac{\sin(k_1d_{12}/2)}{k_1d_{12}/2} \sin(k_2(L_{22} + L_{21})/4)$$

Therefore the power radiation formula is:

$$P_r = P_r^+ + P_r^-$$

$$P_r = J_1^2 S_1 = I_1^2 Z_1.$$

and

$$Z_4^{\pm} = Z_0 \frac{c}{c_A} \int \left(\frac{2}{(2\pi)^{3/2}} \frac{1}{\sqrt{S(w)}} \frac{L_{22} dw}{V}\right.$$
$$\left.\left(\frac{1}{2d_{12}(L_{22}-L_{21})/2} \frac{\sin(k_1 d_{12}/2)}{k_1 d_{12}/2}\right)^2 [f_3(0) - f_3(\frac{1+L_{21}/L_{22}}{2})]\right. \quad \text{(A.8)}$$

f)For a system with current flowing in and out through every surfaces of the end box(see Fig), the results can be obtained based on the above discussions. Now total current

$$I_{tot} = I_2 + I_4 + 2I_1 + 2I_3$$

and total collecting area

$$A_a = A_2 + A_4 + 2A_1 + 2A_3$$

where

$$A_t = d_{11} d_{31}, \quad A_2 = d_{12} d_{32}, \quad A_4 = A_2 - A_t$$
$$A_3 = d_{12}(L_{22} - L_{21})/2, \quad A_1 = d_{32}(L_{22} - L_{21})/2$$

The current densities at each surface are given by:

$$J_1 = I_1/A_1, \quad J_2 = I_2/A_2, \quad J_3 = I_3/A_3, \quad J_4 = I_4/A_4.$$

The term $|\vec{j_s} \cdot \vec{k}|$ is in a superposition form of the above obtained results

$$|\vec{j_s} \cdot \vec{k}| = \frac{2}{(2\pi)^{3/2}} \left\{ \frac{I_2}{A_2} [(d_{12} d_{32} \frac{\sin(k_1 d_{12}/2)}{k_1 d_{12}/2} \frac{\sin(k_3 d_{32}/2)}{k_3 d_{32}/2}\right.$$
$$\sin(k_2 L_{22}/2)] + \frac{I_4}{A_4} [(d_{12} d_{32}) \frac{\sin(k_1 d_{12}/2)}{k_1 d_{12}/2} \frac{\sin(k_3 d_{32}/2)}{k_3 d_{32}/2}$$
$$-(d_{11} d_{31}) \frac{\sin(k_1 d_{11}/2)}{k_1 d_{11}/2} \frac{\sin(k_3 d_{31}/2)}{k_3 d_{31}/2}] \sin(k_2 L_{21}/2)]$$
$$+ \frac{I_1}{A_1} [2 d_{32} \frac{(L_{22}-L_{21})}{2}] [\frac{\sin(k_2(L_{22}-L_{21})/4)}{k_2(L_{22}-L_{21})/4}$$
$$\cos(k_1 d_{12}/2) \frac{\sin(k_3 d_{32}/2)}{k_3 d_{32}/2} \sin k_2(L_{22} + L_{21})/4$$
$$+ \frac{I_3}{A_3} [2 d_{12} \frac{(L_{22}-L_{21})}{2}] [\frac{\sin(k_2(L_{22}-L_{21})/4)}{k_2(L_{22}-L_{21})/4}$$
$$\left.\cos(k_3 d_{32}/2) \frac{\sin(k_1 d_{12}/2)}{k_1 d_{12}/2} \sin k_2(L_{22} + L_{21})/4 \right\}$$

If we further assume that the boundary current densities at each direction are the same,

$$J_1 = J_2 = J_3 = J_4 = J_a$$

then

$$\begin{aligned}
|\vec{j_s} \cdot \vec{k}| = \tfrac{2}{(2\pi)^{3/2}} J_a \Big\{ & [(d_{12}d_{32} \tfrac{\sin(k_1 d_{12}/2)}{k_1 d_{12}/2} \tfrac{\sin(k_3 d_{32}/2)}{k_3 d_{32}/2} \sin(k_2 L_{22}/2)] \\
& + [(d_{12}d_{32}) \tfrac{\sin(k_1 d_{12}/2)}{k_1 d_{12}/2} \tfrac{\sin(k_3 d_{32}/2)}{k_3 d_{32}/2} \\
& - (d_{11}d_{31}) \tfrac{\sin(k_1 d_{11}/2)}{k_1 d_{11}/2} \tfrac{\sin(k_3 d_{31}/2)}{k_3 d_{31}/2}] \sin(k_2 L_{21}/2)] \\
& + [2d_{32} \tfrac{(L_{22}-L_{21})}{2}][\tfrac{\sin(k_2(L_{22}-L_{21})/4}{)} k_2(L_{22}-L_{21})/4 \\
& \cos(k_1 d_{12}/2) \tfrac{\sin(k_3 d_{32}/2)}{k_3 d_{32}/2} \sin k_2(L_{22}+L_{21})/4 \\
& + [2d_{12} \tfrac{(L_{22}-L_{21})}{2}][\tfrac{\sin k_2(L_{22}-L_{21})/4}{k_2(L_{22}-L_{21})/4} \\
& \cos(k_3 d_{32}/2) \tfrac{\sin(k_1 d_{12}/2)}{k_1 d_{12}/2} \sin k_2(L_{22}+L_{21})/4 \Big\}
\end{aligned}$$

Therefore the power radiation formula is:

$$P_r = P_r^+ + P_r^-$$

$$P_r = J_a^2 S_a = I_a^2 Z_a.$$

and the radiation impedance:

$$\begin{aligned}
Z_a^{\pm} = Z_0 \tfrac{c}{c_A} \Big\{ & \int (\tfrac{2}{(2\pi)^{3/2}} \tfrac{1}{\sqrt{S(w)}} \tfrac{L_{22} dw}{V} \\
& [d_{12}d_{32} \tfrac{\sin(k_1 d_{12}/2)}{k_1 d_{12}/2}]^2 [f_2(0) - f_2(1)] \\
& + [d_{12}d_{32} \tfrac{\sin(k_1 d_{12}/2)}{k_1 d_{12}/2}]^2 [f_2(0) - f_2(L_{21}/L_{22})] \\
& + [2d_{32} \tfrac{(L_{22}-L_{21})}{2} \cos(k_1 d_{12}/2)]^2 [f_1(0) - f_1(\tfrac{1+L_{21}/L_{22}}{2})] \\
& + [2d_{12} \tfrac{(L_{22}-L_{21})}{2} \tfrac{\sin(k_1 d_{12}/2)}{k_1 d_{12}/2}]^2 [f_3(0) - f_3(\tfrac{1+L_{21}/L_{22}}{2})] \\
& + 2[(d_{12}d_{32} \tfrac{\sin(k_1 d_{12}/2)}{k_1 d_{12}/2}]^2 [f_2(\tfrac{1-L_{21}/L_{22}}{2}) - f_2(\tfrac{1+L_{21}/L_{22}}{2})] \\
& + 2[d_{12}d_{32} \tfrac{\sin(k_1 d_{12}/2)}{k_1 d_{12}/2}][2d_{32} \tfrac{(L_{22}-L_{21})}{2} \cos(k_1 d_{12}/2)]^2
\end{aligned}$$

$$[f_{21}(\tfrac{1-L_{21}/L_{22}}{4}) - f_{21}(\tfrac{3+L_{21}/L_{22}}{4})]$$
$$+2[d_{12}d_{32}\tfrac{\sin(k_1d_{12}/2)}{k_1d_{12}/2}][2d_{12}\tfrac{(L_{22}-L_{21})}{2}\tfrac{\sin(k_1d_{12}/2)}{k_1d_{12}/2}]$$
$$[f_{23}(\tfrac{1-L_{21}/L_{22}}{4}) - f_{23}(\tfrac{3+L_{21}/L_{22}}{4})]$$
$$+2[d_{12}d_{32}\tfrac{\sin(k_1d_{12}/2)}{k_1d_{12}/2}][2d_{32}\tfrac{(L_{22}-L_{21})}{2}\cos(k_1d_{12}/2)]$$
$$[f_{21}(\tfrac{1-L_{21}/L_{22}}{4}) - f_{21}(\tfrac{1+3L_{21}/L_{22}}{4})]$$
$$+2[d_{12}d_{32}\tfrac{\sin(k_1d_{12}/2)}{k_1d_{12}/2}][2d_{12}\tfrac{(L_{22}-L_{21})}{2}\tfrac{\sin(k_1d_{12}/2)}{k_1d_{12}/2}]$$
$$[f_{23}(\tfrac{1-L_{21}/L_{22}}{4}) - f_{23}(\tfrac{1+3L_{21}/L_{22}}{4})]$$
$$+2[2d_{32}\tfrac{(L_{22}-L_{21})}{2}\cos(k_1d_{12}/2)][2d_{12}\tfrac{(L_{22}-L_{21})}{2}\tfrac{\sin(k_1d_{12}/2)}{k_1d_{12}/2}]$$
$$[f_{13}(0) - f_{13}(\tfrac{1+L_{21}/L_{22}}{2})]$$
$$+[d_{11}d_{31}\tfrac{\sin(k_1d_{11}/2)}{k_1d_{11}/2}]^2[f_4(0) - f_4(L_{21}/L_{22})]$$
$$-2[d_{11}d_{31}\tfrac{\sin(k_1d_{11}/2)}{k_1d_{11}/2}][d_{12}d_{32}\tfrac{\sin(k_1d_{12}/2)}{k_1d_{12}/2}]$$
$$[f_{42}(\tfrac{1-L_{21}/L_{22}}{2}) - f_{42}(\tfrac{1+L_{21}/L_{22}}{2})]$$
$$-2[d_{11}d_{31}\tfrac{\sin(k_1d_{11}/2)}{k_1d_{11}/2}][d_{12}d_{32}\tfrac{\sin(k_1d_{12}/2)}{k_1d_{12}/2}]$$
$$[f_{42}(0) - f_{42}(L_{21}/L_{22})]$$
$$-2[d_{11}d_{31}\tfrac{\sin(k_1d_{11}/2)}{k_1d_{11}/2}][2d_{32}\tfrac{(L_{22}-L_{21})}{2}\cos(k_1d_{12}/2)]$$
$$[f_{41}(\tfrac{1-L_{21}/L_{22}}{4}) - f_{41}(\tfrac{1+3L_{21}/L_{22}}{4})]$$
$$-2[d_{11}d_{31}\tfrac{\sin(k_1d_{11}/2)}{k_1d_{11}/2}][2d_{12}\tfrac{(L_{22}-L_{21})}{2}\tfrac{\sin(k_1d_{12}/2)}{k_1d_{12}/2}]$$
$$[f_{43}(\tfrac{1-L_{21}/L_{22}}{4}) - f_{43}(\tfrac{1+3L_{21}/L_{22}}{4})]\Big\} \qquad \text{(A.9)}$$

In the above expressions, The functions f_1,f_2,etc are the Fourier cosine transformations:

$$f_1(x) = \int_0^\infty d\overline{k}_2 \cos(\overline{k}_2 x)\left\{\frac{\sin(k_3d_{32}/2)}{k_3d_{32}/2}\frac{\sin(\frac{k_2(L_{22}-L_{21})}{4})}{\frac{k_2(L_{22}-L_{21})}{4}}Q\right\}$$

$$f_2(x) = \int_0^\infty d\bar{k}_2 \cos(\bar{k}_2 x) \left\{ [\frac{\sin(k_3 d_{32}/2)}{k_3 d_{32}/2}]^2 Q \right\}$$

$$f_3(x) = \int_0^\infty d\bar{k}_2 \cos(\bar{k}_2 x) \left\{ \cos(k_3 d_{32}/2) \frac{\sin(\frac{k_2(L_{22}-L_{21})}{4})}{\frac{k_2(L_{22}-L_{21})}{4}} Q \right\}$$

$$f_4(x) = \int_0^\infty d\bar{k}_2 \cos(\bar{k}_2 x) \left\{ [\frac{\sin(k_3 d_{31}/2)}{k_3 d_{31}/2}]^2 Q \right\}$$

$$f_{21}(x) = \int_0^\infty d\bar{k}_2 \cos(\bar{k}_2 x) \left\{ [\frac{\sin(k_3 d_{32}/2)}{k_3 d_{32}/2}]^2 \frac{\sin(\frac{k_2(L_{22}-L_{21})}{4})}{\frac{k_2(L_{22}-L_{21})}{4}}] Q \right\}$$

$$f_{23}(x) = \int_0^\infty d\bar{k}_2 \cos(\bar{k}_2 x) \left\{ [\frac{\sin(k_3 d_{32}/2)}{k_3 d_{32}/2} \cos(k_3 d_{32}/2) \frac{\sin(\frac{k_2(L_{22}-L_{21})}{4})}{\frac{k_2(L_{22}-L_{21})}{4}} Q \right\}$$

$$f_{13}(x) = \int_0^\infty d\bar{k}_2 \cos(\bar{k}_2 x) \left\{ \frac{\sin(k_3 d_{32}/2)}{k_3 d_{32}/2} [\frac{\sin(\frac{k_2(L_{22}-L_{21})}{4})}{\frac{k_2(L_{22}-L_{21})}{4}}]^2 \cos(k_3 d_{32}/2) Q \right\}$$

$$f_{41}(x) = \int_0^\infty d\bar{k}_2 \cos(\bar{k}_2 x) \left\{ \frac{\sin(k_3 d_{32}/2)}{k_3 d_{32}/2} \frac{\sin(\frac{k_2(L_{22}-L_{21})}{4})}{\frac{k_2(L_{22}-L_{21})}{4}} \frac{\sin(k_3 d_{31}/2)}{k_3 d_{31}/2} Q \right\}$$

$$f_{42}(x) = \int_0^\infty d\bar{k}_2 \cos(\bar{k}_2 x) \left\{ \frac{\sin(k_3 d_{32}/2)}{k_3 d_{32}/2} \frac{\sin(k_3 d_{31}/2)}{k_3 d_{31}/2} Q \right\}$$

$$f_{43}(x) = \int_0^\infty d\bar{k}_2 \cos(\bar{k}_2 x) \left\{ \frac{\sin(\frac{k_2(L_{22}-L_{21})}{4})}{\frac{k_2(L_{22}-L_{21})}{4}} \frac{\sin(k_3 d_{31}/2)}{k_3 d_{31}/2} cos(k_3 d_{32}/2) Q \right\}$$

where $\bar{k}_2 = k_2 L_{22}$.

A.2 Computer Code Listing

```
c This code calculates the radiation impedance of a space system with
c induced AC current in a multi-ion species environment.  The space
c system is modeled to be a box structure and current can flow into it
c through any surfaces of the two terminators.  The impedances corresponding
c to different boundary current pattern of a given structure is calculated
c at the desired AC frequency.
c-----------------------------------------------------------------------
c Main program: radiation in a two ion species environment.(It can be applied
c to single ion species or three ion species with slight modification.)
c Setting environment and structure parameters, performing integral over w
c and comparing the radiation results of different systems.
c Input variables:
c xl21,xl22,di1,di2,d31,d32:   dimensions of box-structure
c bfield: value of B field.    te:  electron temperature
c den: density of electron ne. NION: number of ion species
c A1, A2: ratio of ion density, ni/ne & n2/ne.
c mass1, mass2:  ion mass, mass1>mass2
c WLH1,WLH2:     roots of S(w)=0.
c WSha(i):    AC frequency.    nhz: number of AC frequencies
c eabs1,eabs2,eabs4:  accuracy control variable for k2 integral
c nki: point for gaussian integral
c Output results:
c wsh: AC frequency.   Numban:  identification of radiation bands
c current collecting surface area: AR1,AR2,AR3,AR4,AR5,ARA,AR
c radiation impedances:
c zint1, zint2: oblong body with I2, length=L22 and L21.
c zini-current from every surface, Itot=I2+2I1+2I3+I4
c zin2-only I2, zin3-only I3, zin4-only I1, zin5-only I4
c comparsion of power radiation from different system:
c ZP1,ZP2,ZN2,ZN3,ZN4,ZN5,ZA,ZA1,ZA2,ZA3,ZA4,ZA5
c
c Subroutine called:
c omint--- obtain dP/dw
c          subroutine called by omint:
c               dqawf--obtain Fourier cosine integral for k2
c          function subroutine called by omint:
c               s--function S(w)
c               integrand of Fourier cosine integral:
c               fchat1,fchat2,fchat3,fchat4,fchat5
c               fchat6,fchat7,fchat8,fchat9,fchat10
c               fch1,fch2,fch3,fch4,fch5,fch6,fch7,fch8,fch9,fch10
c                   function subroutine called by the above fchat's:
c                        Pw--function P(w)
c abwt---- set up the integration for w.
c          subroutine called by abwt:
c                zstop--- stop the program
c.....................................................................
```

```
c-------------------------------------------------------
        implicit real*8 (a-h,o-z)
        real*8 massi,MASS1,MASS2,MASS3,MASSE
        dimension wsha(12),DPDT1(64),DPDT2(64),DPDW1(64),
     &dpdw2(64),DPDW3(64),DPDW4(64),DPDW5(64)
        DIMENSION WI(4),WLH(4)
        real*4 wf(64),wa(64)
        common/int/omegaa(64),wom(64),nk1
        COMMON/FREQ/WI1,WI2,WE,WP1,WP2,WP,
     & WLH1,WLH2
        common/band/wmin,wmax,wnorm,numban
        common/param/den,A1,A2,A3,bfield,masse,mass1,mass2,
     &nion,cL,vsat,ws,pi,ca,te
        common/size/xl21,xl22,d11,d12,d31,d32,arear
        common/xhatc/xhata(5)
        common/tol/epsabs,eabs1,EABS2,EABS3,EABS4
        common/forbac/isgn
c
        DATA DEN,BFIELD,MASSI,CL,VSAT,te/2.d5,0.33,16.,3.d10,7.3d5,0.1/
        data xl21,xl22,d11,d12,d31,d32/8.d3,1.d4,5.d2,2.d3,5.e1,5.e1/
        DATA WS/0./
c
        pi=acos(-1.d0)
c
        OPEN(50,FILE='$disk1:[user.group1.wang]APOWER.in',
     &STATUS='old')
        OPEN(60,FILE='$disk1:[user.group1.wang]APOWER.out',
     &STATUS='new')
        open(70,file='$disk1:[user.group1.wang]APOWER.plt',
     &status='new')
c
c Input dimensions of the box structure, plasma parameter,
c AC frequency and contral parameter.
        read(50,*)xl21,xl22,d11,d12,d31,d32
        read(50,*)den,A1,A2,A3,bfield,mass1,MASS2,te
        READ(50,*)WLH1,WLH2,NION
        read(50,*)nhz,nk1,eabs1,EABS2,EABS4
        do 98 i=1,nhz
98      READ(50,*)WSha(i)
c wp,wp1,wp2--electronic and ionic angular plasma frequency
c we,wi1,wi2--electronic and ionic gyrofrequencies
c masse--electron mass,  massi--average ion mass
c cL--speed of light, CA--alfven velocity, vsat--source velocity
        MASSE=1/1836.
        WP=5.64E4*SQRT(DEN)
        WP1=WP*SQRT(MASSE/MASS1*A1)
        WP2=WP*SQRT(MASSE/MASS2*A2)
C       WP3=WP*SQRT(MASSE/MASS3*A3)
        WE=1.76E7*BFIELD
        WI1=WE*MASSE/MASS1
        WI2=WE*MASSE/MASS2
```

```
C       WI3=WE*MASSE/MASS3
c       wuh=sqrt(we**2+wp**2)
c       wlh=sqrt(we*wi)*wp/wuh
        massi=A1*mass1+A2*mass2
        CA=2.18d11/SQRT(MASSI)/SQRT(DEN)*BFIELD
        z0=ca/cl**2*9.d11
c
        write(60,99)nk1,nhz,eabs1,EABS2,EABS4,C4
99      format(' nk1 = ',i5
     &,' nhz = ',i5,' eabs =',(1pe12.3)/)
c
        rhoe=vsat/we
        rhop=vsat/wp
c
        write(60,101)xl21,xl22,d11,d12,d31,d32,rhoe,rhop,ca,vsat
101     format(' l21 = ',1pe10.3,' cm'/
     &         ' l22 = ',1pe10.3,' cm'/
     &         ' d11 = ',1pe10.3,' cm'/
     &         ' d12 = ',1pe10.3,' cm'/
     &         ' d31 = ',1pe10.3,' cm'/
     &         ' d32 = ',1pe10.3,' cm'/
     &         ' vsat/we = ',1pe10.3,' cm'/
     &         ' vsat/wp = ',1pe10.3,' cm'/
     &         ' alfven velocity = ',1pe10.3,' cm/sec'/
     &         ' source velocity = ',1pe10.3,' cm/sec')
c
        write(60,103)den,A1,A2,bfield,mass1,MASS2,te
103     format(' electron density    =',1pe12.3,' /cm**3'/
     &         ' N1/Ne=',1pe12.3,' N2/Ne=',1pe12.3,/
     &         ' magnetic field      =',1pe12.3,' gauss '/
     &         ' ion mass 1          =',1pe12.3,' amu '/
     &         ' ion mass 2          =',1pe12.3/
     &         ' electron temperature=',1pe12.3,' eV')
c
        WRITE(60,100)WI1,WLH1,WI2,WLH2,WE,WP,WP1,WP2,z0
100     FORMAT( ' wi1  =',1PE10.3,' /sec',' WLH1 =',1PE10.3/
     &     ' wI2 =',1PE10.3,' /sec',' WLH2 =',1PE10.3/
     &     ' we  =',1PE10.3,' /sec'/
     &     ' wp  =',1PE10.3,' /sec',' WP1=',1PE10.3/
     &      ' WP2 =',1PE10.3,' /SEC'/
     &     ' z0  =',1PE10.3,' ohms')
c
        do 1000 ihz=1,nhz
        wsh=wsha(ihz)
        ws=wsh*2.*pi
c
        WRITE(60,102)wsh,WS
102     FORMAT(' wsh  =',1PE10.3,' Hz'/
     &     ' ws  =',1PE10.3/
     &      ' source freq Hz','    band no. ',' impedance ')
c
```

```
c     sum over bands
         nbands=nion+1
         do 1 j=1,NBANDS
         numban=j
c
         if(numban.eq.1)then
         wnorm=wi1
         wmin=0.
         wmax=1.
         EPSABS=EABS1
         end if
c
         if(numban.EQ.2)theN
         wnorm=wlh1
         wmin=1.
         wmax=WI2/WLH1
         EPSABS=EABS2
         end if
c
         if(nbands.gt.1.and.numban.eq.nbands)theN
         wnorm=wlh2
         wmin=1.
         wmax=we/wlh2
         EPSABS=EABS4
         end if
c
         call abwt(nk1,omegaa,wom)
c ipass=1,integral at -w*; ipass=2, integral at +w*; ipass=3, finish.
         ipass=1
60       continue
         if(ipass.eq.1) then
         isgn=-1
         zint1=0.
         zint2=0.
         zint3=0.
         zint4=0.
         zint5=0.
         end if
         if(ipass.eq.2) isgn=1
c Integrating over k2
         call omint(dpdT1,DPDT2,DPDW1,DPDW2,DPDW3,DPDW4,DPDW5)
c Integrating over w
         zint1=0.
         ZINT2=0.
         ZIN1=0.
         ZIN2=0.
         ZIN3=0.
         ZIN4=0.
         ZIN5=0.
         do 2 i=1,nk1
         if(dpdt1(i).lt.0)then
```

```
        dpdt1(i)=0.
        end if
        if(dpdt2(i).lt.0)then
        dpdt2(i)=0.
        end if
        if(dpdw1(i).lt.0)then
        dpdw1(i)=0.
        end if
        if(dpdw2(i).lt.0)then
        dpdw2(i)=0.
        end if
        if(dpdw3(i).lt.0)then
        dpdw3(i)=0.
        end if
        if(dpdw4(i).lt.0)then
        dpdw4(i)=0.
        end if
        if(dpdw5(i).lt.0)then
        dpdw5(i)=0.
        end if
16      FORMAT(9(1X,1PE10.3))
c dpdt1,dpdw1,etc: dZ/dw.  wom: dw.
        zint1=zint1+dpdT1(i)*wom(i)
        ZINT2=ZINT2+DPDT2(I)*WOM(I)
        ZIN1=ZIN1+DPDW1(I)*WOM(I)
        ZIN2=ZIN2+DPDW2(I)*WOM(I)
        ZIN3=ZIN3+DPDW3(I)*WOM(I)
        ZIN4=ZIN4+DPDW4(I)*WOM(I)
        ZIN5=ZIN5+DPDW5(I)*WOM(I)
2       continue
c
        ipass=ipass+1
        if(ipass.lt.3) goto 60
c Comparing the power radiated by different systems
c Let P=(j)**2*Zs, j-current density. Assuming same j, compare Zs.
        if(abs(zint1).gt.1.e-30)then
        ZP1=ZIN1/ZINT1
        ZP2=ZIN1/ZINT2
        end if
        if(abs(zin1).gt.1.e-30)then
        ZN2=ZIN2/ZIN1
        ZN3=ZIN3/ZIN1
        ZN4=ZIN4/ZIN1
        ZN5=ZIN5/ZIN1
        end if
        WRITE(60,17) NUMBAN,ZINT1,ZINT2,ZIN1,ZIN2,ZIN3,ZIN4,
     &ZIN5,ZP1,ZP2,ZN2,ZN3,ZN4,ZN5
17 FORMAT(' NUMBAN=',I2/' P=j*Zs Zs=',7(1PE12.4)/
     &' SAME j  Pa/Pt=',2(1pe10.3),' end  P2/Pa,P3/Pa,P1/Pa,P24/Pa'
     &,4(1pe10.3))
c
```

```
c Let P=I**2*Zr. I-current.  Assuming same total current, compare Zr.
c zint1,zint2 are impedane for tether with length=L22 and L21.
c zin1-current come through every end surface, Itot=I2+I1+I3+I4.
c zin2-only I2. zin3-only I3. zin4-only I1. zin5-only I4.
        AR=D11*D31
        AR2=D12*D32
        AR3=D12*(XL22-XL21)/2.
        AR1=D32*(XL22-XL21)/2.
        AR4=AR2-AR
        ARA=AR2+AR4+AR1*2.+AR3*2.
        zint1=zint1*Z0*(CL/CA)/AR**2
        ZINT2=ZINT2*Z0*(CL/CA)/AR**2
        ZIN1=ZIN1*Z0*(CL/CA)/ARA**2
        ZIN2=ZIN2*Z0*(CL/CA)/AR2**2
        ZIN3=ZIN3*Z0*(CL/CA)/(2*AR3)**2
        ZIN4=ZIN4*Z0*(CL/CA)/(2*AR1)**2
        ZIN5=ZIN5*Z0*(CL/CA)/(AR4)**2
if(abs(zint2).gt.1.e-30) then
        ZA1=ZIN1/ZINT2
        end if
        if(abs(zint1).gt.1.e-30)then
        ZA=ZIN1/ZINT1
        ZA2=ZIN2/ZINT1
        ZA3=ZIN3/ZINT1
        ZA4=ZIN4/ZINT1
        ZA5=ZIN5/ZINT1
        end if
C
        write(60,3)wsh,numban,zint1,ZINT2,ZIN1,ZIN2,
     &ZIN3,ZIN4,ZIN5
c
C        if(zint.lt.0.) ZINT=0.
        write(70,3)wsh,numBAN,zint1,ZINT2,ZIN1,ZIN2,ZIN3,ZIN4,ZIN5
3       format(1pe12.3,i10,7(1pe12.4,1x))
        WRITE(60,18)AR,ARA,AR2,AR3,AR4,AR1,ZA,ZA1,ZA2,ZA3,ZA4,ZA5
18      FORMAT(' AREA At,Aa,A2,A3,A4,A1=',6(1PE10.3)/ ' SAME I
     &P/Pt,P2/Pt,P3/Pt,P1/Pt,P24/Pt',6(1PE10.3))
c
1       continue
c
1000    continue
c
        CALL EXIT
        END
c
c
```

```
c-------------------------------------------------------------
      subroutine abwt(nzx,vz,wz)
c*************************************************************
c*****abwt sets up the outer integrations
c*************************************************************
      implicit real*8 (a-h,o-z)
      common/band/wmin,wmax,wnorm,numban
      dimension vz(64),wz(64),w(64),x(64)
      external d01baz
      data zero,one/0.d0,1.d0/
c
      xmin=wmin
      xmax=wmax
c
      if (nzx.le.6 .or. nzx.eq.8) go to 50
      if (nzx.eq.10 .or. nzx.eq.12) go to 50
      if (nzx.eq.14 .or. nzx.eq.16) go to 50
      if (nzx.eq.20 .or. nzx.eq.24) go to 50
      if (nzx.eq.32 .or. nzx.eq.48) go to 50
      if (nzx.eq.64) go to 50
c
      write (6,20)
   20 format (1x,20hcheck nzx and/or ncx)
c
      call zstop(4,6)
c
   50 continue
c
      ifail=1
      call d01bbf(d01baz,xmin,xmax,1,nzx,w,x,ifail)
c
      do 309 i=1,nzx
      j=nzx+1-i
      vz(i)=x(j)
      wz(i)=w(j)
  309 continue
c
      return
      end
c
c
      subroutine zstop(n,nunit)
c*************************************************************
c****stop code
c*************************************************************
      write(6,1) n
      write(nunit,1) n
1     format(6h stop ,i10,6h *****)
      stop
      end
c
```

```
c-----------------------------------------------------------------------
c subroutine   omint
c Calculating dZ/dw for integral over w.
c Fourier cosine integral over k2 is performed in subroutine dqawf
c dpdt1,dpdt2,dpdw1,dpdw2,dpdw3,dpdw4,dpdw5:
c dZ/dw for zint1,zint2,zin1,zin2,zin3,zin4,zin5.
c fchat's, fch's: integrand for Fourier integral,
c fc(i): results after Fourier integral.
c-----------------------------------------------------------------------
      subroutine omint(dpdT1,DPDT2,DPDW1,DPDW2,DPDW3,DPDW4,DPDW5)
      implicit real*8 (a-h,o-z)
      real*8 massi,MASSE,MASS1,MASS2,MASS3
c
      dimension dpdT1(64),iwork(2000),work(5500),fc(28),DPDT2(64),
     &DPDW1(64),DPDW2(64),DPDW3(64),DPDW4(64),DPDW5(64),X2(28)
c
      common/fixed/omega,xk1,xk1hat,sw
      common/int/omegaa(64),wom(64),nk1
      COMMON/FREQ/WI1,WI2,WE,WP1,WP2,WP,
     &WLH1,WLH2
      common/band/wmin,wmax,wnorm,numban
      common/param/den,A1,A2,A3,bfield,massE,MASS1,MASS2,
     &NION,cl,vsat,ws,pi,ca,te
      common/size/xl21,xl22,d11,d12,d31,d32,arear
      common/xhatc/xhata(5)
      common/tol/epsabs,eabs1,EABS2,EABS3,EABS4
      common/rat/rat1,rat2
      common/forbac/isgn
      external fchat1,fchat2,FCHAT3,FCHAT4,FCHAT5,FCHAT6,FCHAT7,
     &FCHAT8,FCHAT9,FCH1,FCH2,FCH3,FCH4,FCH5,FCH6,FCH7,FCH8,FCH9,
     &FCHAT10,FCH10
c
      data integr,limlst,leniw,maxpl,lenw/1,1000,2000,60,5500/
c
c Calculating integrand function at each w
      do 1 i=1,nk1
c
      omega=omegaa(i)*wnorm
       xk1=abs(omega+isgn*ws)/vsat
      sw=abs(s(omega))
      omoc=omega/cl*d32/2.
      xk1hat=xk1*xl22
c
C set sin and cosine function involved
        SI1=SIN(XK1*D11/2.)
        SI2=SIN(XK1*D12/2.)
        CO1=COS(XK1*D12/2.)
        IF(ABS(XK1*D11).LT.1.E-8)THEN
        ST=1.*D11*D31
        ELSE
        ST=SI1/(XK1*D11/2.)*D11*D31
```

```
        END IF
        IF(ABS(XK1*D12).LT.1.E-8)THEN
        SD12=1.*D12*D32
        SA3=1.*(XL22-XL21)/2.*D12*2.
        ELSE
        sd12=SI2/(XK1*D12/2.)*D12*D32
        SA3=SI2/(XK1*D12/2.)*(XL22-XL21)/2.*D12*2.
        END IF
        CA1=2*(XL22-XL21)/2.*D32*C01
c setting nodimensional parameters for Fourier integral
C  F2   FCHAT2
        X2(1)=0.
        X2(2)=XL21/XL22
        X2(3)=(1-XL21/XL22)/2.
        X2(4)=(1+XL21/XL22)/2.
        X2(5)=1.
C F1    FCHAT1
        X2(6)=0.
        X2(7)=(1+XL21/XL22)/2.
C F3    FCHAT3
        X2(8)=0.
        X2(9)=(1+XL21/XL22)/2.
C F21   FCHAT4
        X2(10)=(1-XL21/XL22)/4.
        X2(11)=(3+XL21/XL22)/4.
        X2(12)=(1+3*XL21/XL22)/4.
C F23   FCHAT5
        X2(13)=(1-XL21/XL22)/4.
        X2(14)=(3+XL21/XL22)/4.
        X2(15)=(1+3*XL21/XL22)/4.
C F13   FCHAT6
        X2(16)=0.
        X2(17)=(1+XL21/XL22)/2.
C F4    FCHAT7
        X2(18)=0.
        X2(19)=XL21/XL22
        X2(20)=1.
C F42   FCHAT8
        X2(21)=0.
        X2(22)=XL21/XL22
        X2(23)=(1-XL21/XL22)/2.
        X2(24)=(1+XL21/XL22)/2.
C F41   FCHAT9
        X2(25)=(1-XL21/XL22)/4.
        X2(26)=(1+3*XL21/XL22)/4.
C F43   FCHAT10
        X2(27)=(1-XL21/XL22)/4.
        X2(28)=(1+3*XL21/XL22)/4.
        IF(NUMBAN.LT.2) THEN
        DO 2 J=1,5
c
```

```
c Fourier Integral
       call dqawf(fchat2,0.,x2(J),integr,epsabs,fc(j),abserr,
     &neval,ier,limlst,lst,leniw,maxpl,lenw,iwork,work)
c
      if(ier.ne.0)
     &write(60,90)ier,J,x2(J),fc(j),abserr,epsabs,numban,xk1hat
c
2     continue
       DO 21 J=6,7
       call dqawf(fchat1,0.,x2(J),integr,epsabs,fc(j),abserr,
     &neval,ier,limlst,lst,leniw,maxpl,lenw,iwork,work)
c
      if(ier.ne.0)
     &write(60,90)ier,J,x2(J),fc(j),abserr,epsabs,numban,xk1hat
21       CONTINUE
         DO 22 J=8,9
       call dqawf(fchat3,0.,x2(J),integr,epsabs,fc(j),abserr,
     &neval,ier,limlst,lst,leniw,maxpl,lenw,iwork,work)
c
      if(ier.ne.0)
     &write(60,90)ier,J,x2(J),fc(j),abserr,epsabs,numban,xk1hat
22       CONTINUE
         DO 23 J=10,12
       call dqawf(fchat4,0.,x2(J),integr,epsabs,fc(j),abserr,
     &neval,ier,limlst,lst,leniw,maxpl,lenw,iwork,work)
c
      if(ier.ne.0)
     &write(60,90)ier,J,x2(J),fc(j),abserr,epsabs,numban,xk1hat
23       CONTINUE
         DO 24 J=13,15
       call dqawf(fchat5,0.,x2(J),integr,epsabs,fc(j),abserr,
     &neval,ier,limlst,lst,leniw,maxpl,lenw,iwork,work)
c
      if(ier.ne.0)
     &write(60,90)ier,J,x2(J),fc(j),abserr,epsabs,numban,xk1hat
24       CONTINUE
C
         DO 25 J=16,17
       call dqawf(fchat6,0.,x2(J),integr,epsabs,fc(j),abserr,
     &neval,ier,limlst,lst,leniw,maxpl,lenw,iwork,work)
c
      if(ier.ne.0)
     &write(60,90)ier,J,x2(J),fc(j),abserr,epsabs,numban,xk1hat
25       CONTINUE
C
         DO 26 J=18,20
    call dqawf(fchat7,0.,x2(J),integr,epsabs,fc(j),abserr,
     &neval,ier,limlst,lst,leniw,maxpl,lenw,iwork,work)
c
       if(ier.ne.0)
     &write(60,90)ier,J,x2(J),fc(j),abserr,epsabs,numban,xk1hat
```

```
26      CONTINUE
        DO 27 J=21,24
     call dqawf(fchat8,0.,x2(J),integr,epsabs,fc(j),abserr,
     &neval,ier,limlst,lst,leniw,maxpl,lenw,iwork,work)
c
      if(ier.ne.0)
     &write(60,90)ier,J,x2(J),fc(j),abserr,epsabs,numban,xk1hat
27      CONTINUE
        DO 28 J=25,26
     call dqawf(fchat9,0.,x2(J),integr,epsabs,fc(j),abserr,
     &neval,ier,limlst,lst,leniw,maxpl,lenw,iwork,work)
c
      if(ier.ne.0)
     &write(60,90)ier,J,x2(J),fc(j),abserr,epsabs,numban,xk1hat
28      CONTINUE
        DO 29 J=27,28
     call dqawf(fchat10,0.,x2(J),integr,epsabs,fc(j),abserr,
     &neval,ier,limlst,lst,leniw,maxpl,lenw,iwork,work)
c
      if(ier.ne.0)
     &write(60,90)ier,J,x2(J),fc(j),abserr,epsabs,numban,xk1hat
29    CONTINUE
C
90    format(' ier=',i2,' J=',I2,' x=',1pe10.3,' fc=',1pe10.3,' err=',
     &1pe10.3,' ep=',1pe10.3,' numban =',i2,' k1hat=',1pe10.3)
C
        COEF=WNORM/VSAT*XL22/SQRT(SW)*(4/(2*PI)**3)/1000.

        ELSE
C
        DO 3 J=1,5
      x2(J)=x2(J)*xk1hat
        call dqawf(fch2,0.,x2(J),integr,epsabs,fc(j),abserr,
     &neval,ier,limlst,lst,leniw,maxpl,lenw,iwork,work)
c
      if(ier.ne.0)
     &write(60,90)ier,J,x2(J),fc(j),abserr,epsabs,numban,xk1hat
c
3       continue
        DO 31 J=6,7
      x2(J)=x2(J)*xk1hat
        call dqawf(fch1,0.,x2(J),integr,epsabs,fc(j),abserr,
     &neval,ier,limlst,lst,leniw,maxpl,lenw,iwork,work)
c
      if(ier.ne.0)
     &write(60,90)ier,J,x2(J),fc(j),abserr,epsabs,numban,xk1hat
31      CONTINUE
c
        DO 32 J=8,9
      x2(J)=x2(J)*xk1hat
        call dqawf(fch3,0.,x2(J),integr,epsabs,fc(j),abserr,
```

```
     &neval,ier,limlst,lst,leniw,maxpl,lenw,iwork,work)
c
      if(ier.ne.0)
     &write(60,90)ier,J,x2(J),fc(j),abserr,epsabs,numban,xk1hat
32      CONTINUE
C
        DO 33 J=10,12
       x2(J)=x2(J)*xk1hat
        call dqawf(fch4,0.,x2(J),integr,epsabs,fc(j),abserr,
     &neval,ier,limlst,lst,leniw,maxpl,lenw,iwork,work)
c
      if(ier.ne.0)
     &write(60,90)ier,J,x2(J),fc(j),abserr,epsabs,numban,xk1hat
33      CONTINUE
C
        DO 34 J=13,15
       x2(J)=x2(J)*xk1hat
        call dqawf(fch5,0.,x2(J),integr,epsabs,fc(j),abserr,
     &neval,ier,limlst,lst,leniw,maxpl,lenw,iwork,work)
c
      if(ier.ne.0)
     &write(60,90)ier,J,x2(J),fc(j),abserr,epsabs,numban,xk1hat
34      CONTINUE
C
        DO 35 J=16,17
        x2(J)=x2(J)*xk1hat
        call dqawf(fch6,0.,x2(J),integr,epsabs,fc(j),abserr,
     &neval,ier,limlst,lst,leniw,maxpl,lenw,iwork,work)
c
      if(ier.ne.0)
     &write(60,90)ier,J,x2(J),fc(j),abserr,epsabs,numban,xk1hat
35      CONTINUE
        DO 36 J=18,20
        x2(J)=x2(J)*xk1hat
    call dqawf(fch7,0.,x2(J),integr,epsabs,fc(j),abserr,
     &neval,ier,limlst,lst,leniw,maxpl,lenw,iwork,work)
c
        if(ier.ne.0)
     &write(60,90)ier,J,x2(J),fc(j),abserr,epsabs,numban,xk1hat
36      CONTINUE
        DO 37 J=21,24
        X2(J)=X2(J)*XK1HAT
    call dqawf(fch8,0.,x2(J),integr,epsabs,fc(j),abserr,
     &neval,ier,limlst,lst,leniw,maxpl,lenw,iwork,work)
c
      if(ier.ne.0)
     &write(60,90)ier,J,x2(J),fc(j),abserr,epsabs,numban,xk1hat
37      CONTINUE
        DO 38 J=25,26
         X2(J)=X2(J)*XK1HAT
    call dqawf(fch9,0.,x2(J),integr,epsabs,fc(j),abserr,
```

```
     &neval,ier,limlst,lst,leniw,maxpl,lenw,iwork,work)
c
      if(ier.ne.0)
     &write(60,90)ier,J,x2(J),fc(j),abserr,epsabs,numban,xk1hat
38       CONTINUE
         DO 39 J=27,28
         X2(J)=X2(J)*XK1HAT
     call dqawf(fch10,0.,x2(J),integr,epsabs,fc(j),abserr,
     &neval,ier,limlst,lst,leniw,maxpl,lenw,iwork,work)
c
      if(ier.ne.0)
     &write(60,90)ier,J,x2(J),fc(j),abserr,epsabs,numban,xk1hat
39       CONTINUE
c
c
        COEF=(4/(2*PI)**3)/XK1HAT
        end if
         DO 44 II=1,28
         IF(ABS(FC(II)).GT.1.E100) FC(II)=0.
44       CONTINUE
c
c k*j term after Fourier Integral. k*j term for different systems
c
c Tether without end connector or station without solar array
c only I2 current
         TET1=(ST)**2*(FC(18)-FC(20))
         dpDT1(i)=COEF*teT1
         TET2=(ST)**2*(FC(18)-FC(19))
         DPDT2(I)=COEF*TET2
c Tether with end connector or station with solar array
c  current flow in and out at every surfaces of the end connectors
         TEMP1=SD12**2*(FC(1)-FC(5))+SD12**2*(FC(1)-FC(2))
     &+(CA1)**2*(FC(6)-FC(7))+SA3**2*(FC(8)-FC(9))
     &+2*SD12**2*(FC(3)-FC(4))+2*(SD12*CA1)*(FC(10)-FC(11))
     &+2*SD12*SA3*(FC(13)-FC(14))
     &+2*SD12*CA1*(FC(10)-FC(12))+2*SD12*SA3*(FC(13)-FC(15))
     &+2*CA1*SA3*(FC(16)-FC(17))
     &+ST**2*(FC(18)-FC(19))
     &-2*ST*SD12*(FC(23)-FC(24))-2*ST*SD12*(FC(21)-FC(22))
     &-2*ST*CA1*(FC(25)-FC(26))-2*ST*SA3*(FC(27)-FC(28))
         DPDW1(I)=COEF*TEMP1
c  current flow in and out through one pair of the end surfaces
         TEMP2=(SD12)**2*(FC(1)-FC(5))
         DPDW2(I)=COEF*TEMP2
         TEMP3=SA3**2*(FC(8)-FC(9))
         DPDW3(I)=COEF*TEMP3
         TEMP4=CA1**2*(FC(6)-FC(7))
         DPDW4(I)=COEF*TEMP4
         TEMP5=SD12**2*(FC(1)-FC(2))+ST**2*(FC(18)-FC(19))
     &-2*SD12*ST*(FC(21)-FC(22))
         DPDW5(I)=COEF*TEMP5
```

```
C
1     continue
c
100     FORMAT(' N=',I2,'COEF',1PE10.3,' SA3',4(1PE10.3))
102     FORMAT(' FC7',6(1PE10.3),' S',2(1PE10.3)/' FC2',4(1PE10.3))
      return
      end
c
```

```
c
c Environmental factor terms in the Fourier integral
c--------------------------------------------------------------------
c P(w) function for two ion species
        double precision FUNCTION Pw(W)
        implicit real*8 (a-h,o-z)
        COMMON/FREQ/WI1,WI2,WE,WP1,WP2,WP,
     &WLH1,WLH2
        Pw=wp**2+WP1**2+WP2**2+-w**2
        RETURN
        END
c
c--------------------------------------------------------------------
c S(w) function for two ion species
        double precision FUNCTION S(W)
        implicit real*8 (a-h,o-z)
        COMMON/FREQ/WI1,WI2,WE,WP1,WP2,WP,
     &WLH1,WLH2
        S=1+WP**2/(WE**2-W**2)+WP1**2/(WI1**2-W**2)+
     &WP2**2/(WI2**2-W**2)
        RETURN
        END
c
c
```

```
c-----------------------------------------------------------------------
c Integrand function for the Fourier cosine integrals
c-----------------------------------------------------------------------
      double precision function fchat2(xk2hat)
      implicit real*8 (a-h,o-z)
      real*8 massi,MASS1,MASS2,MASS3,MASSE
      common/fixed/omega,xk1,xk1hat,sw
      common/param/den,A1,A2,A3,bfield,massE,MASS1,MASS2,
     &NION,cL,vsat,ws,pi,ca,te
      common/size/xl21,xl22,d11,d12,d31,d32,arear
      common/rat/rat1,rat2
c
      xkpht2=xk1hat**2+xk2hat**2
      rhoe=2.38*sqrt(te)/bfield
      therm=(xl22/rhoe)**2
      if(xkpht2.gt.therm) go to 1
c
      comp=abs((1.+xkpht2*(cl/xl22)**2/pw(omegA)))
      omoc=omega/cL*d32/2.
      xk3hat=omoc*sqrt(sw*comp)
c
        IF(ABS(XK3HAT).LT.1.E-10)THEN
        SINK3=1.
        ELSE
        SINK3=SIN(XK3HAT)/XK3HAT
        END IF
      fchat2=SINK3**2
     &*sqrt(comp)/xkpht2
     &*(4*PI**2)*1000.
c
      return
1     fchat2=0.d0
      return
      end
c-----------------------------------------------------------------------
      double precision function fchat1(xk2hat)
      implicit real*8 (a-h,o-z)
      real*8 massi,MASS1,MASS2,MASS3,MASSE
      common/fixed/omega,xk1,xk1hat,sw
      common/param/den,A1,A2,A3,bfield,massE,MASS1,MASS2,
     &NION,cL,vsat,ws,pi,ca,te
      common/size/xl21,xl22,d11,d12,d31,d32,arear
      common/rat/rat1,rat2
c
      xkpht2=xk1hat**2+xk2hat**2
      rhoe=2.38*sqrt(te)/bfield
      therm=(xl22/rhoe)**2
      if(xkpht2.gt.therm) go to 1
c
      comp=abs((1.+xkpht2*(cl/xl22)**2/pw(omegA)))
      omoc=omega/cL*d32/2.
```

```
      xk3hat=omoc*sqrt(sw*comp)
c
        IF(ABS(XK3HAT).LT.1.E-10)THEN
        SINK3=1.
        ELSE
        SINK3=SIN(XK3HAT)/XK3HAT
        END IF
        XLL=XK2HAT*(1-XL21/XL22)/4.
        IF(ABS(XLL).LT.1.E-10)THEN
        SINK2=1.
        ELSE
        SINK2=SIN(XLL)/XLL
        END IF
      fchat1=(SINK3*SINK2)**2
     &*sqrt(comp)/xkpht2
     &*(4*PI**2)*1000.
c
      return
1     fchat1=0.d0
      return
      end
c-----------------------------------------------------------------------
      double precision function fchat3(xk2hat)
      implicit real*8 (a-h,o-z)
      real*8 massi,MASS1,MASS2,MASS3,MASSE
      common/fixed/omega,xk1,xk1hat,sw
      common/param/den,A1,A2,A3,bfield,massE,MASS1,MASS2,
     &NION,cL,vsat,ws,pi,ca,te
      common/size/xl21,xl22,d11,d12,d31,d32,arear
      common/rat/rat1,rat2
c
      xkpht2=xk1hat**2+xk2hat**2
      rhoe=2.38*sqrt(te)/bfield
      therm=(xl22/rhoe)**2
      if(xkpht2.gt.therm) go to 1
c
      comp=abs((1.+xkpht2*(cl/xl22)**2/pw(omegA)))
      omoc=omega/cL*d32/2.
      xk3hat=omoc*sqrt(sw*comp)
c
        XLL=XK2HAT*(1-XL21/XL22)/4.
        IF(ABS(XLL).LT.1.E-10)THEN
        SINK2=1.
        ELSE
        SINK2=SIN(XLL)/XLL
        END IF
        COK3=COS(XK3HAT)
      fchat3=(COK3*SINK2)**2
     &*sqrt(comp)/xkpht2
     &*(4*PI**2)*1000.
c
```

```
      return
1     fchat3=0.d0
      return
      end
c-----------------------------------------------------------------------
      double precision function fchat4(xk2hat)
      implicit real*8 (a-h,o-z)
      real*8 massi,MASS1,MASS2,MASS3,MASSE
      common/fixed/omega,xk1,xk1hat,sw
      common/param/den,A1,A2,A3,bfield,massE,MASS1,MASS2,
     &NION,cL,vsat,ws,pi,ca,te
      common/size/xl21,xl22,d11,d12,d31,d32,arear
      common/rat/rat1,rat2
c
      xkpht2=xk1hat**2+xk2hat**2
      rhoe=2.38*sqrt(te)/bfield
      therm=(xl22/rhoe)**2
      if(xkpht2.gt.therm) go to 1
c
      comp=abs((1.+xkpht2*(cl/xl22)**2/pw(omegA)))
      omoc=omega/cL*d32/2.
      xk3hat=omoc*sqrt(sw*comp)
c
        IF(ABS(XK3HAT).LT.1.E-10)THEN
        SINK3=1.
        ELSE
        SINK3=SIN(XK3HAT)/XK3HAT
        END IF
        XLL=XK2HAT*(1-XL21/XL22)/4.
        IF(ABS(XLL).LT.1.E-10)THEN
        SINK2=1.
        ELSE
        SINK2=SIN(XLL)/XLL
        END IF
      fchat4=(SINK3)**2*SINK2
     &*sqrt(comp)/xkpht2
     &*(4*PI**2)*1000.
c
      return
1     fchat4=0.d0
      return
      end
C-----------------------------------------------------------------------
      double precision function fchat5(xk2hat)
      implicit real*8 (a-h,o-z)
      real*8 massi,MASS1,MASS2,MASS3,MASSE
      common/fixed/omega,xk1,xk1hat,sw
      common/param/den,A1,A2,A3,bfield,massE,MASS1,MASS2,
     &NION,cL,vsat,ws,pi,ca,te
      common/size/xl21,xl22,d11,d12,d31,d32,arear
      common/rat/rat1,rat2
```

```
c
      xkpht2=xk1hat**2+xk2hat**2
      rhoe=2.38*sqrt(te)/bfield
      therm=(xl22/rhoe)**2
      if(xkpht2.gt.therm) go to 1
c
      comp=abs((1.+xkpht2*(cl/xl22)**2/pw(omegA)))
      omoc=omega/cL*d32/2.
      xk3hat=omoc*sqrt(sw*comp)
c
        COSK3=COS(XK3HAT)
        IF(ABS(XK3HAT).LT.1.E-10)THEN
        SINK3=1.
        ELSE
        SINK3=SIN(XK3HAT)/XK3HAT
        END IF
        XLL=XK2HAT*(1-XL21/XL22)/4.
        IF(ABS(XLL).LT.1.E-8)THEN
        SINK2=1.
        ELSE
        SINK2=SIN(XLL)/XLL
        END IF
      fchat5=(SINK3*SINK2*COSK3)
     &*sqrt(comp)/xkpht2
     &*(4*PI**2)*1000.
c
      return
1     fchat5=0.d0
      return
      end
C-------------------------------------------------------------------------
      double precision function fchat6(xk2hat)
      implicit real*8 (a-h,o-z)
      real*8 massi,MASS1,MASS2,MASS3,MASSE
      common/fixed/omega,xk1,xk1hat,sw
      common/param/den,A1,A2,A3,bfield,massE,MASS1,MASS2,
     &NION,cL,vsat,ws,pi,ca,te
      common/size/xl21,xl22,d11,d12,d31,d32,arear
      common/rat/rat1,rat2
c
      xkpht2=xk1hat**2+xk2hat**2
      rhoe=2.38*sqrt(te)/bfield
      therm=(xl22/rhoe)**2
      if(xkpht2.gt.therm) go to 1
c
      comp=abs((1.+xkpht2*(cl/xl22)**2/pw(omegA)))
      omoc=omega/cL*d32/2.
      xk3hat=omoc*sqrt(sw*comp)
c
        COSK3=COS(XK3HAT)
        IF(ABS(XK3HAT).LT.1.E-10)THEN
```

```
        SINK3=1.
        ELSE
        SINK3=SIN(XK3HAT)/XK3HAT
        END IF
        XLL=XK2HAT*(1-XL21/XL22)/4.
        IF(ABS(XLL).LT.1.E-10)THEN
        SINK2=1.
        ELSE
        SINK2=SIN(XLL)/XLL
        END IF
      fchat6=(SINK3*COSK3*SINK2**2)
     &*sqrt(comp)/xkpht2
     &*(4*PI**2)*1000.
c
      return
1     fchat6=0.d0
      return
      end
C-------------------------------------------------------------------------
      double precision function fchat7(xk2hat)
      implicit real*8 (a-h,o-z)
      real*8 massi,MASS1,MASS2,MASS3,MASSE
      common/fixed/omega,xk1,xk1hat,sw
      common/param/den,A1,A2,A3,bfield,massE,MASS1,MASS2,
     &NION,cL,vsat,ws,pi,ca,te
      common/size/xl21,xl22,d11,d12,d31,d32,arear
      common/rat/rat1,rat2
c
      xkpht2=xk1hat**2+xk2hat**2
      rhoe=2.38*sqrt(te)/bfield
      therm=(xl22/rhoe)**2
      if(xkpht2.gt.therm) go to 1
c
      comp=abs((1.+xkpht2*(cl/xl22)**2/pw(omegA)))
      omoc=omega/cL*d31/2.
      xk3hat=omoc*sqrt(sw*comp)
c
        IF(ABS(XK3HAT).LT.1.E-10)THEN
        SINK3=1.
        ELSE
        SINK3=SIN(XK3HAT)/XK3HAT
        END IF
      fchat7=SINK3**2
     &*sqrt(comp)/xkpht2
     &*(4*PI**2)*1000.
c
      return
1     fchat7=0.d0
      return
      end
C-------------------------------------------------------------------------
```

```
      double precision function fchat8(xk2hat)
      implicit real*8 (a-h,o-z)
      real*8 massi,MASS1,MASS2,MASS3,MASSE
      common/fixed/omega,xk1,xk1hat,sw
      common/param/den,A1,A2,A3,bfield,massE,MASS1,MASS2,
     &NION,cL,vsat,ws,pi,ca,te
      common/size/xl21,xl22,d11,d12,d31,d32,arear
      common/rat/rat1,rat2
c
      xkpht2=xk1hat**2+xk2hat**2
      rhoe=2.38*sqrt(te)/bfield
      therm=(xl22/rhoe)**2
      if(xkpht2.gt.therm) go to 1
c
      comp=abs((1.+xkpht2*(cl/xl22)**2/pw(omegA)))
      omoc=omega/cL*d31/2.
      OMOC2=OMEGA/CL*D32/2.
      xk3hat=omoc*sqrt(sw*comp)
       XK3HAT2=OMOC2*SQRT(SW*COMP)
c
        IF(ABS(XK3HAT).LT.1.E-10)THEN
        SINK3=1.
        ELSE
        SINK3=SIN(XK3HAT)/XK3HAT
        END IF
        IF(ABS(XK3HAT2).LT.1.E-10)THEN
        SINK32=1.
        ELSE
        SINK32=SIN(XK3HAT2)/XK3HAT2
        END IF
      fchat8=SINK3*SINK32
     &*sqrt(comp)/xkpht2
     &*(4*PI**2)*1000.
c
      return
1     fchat8=0.d0
      return
      end
C-------------------------------------------------------------------------
      double precision function fchat9(xk2hat)
      implicit real*8 (a-h,o-z)
      real*8 massi,MASS1,MASS2,MASS3,MASSE
      common/fixed/omega,xk1,xk1hat,sw
      common/param/den,A1,A2,A3,bfield,massE,MASS1,MASS2,
     &NION,cL,vsat,ws,pi,ca,te
      common/size/xl21,xl22,d11,d12,d31,d32,arear
      common/rat/rat1,rat2
c
      xkpht2=xk1hat**2+xk2hat**2
      rhoe=2.38*sqrt(te)/bfield
      therm=(xl22/rhoe)**2
```

```
      if(xkpht2.gt.therm) go to 1
c
      comp=abs((1.+xkpht2*(cl/xl22)**2/pw(omegA)))
      omoc=omega/cL*d31/2.
      OMOC2=OMEGA/CL*D32/2.
      xk3hat=omoc*sqrt(sw*comp)
      XK3HAT2=OMOC2*SQRT(SW*COMP)
c
       IF(ABS(XK3HAT).LT.1.E-10)THEN
        SINK3=1.
        ELSE
        SINK3=SIN(XK3HAT)/XK3HAT
        END IF
        IF(ABS(XK3HAT2).LT.1.E-10)THEN
        SINK32=1.
        ELSE
        SINK32=SIN(XK3HAT2)/XK3HAT2
        END IF
        XLL=XK2HAT*(1-XL21/XL22)/4.
        IF(ABS(XLL).LT.1.E-10)THEN
        SINK2=1.
        ELSE
        SINK2=SIN(XLL)/XLL
        END IF
      fchat9=SINK3*SINK32*SINK2
     &*sqrt(comp)/xkpht2
     &*(4*PI**2)*1000.
c
      return
1     fchat9=0.d0
      return
      end
C-------------------------------------------------------------------------
      double precision function fchat10(xk2hat)
      implicit real*8 (a-h,o-z)
      real*8 massi,MASS1,MASS2,MASS3,MASSE
      common/fixed/omega,xk1,xk1hat,sw
      common/param/den,A1,A2,A3,bfield,massE,MASS1,MASS2,
     &NION,cL,vsat,ws,pi,ca,te
      common/size/xl21,xl22,di1,di2,d31,d32,arear
      common/rat/rat1,rat2
c
      xkpht2=xk1hat**2+xk2hat**2
      rhoe=2.38*sqrt(te)/bfield
      therm=(xl22/rhoe)**2
      if(xkpht2.gt.therm) go to 1
c
      comp=abs((1.+xkpht2*(cl/xl22)**2/pw(omegA)))
      omoc=omega/cL*d31/2.
        OMOC2=OMEGA/CL*D32/2.
      xk3hat=omoc*sqrt(sw*comp)
```

```
        XK3HAT2=OMOC2*SQRT(SW*COMP)
c
        IF(ABS(XK3HAT).LT.1.E-10)THEN
        SINK3=1.
        ELSE
        SINK3=SIN(XK3HAT)/XK3HAT
        END IF
        XLL=XK2HAT*(1-XL21/XL22)/4.
        IF(ABS(XLL).LT.1.E-10)THEN
        SINK2=1.
        ELSE
        SINK2=SIN(XLL)/XLL
        END IF
        CK3=COS(XK3HAT2)
      fchat10=SINK3*SINK2*CK3
     &*sqrt(comp)/xkpht2
     &*(4*PI**2)*1000.
c
      return
1     fchat10=0.d0
      return
      end
C-----------------------------------------------------------------------
      double precision function fch2(y)
      implicit real*8 (a-h,o-z)
      real*8 massi,MASS1,MASS2,MASS3,MASSE
      common/band/wmin,wmax,wnorm,numban
      common/fixed/omega,xk1,xk1hat,sw
      common/param/den,A1,A2,A3,bfield,massE,MASS1,MASS2,
     &NION,cl,vsat,ws,pi,ca,te
      common/size/xl21,xl22,d11,d12,d31,d32,arear
      common/rat/rat1,rat2
      cLd=cL
      xl22d=xl22
      swd=sw
c
      xk2hat=xk1hat*y
      xkpht2=xk1hat**2+xk2hat**2
      rhoe=2.38*sqrt(te)/bfield
      therm=(xl22/rhoe)**2
      if(xkpht2.gt.therm) go to 1
c
      pwo=pw(omega)
      comp=dabs((1.+xkpht2*(cLd/xl22d)**2/pwo))
      omoc=omega/cLd*d32/2.
      xk3hat=omoc*dsqrt(sw*comp)
        IF(ABS(XK3HAT).LT.1.E-14)THEN
        SINK3=1.
        ELSE
        SINK3=SIN(XK3HAT)/XK3HAT
        END IF
```

```
c
      fch2=sinK3**2
     &*sqrt(comp)/(1+y**2)
     &/SQRT(SW)*WNORM/VSAT*XL22*(4*PI**2)
c
      return
1     fch2=0.d0
      return
      end
c-----------------------------------------------------------------------
      double precision function fch1(y)
      implicit real*8 (a-h,o-z)
      real*8 massi,MASS1,MASS2,MASS3,MASSE
      common/band/wmin,wmax,wnorm,numban
      common/fixed/omega,xk1,xk1hat,sw
      common/param/den,A1,A2,A3,bfield,massE,MASS1,MASS2,
     &NION,cl,vsat,ws,pi,ca,te
      common/size/xl21,xl22,d11,d12,d31,d32,arear
      common/rat/rat1,rat2
      cLd=cL
      xl22d=xl22
      swd=sw
c
      xk2hat=xk1hat*y
      xkpht2=xk1hat**2+xk2hat**2
      rhoe=2.38*sqrt(te)/bfield
      therm=(xl22/rhoe)**2
      if(xkpht2.gt.therm) go to 1
c
      pwo=pw(omega)
      comp=dabs((1.+xkpht2*(cLd/xl22d)**2/pwo))
      omoc=omega/cLd*d32/2.
      xk3hat=omoc*dsqrt(sw*comp)
        IF(ABS(XK3HAT).LT.1.E-14)THEN
        SINK3=1.
        ELSE
        SINK3=SIN(XK3HAT)/XK3HAT
        END IF
        XLL=XK2HAT*(1-XL21/XL22)/4.
        IF(ABS(XLL).LT.1.E-14)THEN
        SINK2=1.
        ELSE
        SINK2=SIN(XLL)/XLL
        END IF
c
      fch1=(sinK3*SINK2)**2
     &*sqrt(comp)/(1+y**2)
     &/SQRT(SW)*WNORM/VSAT*XL22*(4*PI**2)
c
      return
1     fch1=0.d0
```

```
      return
      end
c-----------------------------------------------------------------------
      double precision function fch3(y)
      implicit real*8 (a-h,o-z)
      real*8 massi,MASS1,MASS2,MASS3,MASSE
      common/band/wmin,wmax,wnorm,numban
      common/fixed/omega,xk1,xk1hat,sw
      common/param/den,A1,A2,A3,bfield,massE,MASS1,MASS2,
     &NION,cl,vsat,ws,pi,ca,te
      common/size/xl21,xl22,d11,d12,d31,d32,arear
      common/rat/rat1,rat2
      cLd=cL
      xl22d=xl22
      swd=sw
c
      xk2hat=xk1hat*y
      xkpht2=xk1hat**2+xk2hat**2
      rhoe=2.38*sqrt(te)/bfield
      therm=(xl22/rhoe)**2
      if(xkpht2.gt.therm) go to 1
c
      pwo=pw(omega)
      comp=dabs((1.+xkpht2*(cLd/xl22d)**2/pwo))
      omoc=omega/cLd*d32/2.
      xk3hat=omoc*dsqrt(sw*comp)
        COSK3=COS(XK3HAT)
        XLL=XK2HAT*(1-XL21/XL22)/4.
        IF(ABS(XLL).LT.1.E-14)THEN
        SINK2=1.
        ELSE
        SINK2=SIN(XLL)/XLL
        END IF
c
      fch3=(COSK3*SINK2)**2
     &*sqrt(comp)/(1+y**2)
     &/SQRT(SW)*WNORM/VSAT*XL22*(4*PI**2)
c
      return
1     fch3=0.d0
      return
      end
c-----------------------------------------------------------------------
      double precision function fch4(y)
      implicit real*8 (a-h,o-z)
      real*8 massi,MASS1,MASS2,MASS3,MASSE
      common/band/wmin,wmax,wnorm,numban
      common/fixed/omega,xk1,xk1hat,sw
      common/param/den,A1,A2,A3,bfield,massE,MASS1,MASS2,
     &NION,cl,vsat,ws,pi,ca,te
      common/size/xl21,xl22,d11,d12,d31,d32,arear
```

```
      common/rat/rat1,rat2
      cLd=cL
      xl22d=xl22
      swd=sw
c
      xk2hat=xk1hat*y
      xkpht2=xk1hat**2+xk2hat**2
      rhoe=2.38*sqrt(te)/bfield
      therm=(xl22/rhoe)**2
      if(xkpht2.gt.therm) go to 1
c
      pwo=pw(omega)
      comp=dabs((1.+xkpht2*(cLd/xl22d)**2/pwo))
      omoc=omega/cLd*d32/2.
      xk3hat=omoc*dsqrt(sw*comp)
        IF(ABS(XK3HAT).LT.1.E-14)THEN
        SINK3=1.
        ELSE
        SINK3=SIN(XK3HAT)/XK3HAT
        END IF
        XLL=XK2HAT*(1-XL21/XL22)/4.
        IF(ABS(XLL).LT.1.E-14)THEN
        SINK2=1.
        ELSE
        SINK2=SIN(XLL)/XLL
        END IF
c
      fch4=(sinK3)**2*SINK2
     &*sqrt(comp)/(1+y**2)
     &/SQRT(SW)*WNORM/VSAT*XL22*(4*PI**2)
c
      return
1     fch4=0.d0
      return
      end
C-----------------------------------------------------------------------
      double precision function fch5(y)
      implicit real*8 (a-h,o-z)
      real*8 massi,MASS1,MASS2,MASS3,MASSE
      common/band/wmin,wmax,wnorm,numban
      common/fixed/omega,xk1,xk1hat,sw
      common/param/den,A1,A2,A3,bfield,massE,MASS1,MASS2,
     &NION,cl,vsat,ws,pi,ca,te
      common/size/xl21,xl22,d11,d12,d31,d32,arear
      common/rat/rat1,rat2
      cLd=cL
      xl22d=xl22
      swd=sw
c
      xk2hat=xk1hat*y
      xkpht2=xk1hat**2+xk2hat**2
```

```
      rhoe=2.38*sqrt(te)/bfield
      therm=(xl22/rhoe)**2
      if(xkpht2.gt.therm) go to 1
c
      pwo=pw(omega)
      comp=dabs((1.+xkpht2*(cLd/xl22d)**2/pwo))
      omoc=omega/cLd*d32/2.
      xk3hat=omoc*dsqrt(sw*comp)
        COSK3=COS(XK3HAT)
        IF(ABS(XK3HAT).LT.1.E-14)THEN
        SINK3=1.
        ELSE
        SINK3=SIN(XK3HAT)/XK3HAT
        END IF
        XLL=XK2HAT*(1-XL21/XL22)/4.
        IF(ABS(XLL).LT.1.E-14)THEN
        SINK2=1.
        ELSE
        SINK2=SIN(XLL)/XLL
        END IF
c
      fch5=(sinK3*SINK2*COSK3)
     &*sqrt(comp)/(1+y**2)
     &/SQRT(SW)*WNORM/VSAT*XL22*(4*PI**2)
c
      return
1     fch5=0.d0
      return
      end
C-------------------------------------------------------------------------------
      double precision function fch6(y)
      implicit real*8 (a-h,o-z)
      real*8 massi,MASS1,MASS2,MASS3,MASSE
      common/band/wmin,wmax,wnorm,numban
      common/fixed/omega,xki,xkihat,sw
      common/param/den,A1,A2,A3,bfield,massE,MASS1,MASS2,
     &NION,cl,vsat,ws,pi,ca,te
      common/size/xl21,xl22,di1,di2,d31,d32,arear
      common/rat/rat1,rat2
      cLd=cL
      xl22d=xl22
      swd=sw
c
      xk2hat=xkihat*y
      xkpht2=xkihat**2+xk2hat**2
      rhoe=2.38*sqrt(te)/bfield
      therm=(xl22/rhoe)**2
      if(xkpht2.gt.therm) go to 1
c
      pwo=pw(omega)
      comp=dabs((1.+xkpht2*(cLd/xl22d)**2/pwo))
```

```
      omoc=omega/cLd*d32/2.
      xk3hat=omoc*dsqrt(sw*comp)
        COSK3=COS(XK3HAT)
        IF(ABS(XK3HAT).LT.1.E-14)THEN
        SINK3=1.
        ELSE
        SINK3=SIN(XK3HAT)/XK3HAT
        END IF
        XLL=XK2HAT*(1-XL21/XL22)/4.
        IF(ABS(XLL).LT.1.E-14)THEN
        SINK2=1.
        ELSE
        SINK2=SIN(XLL)/XLL
        END IF
c
      fch6=(sinK3*COSK3)*SINK2
     &*sqrt(comp)/(1+y**2)
     &/SQRT(SW)*WNORM/VSAT*XL22*(4*PI**2)
c
      return
1     fch6=0.d0
      return
      end
c-----------------------------------------------------------------------
      double precision function fch7(y)
      implicit real*8 (a-h,o-z)
      real*8 massi,MASS1,MASS2,MASS3,MASSE
      common/band/wmin,wmax,wnorm,numban
      common/fixed/omega,xk1,xk1hat,sw
      common/param/den,A1,A2,A3,bfield,massE,MASS1,MASS2,
     &NION,cl,vsat,ws,pi,ca,te
      common/size/xl21,xl22,d11,d12,d31,d32,arear
      common/rat/rat1,rat2
      cLd=cL
      xl22d=xl22
      swd=sw
c
      xk2hat=xk1hat*y
      xkpht2=xk1hat**2+xk2hat**2
      rhoe=2.38*sqrt(te)/bfield
      therm=(xl22/rhoe)**2
      if(xkpht2.gt.therm) go to 1
c
      pwo=pw(omega)
      comp=dabs((1.+xkpht2*(cLd/xl22d)**2/pwo))
      omoc=omega/cLd*d31/2.
      xk3hat=omoc*dsqrt(sw*comp)
        IF(ABS(XK3HAT).LT.1.E-14)THEN
        SINK3=1.
        ELSE
        SINK3=SIN(XK3HAT)/XK3HAT
```

```
        END IF
c
      fch7=sinK3**2
     &*sqrt(comp)/(1+y**2)
     &/SQRT(SW)*WNORM/VSAT*XL22*(4*PI**2)
c
      return
1     fch7=0.d0
      return
      end
C-----------------------------------------------------------------------
      double precision function fch8(y)
      implicit real*8 (a-h,o-z)
      real*8 massi,MASS1,MASS2,MASS3,MASSE
      common/band/wmin,wmax,wnorm,numban
      common/fixed/omega,xk1,xk1hat,sw
      common/param/den,A1,A2,A3,bfield,massE,MASS1,MASS2,
     &NION,cl,vsat,ws,pi,ca,te
      common/size/xl21,xl22,d11,d12,d31,d32,arear
      common/rat/rat1,rat2
      cLd=cL
      xl22d=xl22
      swd=sw
c
      xk2hat=xk1hat*y
      xkpht2=xk1hat**2+xk2hat**2
      rhoe=2.38*sqrt(te)/bfield
      therm=(xl22/rhoe)**2
      if(xkpht2.gt.therm) go to 1
c
      pwo=pw(omega)
      comp=dabs((1.+xkpht2*(cLd/xl22d)**2/pwo))
      omoc=omega/cLd*d31/2.
      xk3hat=omoc*dsqrt(sw*comp)
        OMOC2=OMEGA/CLD*D32/2.
        XK3HAT2=OMOC2*DSQRT(SW*COMP)
        IF(ABS(XK3HAT).LT.1.E-14)THEN
        SINK3=1.
        ELSE
        SINK3=SIN(XK3HAT)/XK3HAT
        END IF
        IF(ABS(XK3HAT2).LT.1.E-14)THEN
        SINK32=1.
        ELSE
        SINK32=SIN(XK3HAT2)/XK3HAT2
        END IF
      fch8=SINK3*SINK32
     &*sqrt(comp)/(1+y**2)
     &/SQRT(SW)*WNORM/VSAT*XL22*(4*PI**2)
c
      return
```

```
1     fch8=0.d0
      return
      end
C-----------------------------------------------------------------------
      double precision function fch9(y)
      implicit real*8 (a-h,o-z)
      real*8 massi,MASS1,MASS2,MASS3,MASSE
      common/band/wmin,wmax,wnorm,numban
      common/fixed/omega,xk1,xk1hat,sw
      common/param/den,A1,A2,A3,bfield,massE,MASS1,MASS2,
     &NION,cl,vsat,ws,pi,ca,te
      common/size/xl21,xl22,d11,d12,d31,d32,arear
      common/rat/rat1,rat2
      cLd=cL
      xl22d=xl22
      swd=sw
c
      xk2hat=xk1hat*y
      xkpht2=xk1hat**2+xk2hat**2
      rhoe=2.38*sqrt(te)/bfield
      therm=(xl22/rhoe)**2
      if(xkpht2.gt.therm) go to 1
c
      pwo=pw(omega)
      comp=dabs((1.+xkpht2*(cLd/xl22d)**2/pwo))
      omoc=omega/cLd*d31/2.
      xk3hat=omoc*dsqrt(sw*comp)
        OMOC2=OMEGA/CLD*D32/2.
        XK3HAT2=OMOC2*DSQRT(SW*COMP)
        IF(ABS(XK3HAT).LT.1.E-14)THEN
        SINK3=1.
        ELSE
        SINK3=SIN(XK3HAT)/XK3HAT
        END IF
        IF(ABS(XK3HAT2).LT.1.E-14)THEN
        SINK32=1.
        ELSE
        SINK32=SIN(XK3HAT2)/XK3HAT2
        END IF
        XLL=XK2HAT*(1-XL21/XL22)/4.
        IF(ABS(XLL).LT.1.E-12)THEN
        SINK2=1.
        ELSE
        SINK2=SIN(XLL)/XLL
        END IF
      fch9=SINK3*SINK32*SINK2
     &*sqrt(comp)/(1+y**2)
     &/SQRT(SW)*WNORM/VSAT*XL22*(4*PI**2)
c
      return
1     fch9=0.d0
```

```
      return
      end
C-----------------------------------------------------------------------
      double precision function fch10(y)
      implicit real*8 (a-h,o-z)
      real*8 massi,MASS1,MASS2,MASS3,MASSE
      common/band/wmin,wmax,wnorm,numban
      common/fixed/omega,xk1,xk1hat,sw
      common/param/den,A1,A2,A3,bfield,massE,MASS1,MASS2,
     &NION,cl,vsat,ws,pi,ca,te
      common/size/xl21,xl22,d11,d12,d31,d32,arear
      common/rat/rat1,rat2
      cLd=cL
      xl22d=xl22
      swd=sw
c
      xk2hat=xk1hat*y
      xkpht2=xk1hat**2+xk2hat**2
      rhoe=2.38*sqrt(te)/bfield
      therm=(xl22/rhoe)**2
      if(xkpht2.gt.therm) go to 1
c
      pwo=pw(omega)
      comp=dabs((1.+xkpht2*(cLd/xl22d)**2/pwo))
      omoc=omega/cLd*d31/2.
      xk3hat=omoc*dsqrt(sw*comp)
        OMOC2=OMEGA/CLD*D32/2.
        XK3HAT2=OMOC2*DSQRT(SW*COMP)
        IF(ABS(XK3HAT).LT.1.E-14)THEN
        SINK3=1.
        ELSE
        SINK3=SIN(XK3HAT)/XK3HAT
        END IF
        XLL=XK2HAT*(1-XL21/XL22)/4.
        IF(ABS(XLL).LT.1.E-14)THEN
        SINK2=1.
        ELSE
        SINK2=SIN(XLL)/XLL
        END IF
        CK3=COS(XK3HAT2)
      fch10=SINK3*SINK2*CK3
     &*sqrt(comp)/(1+y**2)
     &/SQRT(SW)*WNORM/VSAT*XL22*(4*PI**2)
c
      return
1     fch10=0.d0
      return
      end
```